The Effect of Facial Protection, Impact Location, and Neckform Stiffness on Peak Linear Acceleration, Risk of Injury, and Energy Loading Measures of Horizontal Impacts on a Hockey Helmet

By: Leigh Jeffries

MSc.
School of Kinesiology
Lakehead University
Thunder Bay, Ontario

Submitted in partial fulfillment
of the requirements of
Master's of Science
In
Kinesiology

Supervisors: Dr. Carlos Zerpa & Dr. Eryk Przysucha

Committee: Dr. Paolo Sanzo

ABSTRACT

Helmets were originally designed and implemented to protect players from skull fractures and traumatic brain injuries by minimizing linear impact accelerations. The sport of hockey, however, has evolved, and now includes faster, larger, and stronger players. As a result, mild traumatic brain injuries or concussions have become more associated with the sport. Some solutions have been proposed to minimize concussions on hockey players by attaching facial shielding to helmets and increasing the neck strength of players, but these solutions have not been extensively explored in the research. Based on these concerns, the first purpose of this study was to assess the durability of a hockey helmet when exposed to multiple impact testing protocols. The second purpose was to investigate the influence of facial shielding and helmet location on the stiffness of a hockey helmet. The third purpose was to examine the influence of impact location, type of facial protection, and neck stiffness on peak linear acceleration, severity index, and the energy loading properties of hockey helmets during dynamic horizontal impacts. For the first purpose of the study, the analysis revealed that attenuation properties of the helmet were not compromised at either location after 200 impacts were administered. This aided in the determination of a threshold impact count to replace the helmet during dynamic testing. For the second purpose, the analysis revealed that adding facial shielding to a hockey helmet increases its stiffness properties. Additionally, this analysis revealed that the stiffness of the helmet varies according to helmet location. For the third purpose, the analyses revealed statistically significant three-way interactions between facial shielding, impact location, and neckform stiffness on measures of peak linear acceleration, F (3.40, 86.77) = 6.31, $p < .001$, $\eta_p^2 = .19$; severity index, F (3.28, 83.72) = 4.51, $p = .004$, $\eta_p^2 = .15$ and energy loading, F (16, 408) = 2.25, $p = .004$, $\eta_p^2 = .08$. Two-way interactions at each level of neckform stiffness were examined for each of the

three dependent variables to help explain the three-way interactions and the results of the analysis revealed statistically significant two way interactions and subsequent simple main effects for impact location and facial shielding. The findings of this work add to previous literature concerning helmeted headform impact testing by examining the role that facial shielding plays in combination with neck strength and impact location in brain injury prevention for the sport of hockey. Finally, the outcome of this study adds to the current understanding of injury mechanisms in the sport of hockey, and have practical applications for helmet designs and manufacturers, standards organizations, coaches and hockey players.

ACKNOWLEDGMENTS

I would like to begin by thanking my thesis supervisors Dr. Carlos Zerpa and Dr. Eryk Przysucha for their support throughout this project. It would not have been possible without your guidance, feedback, and expertise. I am also thankful to have Dr. Paolo Sanzo on my committee, who provided valuable guidance and feedback on this thesis. I also must thank Ms. Gloria Estabrooks and Mrs. Anthea Kyle for their help editing my thesis.

Next, I would like to acknowledge the fourth-year mechanical engineering students Michael Bayley, Rajit Singh, Robert Stubbe, and Kurtis TenHave and their project supervisors Dr. Kefu Liu, Dr. Meilan Liu, and Dr. Carlos Zerpa for designing and constructing the pneumatic horizontal impactor used in my research. Furthermore, I would like to extend thanks to Mr. Kuo Yang and Mr. Glen Patterson, who helped ensure that the impactor worked smoothly throughout my data collection, as well as retrofitting the impactor with new parts. I also would like to thank Dr. Siamak Elyasi for agreeing to be the external examiner of my thesis.

Finally, I would like to thank my family and friends who helped me in various ways over the course of this project. I am so thankful for their encouragement, love, and support. I would not have been able to achieve this goal without you.

Table of Contents

Appendix B

List of Figures

List of Tables

List of Abbreviations

ABS	Acrylonitrile-Butadiene-Styrene
ASTM	American Society for Testing and Materials
AE	Athletic exposures
AS/NZS	Australia and New Zealand Standards
CSA	Canadian Standards Association
EPE	Expanded polyethylene
EPE	Expanded polypropylene
HIC	Head injury criterion
HIT	Helmet Impact Telemetry
HECC	Hockey Equipment Certification Council
ICP	Integrated circuit piezoelectric sensor
ISO	International Organization for Standards
KE	Kinetic energy
mTBI	Mild traumatic brain injury
NCAA	National Collegiate Athletic Association
NHL	National Hockey League
NOCSAE	National Operating Committee on Standards for Athletic Equipment
SI	Severity Index
STAR	Summation of Tests for the Analysis of Risk
TSN	The Sports Network
TBI	Traumatic brain injury
VN	Vinyl nitrile
WSTC	Wayne State Tolerance Curve

Chapter 1 - Introduction

Ice hockey is a collision sport played at high speeds. This attribute of the game has inherently caused hockey players to be at risk for injuries (Agel & Harvey, 2010). Injuries to the head are common to hockey players and can have a profound impact on the well-being of a player (Biasca, Wirth, & Tegner, 2002) since they can potentially lead to neuronal damage in the brain and even death (Post, Oeur, Hoshizaki, & Gilchrist, 2011). After several players died from head injuries sustained while playing hockey (Biasca et al., 2002), players began to fear for their safety.

This concern resulted in the development of protective equipment for the head and brain (Wennberg & Tator, 2003) and helmets became the chosen method to protect hockey players from these injuries (Kis et al., 2013). At their inception, hockey helmets aimed to reduce the incidence of traumatic brain injury (TBI) such as subdural hematoma and skull fracture caused by sudden acceleration and deceleration forces acting on the head and brain (Namjoshi et al., 2013). Hockey helmets significantly minimized the occurrence of TBIs in the sport (Kis et al., 2013). Hockey, however, is now recognized as a sport with an elevated risk of concussion or mild traumatic brain injuries (mTBI; Rowson, Rowson, & Duma, 2015). A concussion is a type of mTBI occurring from static or dynamic loading forces acting on a player's head (direct) or torso (indirect) that temporarily affects brain function (Guskiewicz & Mihalik, 2006; Mayo Clinic, 2017).

Some believe that hockey has become a sport plagued by concussions because of changes to protective equipment, such as the addition of larger padding, combined with increased game speed, player mass, and aggressiveness. The high incidence of concussions may also be

compounded by the fact that current helmet designs are not intended to protect wearers from this kind of injury (Benson, Mieeuwisse, Rizos, Kang, & Burke, 2011).

Current helmet design and head protection characteristics are based on the helmet testing protocols and standard procedures currently in existence. Helmets only need to meet these standards to be sold to consumers. The current testing protocols and criteria have been developed both for research purposes and to prevent brain injuries in sports. All helmet testing is conducted using a surrogate headform with a helmet mounted on it (Carlson et al., 2016). The headform contains an array of accelerometers and mimics the response of a human head during a collision (Carlson et al., 2016). Peak linear acceleration experienced by the helmeted headform is the primary evaluation measure used to assess helmet performance (Post et al., 2011). The maximum value accepted for peak linear impact acceleration for helmet ranges from 275 to 300 gs, depending on the standard (Ouckama, 2013). The measurement unit of g is used when assessing the linear acceleration component of an impact and is a multiple of the acceleration due to gravity ($g = 9.81\ m/s^2$). Other criteria such as the severity index (SI) are used to evaluate helmets, and if all impact conditions are met, then the helmet is determined to be suitable for use in hockey (Carlson et al., 2016).

All current helmet standards employ helmet drop testing for certification; however, this method mimics a mechanism of injury associated with falls (Gwin et al., 2010). Using drop testing to evaluate helmets is concerning since many epidemiological studies examining hockey players' injuries have identified falls as a secondary cause of brain injury; while the primary source reported is collision or body contact (Agel & Harvey, 2010). As a result, the National Operating Committee on the Standards for Athletic Equipment (NOCSAE) has introduced a horizontal linear impactor testing method to more accurately emulate on ice impacts believed to

be responsible for mTBI. As stated by NOCSAE (2006), “it is believed that compliance with this test method will reduce the likelihood of mild traumatic brain injuries” (p. 1). In the linear impact test procedure, a researcher positions a helmet on a headform, which is attached to a neckform assembly and firmly secured to a linear bearing table to allow post impact kinematics. An impactor rod is subsequently propelled at the helmet to achieve the impact, and the resultant peak linear acceleration is recorded (NOCSAE, 2016b).

The use of a linear impactor not only allows for helmet testing certification but also to examine other variables related to concussions in hockey such as neck stiffness, which can be simulated by using a surrogate neckform attached to a headform. This relationship between neck stiffness/compliance and concussions is another area often overlooked in the literature (Rousseau & Hoshizaki, 2009). It is believed that the neck response behaviour can influence the head response acceleration transferred to the head and brain during a collision (Rousseau & Hoshizaki, 2009). Although several studies have examined this relationship using surrogate head and neckforms, there are discrepancies between the studies (Carlson, 2016; Rousseau, & Hoshizaki, 2009). These inconsistencies highlight the need for further investigation to better understand the influence of neck stiffness on head accelerations in simulated tests.

Another element in helmet testing that needs further research is the use of energy measures to better understand the behaviour of helmet material properties in minimizing head injuries such as concussions for different head impact mechanisms. Researchers have used energy analysis techniques to examine the protective capability of soccer headgear, hockey helmets, and bicycle face protection (Carlson, 2016; Marsh, McPherson, & Zerpa, 2008; Monthatipkul, Iovenitti, & Sbarski, 2012; Zerpa, Carlson, Elyasi, Przysucha, & Hoshizaki, 2016), but they have not performed these analysis techniques on hockey helmets with different

types of facial protection. A helmet energy analysis may provide further insight on head and brain injuries specifically for concussions when combined with the traditional measures of peak acceleration (Agel & Harvey, 2010).

In addition, assessing whether facial protection prevents hockey players from sustaining concussions, is an area in the literature with conflicting research and warrants further exploration. Clinical studies report no difference in concussion rates between players who wear facial protection to those who do not (Benson, Mohtadi, Rose, & Meeuwisse, 1999; Benson, Rose, & Meeuwisse, 2002; Stevens, Lassonde, de Beaumount, & Keenan, 2006; Stuart, Smith, Malo-Ortiguera, Fischer, & Larson, 2002). These studies, however, do not take into consideration that game and practice settings have confounding variables. These can include the location and magnitude of the impact, neck strength, facial protection (whether it is used or not), and the number of impacts sustained by a player. Since these variables cannot be controlled in vivo, examining the influence of each of these confounding variables in head injuries requires further investigation beyond testing techniques reported in the literature. A laboratory simulation study, may allow researchers to control these variables and examine their relationship to head injuries, and more specifically, concussions. It is important to highlight that only one biomechanical study by Lemair and Pearsall (2007) examined the effect of facial shields on peak linear acceleration. They found that facial shields do reduce the peak linear acceleration in a drop impact test.

The variables mentioned above are all connected to a hockey player's risk of sustaining a concussion. It is interesting that the interactions of impact location, neckform stiffness, and facial protection on helmeted headform peak linear acceleration, risk of injury, and energy loading measures have not been studied using a linear horizontal impactor to assess helmet performance.

To address this research gap, this study had three purposes. The first purpose was to assess the durability of the helmet when exposed to multiple impacts during helmet testing protocols. The second purpose was to test the helmets in a static setting to investigate the effect of facial shielding and helmet location on measures of helmet stiffness. The third purpose was to examine the effect of impact location, type of facial protection, and neckform stiffness on peak linear acceleration, severity index (SI), and energy loading properties of the hockey helmet during dynamic simulated horizontal impacts.

From the theoretical perspective, the outcome of this study builds upon existing literature concerning facial shield ability to reduce linear acceleration, a variable that could be associated with concussion prevention. Furthermore, this study adds to the existing knowledge base surrounding the influence of neckform stiffness and impact location on concussion in terms of measures of linear acceleration, risk of injury and energy during head collisions. From the practical perspective, it may provide another avenue to assess helmet performance using a horizontal impactor and measures of energy loading, to develop new testing standards and criteria.

Chapter 2 - Literature Review

Brain Injuries and Concussions in Hockey

The sport of ice hockey is considered a high-speed collision sport, and one of the most physically demanding sports due to the unpredictable nature of the game. There is a high potential for forceful impacts or contact between players or with environmental factors, such as the ice, boards, glass, pucks, and sticks. These inherent risks of the sport, subsequently, mean a high likelihood that hockey players may experience head/brain injuries (Post et al., 2011; Wennberg & Tator, 2003). Injuries to the head and face, which are some of the most common locations for hockey injuries, can have a profound impact on the well-being of a player (Biasca et al., 2002).

Brain injuries or concussions that hockey players receive while playing the sport of ice hockey vary regarding both severity and localization of the damage to the brain. Terms such as mild and traumatic are often used to describe the seriousness of the injury, while terms such as focal and diffuse describe whether an injury is concentrated to one area of the brain or if it is widespread (Biasca et al., 2002). This review of literature will include concussion or mTBI as well as diffuse and focal head injuries, which are progressively more traumatic and play a critical role in concussions.

Concussions or mild traumatic brain injuries. Giza and Hovda (2001) described a concussion, more specifically, as a mild diffuse neurological injury resulting from acceleration-deceleration of biomechanical forces acting on the brain. Throughout brain injury literature, the terms concussions and mTBIs are used interchangeably. The results of a concussion are typically transient and reversible, but occasionally produce persistent neurological dysfunction characterized by some, or all of the following symptoms: alterations in consciousness, amnesia,

visual disturbances, concentration problems, headache, vertigo, and balance disturbances (Giza & Hovda, 2001). Concussions alter the physiological processes occurring in the brain. Individuals with concussions may experience reduced cerebral blood flow, over-firing neurons, ion imbalances, and increased glucose metabolism (Giza & Hovda, 2001). These symptoms and physiological disturbances can alter brain functioning for several hours or months depending on the severity of the concussion (McAllister, Sparling, Flashman, & Saykin, 2001). The cognitive, physical, behavioural, and emotional effects, however, can remain long after the concussion (Arciniegas, Anderson, Topkoff, & McAllister, 2005). As no two concussions are same, the outcome for each player depends on a variety of factors including the force of the blow to the head, the level of the metabolic dysfunction, the number of previous concussions, the time between injuries, and the type of tissue damage, whether it is focal, diffuse, or a combination of the two (Biasca et al., 2002).

Diffuse brain injuries. Concussions are a type of diffuse brain injury characterized by widespread neural disruption of the brain (Biasca et al., 2002). This type of injury is caused by the inertial effects of a mechanical blow to the head causing a rapid acceleration-deceleration of the head and brain inside the skull. Stated in the context of a hockey, if a player receives an abrupt body check, it can cause either direct or indirect inertial loading of the head, and, potentially, a diffuse injury (Biasca et al., 2002). Diffuse brain injuries are characterized by progressive widespread damage to the white matter of the brain. The underlying pathologies of diffuse injuries fall on the same continuum. That is, all of them contain a degree of axonal shearing, which determines the severity of the injury. Diffuse brain damage can occur in both the cerebral and cerebellar hemispheres as well as the brainstem (Biasca et al., 2002). Furthermore, this type of brain injury may cause diffuse vascular injuries, hypoxic-ischemic injuries, and

cerebral edema (Andriessen, Jacobs, & Vos, 2010). Diffuse vascular injuries are small hemorrhagic brain lesions from shear forces acting on brain structures (Pittella & Gusmão, 2003). Hypoxic-ischemic injuries occurs when there is a decreased supply of oxygenated blood to the brain tissue and decreased blood perfusion of the brain (Arciniegas, 2012). Cerebral edema is brain swelling due to a build-up of fluids (Silverthorn, Johnson, Ober, Garrison, & Silverthorn, 2009). These associated brain injuries, occur because brain structures are heterogeneous concerning both the degree of fixation to other parts of the brain and skull as well as brain tissue consistency. Therefore, when rapid acceleration-deceleration of the head occurs, it causes certain segments of the brain to move at different rates than others, resulting in shearing, tensile, and compressive forces within the brain (Andriessen et al., 2010). Depending on the magnitude and types of force, the proportion and the total number of axons damaged, and their anatomical location will determine the severity and reversibility of the clinical syndromes and neurological deficits. The extent of traumatic axonal damage ranges from transient disturbance of ionic homeostasis (failure to maintain ion balance within the axon), to swelling and impairment of axoplasmic transport (inability to move material between axon terminal and the cell body), which may lead to delayed secondary axotomy (severing of the axon), and, consequently, irreversible structural brain lesions (Biasca et al., 2002; Silverthorn et al., 2010).

The consequences of a diffuse brain injury can range from a concussion, to coma, or death. In fact, diffuse brain injuries are responsible for approximately 25% of head injury deaths and individuals who survivor can be left with a permanent neurological disability. Furthermore, diffuse brain injuries are characterized by a cumulative effect, which can potentially end an athlete's career (Biasca et al., 2002).

Focal brain injuries. Alternatively, focal brain damage is the result of direct blunt collision forces transmitted through the skull. Brain tissue is compressed below the cranium at the site of impact (coup) or tissue opposite to the impact (contrecoup) which can result in a concussion (Andriessen et al., 2010). Brain tissue under the impact site is damaged but localized to that area of the brain. This type of injury can occur in hockey if a player is struck by a hockey stick or puck, or by falling and hitting his/her head on the ice (Biasca et al., 2002). The location and severity of impact to the skull dictate the associated cerebral pathologies and neurological deficits (Andriessen et al., 2010). Focal injuries include skull fractures, intracranial hematoma (epidural or subdural) (Biasca et al., 2002), intraparenchymal hematomas, and hemorrhagic contusions (Andriessen et al., 2010).

A focal impact on the head can cause the cranium to demonstrate elastic deformation (Ommaya, Goldsmith, & Thibault, 2002). Mechanically, the skull can only deform 4.3 to 5.7 mm depending on location before it ultimately fails and results in the cranial bones fracturing (Ommaya et al. 2002; Yoganandan & Pintar, 2003). There are several ways the skull can fail. Comminuted or depression fracturing to the skull, gives the skull a sunken appearance, as the pieces of the fractured bone are pushed inwards. These pieces can potentially enter the cranium and contact the brain causing significant intracranial damage (Cantu & Cantu, 2011). The most common skull fractures in sports are linear fractures resulting from focal impacts. When this type of break occurs, the bone remains fixed in the same spot (Cantu & Cantu, 2011). Finally, the last type of fracture is an open fracture and occurs when an object penetrates the scalp and skull, or the bone exits through the skin (Cantu & Cantu, 2011).

Focal impacts produce significant strain forces in the brain and may result in a skull fracture. A linear fracture may cause a rupture of the blood vessels in the head, causing them to

rupture and hemorrhage between the dural membranes (Meaney & Smith, 2011). Depending on the location of the bleed, these injuries may result in subdural hematoma, epidural hematoma, or subarachnoid hemorrhage (Andriessen et al., 2010). All types of focal related brain injury, pose a significant threat to brain health and functioning. Focal brain injuries are responsible for approximately half of all hospital admissions due to head injuries, and nearly two-thirds of the deaths caused by head injury (Biasca et al., 2002).

Concussion management. Concussions should be considered as serious as TBIs because the athlete's health and career can be adversely affected if he/she experiences persistent symptoms affecting his/her ability to return to play. In addition, concussions are an area of concern throughout all levels of hockey because many cases go unreported (Daneshvar, Nowinski, McKee, & Cantu, 2011). Even now, with an increased awareness, determining if a player has a concussion can be difficult. For example, some athletes may not realize that they have been concussed and continue to play or may not report the head injury or concussion symptoms to their coaches or trainers. As a result, they are not withheld from competition, which puts them at a higher risk of sustaining a severe brain injury (Gessel, Collins, & Dick, 2007). Furthermore, some coaches may still suggest that the player walk it off and return to the game after receiving the hit (Graham, Rivara, Ford, & Spicer, 2014). Although this second scenario is less likely to occur in hockey today due to the growing awareness of head injuries. Regardless, athletes may still find themselves returning to the game with a concussion or without fully recovering, thereby placing them in a vulnerable position. These athletes are now predisposed to an increased risk of receiving another concussive impact. If another head impact occurs, it is known as second-impact syndrome (Biasca, Wirth, Maxwell, & Simmen, 2005), and may lead to the development of chronic brain injuries or death (Chamard et al., 2012). Consequently, it is

now recommended that after receiving a possible concussion, the hockey player should be removed immediately from the game and assessed accordingly (Halstead et al., 2010). There has been a culture shift regarding acknowledgment, treatment, and management of concussion in hockey that has led to rule changes to prevent head contact, thereby reducing concussion. Even with the cultural shift, epidemiological research reveals that concussion rates are still a concern in hockey of all skill levels, ages, and genders.

Concussion rates. Concussion have been reported as injuries in ice hockey, which make up a significant portion of injuries and hockey related head injuries (Lemair, 2007). Decloe, Meeuwisse, Hagel, and Emery (2014) for example, reported that concussions are a commonly occurring injury among females. Emery and Meeuwisse (2006) also reported that concussions are the most frequently occurring injury among male youth. The concussion rate for female youth was calculated at 0.2 concussions per 1000 player-hours while for male youth, the concussion rate ranged from 0.24 per 1000 player-hours in atom aged players to 0.97 per 1000 player-hours in bantam aged players. The next level of play that researchers focused on is the high school level. Matic and colleagues (2015) determined that concussions were the most frequently reported injury at 6.4 per 10,000 athletic exposures (AEs), and the rates were significantly higher in competition (16.7 per 10,000 AEs) than in practice (1.6 per 10,000 AEs). Next, in a seven-year study of male and female National Collegiate Athletic Association (NCAA) hockey players, Agel and Harvey (2010) found that the rate of concussion was 0.72 per 1000 AEs for men and 0.82 per 1000 AEs for women, with that rate remaining stable over the study period. Another study focusing on collegiate athletes from the Canada West Universities Athletics Association had similar findings, reporting that concussions were the most common injury in both men (0.95 per 1000 AEs) and women (1.2 per 1000 AEs; Schick & Meeuwisse,

2003). Finally, concussions have been investigated at the professional and international levels of hockey, considered to be the highest levels athletes can play. Wennberg and Tator (2003) longitudinally examined the rate of concussions at the highest professional rank, the National Hockey League (NHL), from 1986-87 to the 2001-02 season. The authors found that the rate of concussion remained relatively stable from 1986 to 1996, ranging from 4 to 8 concussions per 1000 games. There was, however, a substantial increase in the rate of concussions from 1997 to 2002. The concussion rate during this period ranged from 13 to 30 per 1000 games. The researchers posit that this increase could be the result of improved concussion detection and reporting (Wennberg & Tator, 2003). Another study by Benson et al. (2011) examined concussions at this level. Over the course of seven NHL seasons (1997-2004), an inclusive cohort of NHL players and teams were included. In this study, team physicians diagnosed 559 concussions over the seven seasons. The concussion rate was calculated to be 1.8 per 1000 player-hours. Finally, at the international level of play, Tuominen et al. published two papers in 2015. The first reported that the concussion rate was 1.4 per 1000 player games for men over a 7-year period from 2006-07 to 2012-13 (Tuominen et al., 2015a). The women's concussion rate was determined to be 1.0 per 1000 player games over an 8-year period from 2006-07 to 2013-14 (Tuominen et al., 2015b). Each of these studies listed player contact or collision mechanisms as the primary cause of the concussion injury. As well, findings demonstrated that concussions are a major concern for the health and well-being of hockey players because of the time lost from play.

Mechanisms of Injury and Head Impact Variables Causing Concussion

Mechanisms of injury. Head injuries can be the result of loading. Loading is initiated by forces acting on a player's head or torso, with most head injuries arising from dynamic loading

(Guskiewicz & Mihalik, 2006). The sudden loading of the head is initiated by either a direct blow to the head (impact) or by a sudden movement of the head (impulse) produced by an impact; for instance, an impact to the torso resulting in a whiplash mechanism (Guskiewicz & Mihalik, 2006). Therefore, mechanisms of head injury are divided into two categories: a) those related to head-contact injuries (i.e., direct impacts) and b) those related to head movement injuries (i.e., inertial loading) (Meaney & Smith, 2011).

Direct or contact loading is the mechanism of injury behind focal injuries. This type of loading is associated with high linear accelerations and can result in focal bending, volume changes, and the propagation of shock waves through the skull (Gurdjian, Hodgson, Thomas, & Patrick, 1968). Conversely, inertial loading is related to the mechanism of injury behind diffuse injuries, because of the associated translation, rotation, and angulation. These factors are synonymous with shear force and high rotational acceleration (Gurdjian, 1972). Head injuries resulting from either mechanism are dependent on the direction, speed, and duration of the head movement. These variables contribute to the severity and areas of the brain affected by an impact. Figure 1 illustrates how different types of head movements can cause compression, shear, and rotation of the brain.

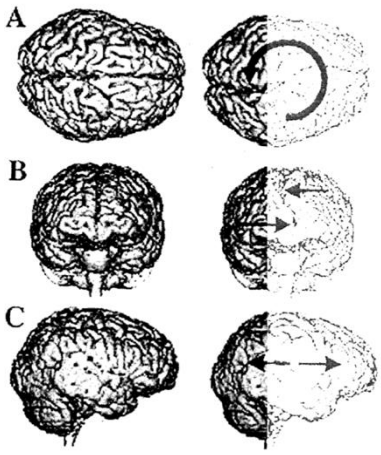

Figure 1. Impact forces that can act upon the brain. These forces include rotational (A), shearing (B), or compressive (C). A combination of these forces may act upon the brain from a single impact. Adapted from "Foundations of Sports-related Brain Injuries," by S. M. Slobounov & W. J. Sebastianelli, 2006, p. 68. Copyright 2006 by Springer Science + Business Media, Inc.

When a player is struck, both inertial and direct loadings to the head can occur. The kinematic response of the brain and neural damage upon head impact is dictated by factors such as: a) if the impact is to the head or not; b) what type of head acceleration occurs (linear or rotational); and c) whether the impact forces act on the centre of mass of the individual's head (centroidal) or not (non-centroidal; Graham et al., 2014). Each scenario influences the level of strain and potential damage to the brain during an impact. Direct loading occurs as a result of an impact on the head itself; whereas inertial loading is the consequence of head motion generated from either an impact or impulsive force (Guskiewicz & Mihalik, 2006). An example of an inertial loading would be if a player experienced rapid acceleration or deceleration of the head with no direct contact to his/her head by from an external object; loading is produced when another portion of the body is impacted (i.e., torso). This type of impact would also be considered a non-centroidal impact, resulting in angular acceleration of the head and brain. On the other hand, if a player's head was struck and the energy was focused through the head's centre of mass, linear acceleration of the brain would occur. Often in sports, the mechanism of a

head injury is the result of a combination of both linear and angular acceleration (Biasca et al., 2002).

Linear acceleration as a measure of brain injury due to head impacts. Peak linear acceleration is a vector quantity representing the rate of change of linear velocity over time and is used by many international helmet standards as a determinant for head injury (Gimbel & Hoshizaki, 2008). This measure has been used to predict the risk of injury for concussions (Zhang, Yang, & King, 2004). In head impact and helmet testing, accelerations are expressed as the resultant vector quantity of linear accelerations experienced in the three planes of motion. Linear acceleration is measured using gs. A g is the experimentally determined rate of change in velocity because of gravity (9.81 m/s^2), or a multiple of the acceleration due to gravity (National Aeronautics and Space Administration, 1965).

Peak linear acceleration has been linked to focal injuries and TBIs such as skull fracture and intracranial bleeding (Andriessen et al., 2010). Impacts transferring high linear accelerations to the head may result in focused damage to the brain. Previously, this mechanism of injury was assumed to be the underlying cause of most head and brain injuries like a concussion (Carlson, 2016). It is now more commonly thought that concussions are associated with angular accelerations (Gennarelli, Ommaya, & Thibault, 1971); however, linear accelerations may still be a factor (Zhang et al., 2004).

Occurrence of impacts. To further understand head injuries, it is important to examine how often an athlete's head is subjected to impact or loading in sport. Researchers conduct applied research to study this relationship between exposure to head impacts and mTBI to improve their understanding of injury mechanisms. A head impact can be defined as any instance where the head contacts an external object such as the ice or an opposing player in hockey

(Graham et al., 2014). To quantify the impacts received by hockey players, researchers fit players with helmets instrumented with the Head Impact Telemetry (HIT) System (Simbex, Lebanon, New Hampshire). These helmets contain six single-axis linear accelerometers and record the number of impact events and their magnitude. Brainard et al. (2012) had participants wear this technology in a study looking at female and male collegiate hockey players over two seasons. They found that female players received an average of M = 105, SD = 17.5 impacts per season while the male players received an average of M = 347.3, SD = 170.2 impacts to the head per season. Regarding the number of impacts per athlete exposure, females received fewer impacts (M = 1.7, SD = 0.7) ranging from 0.2 to 3.2, as compared to males (M = 2.9, SD = 1.2), with impacts ranging from 0.7 to 6.3. Wilcox et al. (2014) also quantified the head impacts sustained in collegiate hockey players. This study monitored 99 athletes over three competitive seasons and reported the median number of head impacts sustained in a season. Female hockey players received a median of 170 impacts with a maximum of 489 impacts. Their male counterparts received a median of 287 impacts to the head with a maximum of 785. Similar to the previous study, the impact frequency median was higher in males at 6.3, while females experienced a median of 3.7 impacts per game.

The occurrence of head impacts has also commonly been examined in youth players, since head injuries are problematic among players at this age level. Mihalik et al. (2012) quantified the number of head impacts sustained by youth players 13-16 years old over two seasons. They determined that each player at this level received a median of 223 head impacts in a season. At this level of hockey, head impacts do not usually exceed the concussive threshold values (150-200 g range). Even though the impacts are below this threshold, they are still concerning due to the high number that hockey player's experience. These repetitive sub-

concussive impacts are thought to lead to future neurological impairment (Bailes, Petraglia, Omalu, Nauman, & Talavage, 2013).

Location of impact. With the total number of impacts occurring in a season or game already quantified, researchers can further examine the impacts based on the location of the impact to the helmet. Analyzing the distribution of impacts amongst the different areas of the helmet is also determined with players wearing HIT helmets instrumented with single-axis linear accelerometers. The studies mentioned above, which addressed the frequency of impacts also reported the frequency that each location was contacted. Brainard et al. (2012) found that at the collegiate level, hockey players received the highest number of impacts to the front (30%) and back (33%) of the helmet followed by the left (14%), right (14%), and top (9%). Other studies examining the frequency of impact by location also reported similar impact frequencies to Brainard et al. (2012). Wilcox et al. (2014) also used collegiate hockey players, while Mihalik et al. (2012) used a Bantam (13-14 years) and Midget (15-16 year old) players to assess how often the different areas of the head were impacted. This applied research measuring how often certain areas of the head were contacted may have consequences for player safety. Knowing where players typically sustain head impacts may have implications for helmet design. Helmet design could also benefit from the laboratory research. This type of investigation has shown that human heads have various dynamic responses to impacts at different locations. Zhang, Yang, and King (2011) found increases in stress felt by intracranial tissue and that the chance of skull deformation was greater from lateral impacts to the head. These findings corresponded with research performed on anesthetized monkeys. Hodgson, Thomas, and Khalil (1983) reproduced concussions to determine the tolerances to concussions at different impact sites. They found that side locations produced longer periods of unconsciousness, as well as, higher linear and

rotational accelerations. They hypothesized that increased concussion tolerance and accelerations at the side location may be caused by the inability of the skull to resist the motion due to its oval shaped geometry and the thinner bone in this region (Yoganandan & Pintar, 2003).

Comparable relationships have also been shown using headform impact testing. Walsh, Rousseau, and Hoshizaki (2011) found differences in peak linear acceleration when impacting the head at different locations. Like Hodgson et al. (1983), the largest peak linear acceleration was experienced at the side location (132.8 g), followed by the front (121.3 g), and rear locations (116.9 g). Conversely, Carlson (2016) found that the front boss impact site was susceptible to the highest peak linear acceleration followed by the front, side, rear, and rear boss. On the other hand, Walsh et al. (2011) found that the areas of the headform with the greatest susceptibilities to linear acceleration were the front, rear, front boss, and rear boss. The discrepancies may be related to the type of impactor used and the helmet, headform, and neckform behaviour properties across impact locations. Although the outcomes of these studies differ, they still suggest that injury risk may be elevated at certain impact sites when compared to others (Carlson, 2016).

Subconcussive impacts. Subconcussive impacts are below the concussive threshold but may lead to effects similar to a severe concussion (Bailes et al., 2013). Concussions have been extensively studied, but little is known about subconcussive impacts and their effects (Gysland et al., 2012). Subconcussive impacts should still be taken seriously based on this logic. If all the magnitude of head impacts experienced by hockey players over the course of a season were plotted in a frequency distribution, one would see that a typical player would receive a greater number of small impacts (subconcussive). As the magnitude of the impacts increases, the frequency of high magnitude impacts would decrease. In other words, the distribution of impacts

is positively skewed towards lower magnitude impacts. This rationale is supported by Brainard et al. (2012) who determined that 95% of all impacts were less than 43.7 g for males and less than 44.9 g for females at the collegiate level. Wilcox et al. (2014) also suggested that the majority of impacts tend to be subconcussive; that is, the median peak linear acceleration was found to be 38.5 g in players that positionally played defense compared to 43.4 g in forwards. For female defense players, the median peak linear acceleration was 40.6 g, while for female forwards it was slightly higher at 40.9 g.

Some researchers believe impacts of this magnitude "reflect the lowest level of trauma related to concussion" (Hoshizaki, Post, Kendall, Karton, & Brien, 2013, p. 4). Subconcussive impacts can produce functional and neuropsychological impairment, just like a concussion. Axonal injuries, neuro-inflammation, and blood-brain barrier permeability changes have been observed following such impacts, without producing the symptoms of a concussion (Bailes et al., 2013). The observations regarding the frequency and magnitude of the impacts experienced by hockey players, along with the reported physiological consequences, suggest that subconcussive impacts could be a major concern in contact sports like hockey.

Neck influence. Another variable not often considered is the influence of neck stiffness on concussion and head injuries (Rousseau & Hoshizaki, 2009). Some researchers posit that increased neck strength allows for greater mass recruitment, thereby, lowering head acceleration and resulting in a lower concussion risk (Rowson et al., 2016). Theoretically, an athlete's ability to resist and absorb the impact accelerations can be achieved by increasing the mass and conditioning the head, neck, and trunk to work in unison (Rousseau & Hoshizaki, 2009). There is some support for the hypothesis that neck muscle training can increase an athlete's ability to attenuate forces. Collins et al. (2014) reported that with a one pound (lb) increase in neck

strength, the odds of an athlete receiving a concussion decreased by 5%. Untrained athletes, especially those with weaker necks, may be at increased risk of injury when exposed to the same impact acceleration (Rousseau & Hoshizaki, 2009). In the literature, there are currently mixed results when considering neck stiffness and the reduced incidence of concussions. Collins et al. (2014) found that neck strength was a significant predictor of concussion among high school basketball, soccer, and lacrosse; whereas Schmidt et al. (2014) suggested that football players with increased neck stiffness may be at reduced risk of sustaining higher magnitude impacts. From their findings, however, the researchers could not support the theory that players with stronger and larger neck muscles mitigated head impact severity more efficiently.

Another component of the neck that may influence head impact severity is the preparedness of the player when receiving the impact. Rousseau and Hoshizaki (2009) suggested that athletes unaware of an impending collision were not equipped to resist the shock; therefore, much of the force was transmitted to the player's head. Athletes who anticipated a hit had sufficient time to contract their neck muscles, allowing for some resistance to the impact with the mass of their head, neck, and upper torso. Therefore, if the impacts to players are equal, the smaller impact mass of the unaware player will result in a higher post impact peak acceleration of the head. This idea was supported by Mihalik et al. (2010) who determined that players who anticipated body contact could decrease the severity of the impending head impact, especially on head impacts of moderate severity.

The response of human neck stiffness during simulated head collision has only been investigated using a headform with a mechanical neck attached to it. Researchers believe the neck stiffness characteristics could influence the linear acceleration transferred to the head and brain during a collision (Rousseau & Hoshizaki, 2009). Rousseau and Hoshizaki (2009) were the

first to investigate how head accelerations changed based on neck stiffness during a simulated collision. In their study, neck compliance was defined as "the ability of the neck to resist motion (in this case, bending, torsion, and compression)" (Rousseau & Hoshizaki, 2009, p. 91). Therefore, higher compliance would offer less resistance to the motion and less compliance would mean more resistance of the neck. Three different neck stiffness levels were used; one representing a 50th percentile human neck (median), then one 30% more compliant (soft), and 30% less compliant (stiff) than the 50th percentile neck. The different compliances of neckforms were connected to a surrogate headform, and then struck at different velocities (5, 7, and 9 m/s). At 5 m/s, the headform attached to the different necks experienced a linear acceleration of 78.4 ± 1.8 g (soft), 79.1 ± 3.7 g (median), and 82.0 ± 2.6 g (stiff). When increased to 7 m/s, the headform experienced peak linear accelerations of 137.3 ± 4.6 g (soft), 134.4 ± 9.4 g (median), and 140.0 ± 3.6 g on the (stiff) neck. Finally, at 9 m/s, the peak linear accelerations experienced by the headform were all relatively similar. The headform with the soft neck compliance experienced accelerations of 210.9 ± 4.4 g, while the headform with median neck compliance experienced accelerations of 214.4 ± 4.3g, and finally the headform with the stiff neck compliance experienced accelerations of 230.9 ± 5.1 g. Researchers reported that neck compliance had a significant effect on peak linear acceleration at 5 m/s and 9 m/s but not at 7 m/s. The results of Rousseau and Hoshizaki's (2009) study also showed that a neckform more capable of resisting motion did not reduce the linear acceleration of the headform. These results suggest that a hockey player who had tensed neck muscles before a hit would have higher peak linear accelerations acting on her/his head, meaning an increased likelihood of concussion. Carlson (2016) also incorporated the concept of neck stiffness into his study but manipulated the impact location and angle of impact using a surrogate headform. This study used three neckform

stiffness conditions; 8.4, 12, and 15.6 in-lbs, which were specific to the custom neckform used. The 8.4 in-lbs represented 30% of the values below the 50th percentile, and the 15.6 in-lbs represented 30% of the values above the 50th percentile (Carlson, 2016). When analyzing the peak linear accelerations, the researcher found there were no significant interaction effects among these independent variables together (location, angle, and neck stiffness) on these measures. He also determined that no significant main effects were observed between the different neck stiffness conditions (neck compliances) when using a custom built neckform. The discrepancies between these studies highlight the need for further investigation of the influence of neck stiffness on head accelerations in simulated tests. The influence of neckform stiffness may also become more pronounced when impacted horizontally rather than vertically. Furthermore, there is a need to consider these concepts when designing helmets and developing new helmet testing protocols (Rousseau & Hoshizaki, 2009).

Hockey Helmets and Current Testing Procedures

Hockey did not always have a connection with head and brain injuries. The sport was first played outdoors on frozen lakes and rivers to help pass the long winter months. Equipment was meant to keep players warm rather than to protect against injury. After the second World War, the sport moved to indoor arenas, which reduced the space available, leading to more interaction between the players and the environment. Consequently, the number of serious head injuries in hockey began to increase, which lead to the implementation of various types of protective equipment to reduce the incidence of these injuries (Biasca et al., 2002). Helmets became the chosen method to protect hockey players' heads from falls to the ice or sticks and pucks to the head.

Helmets. A helmet is a device worn on the head with the intent to reduce the risk of head injury (CSA, 2015a). Helmets are designed to decrease the likelihood of head injuries by attenuating energy and distributing the energy load from biomechanical impacts away from the head (Graham et al., 2014). They also protect the wearer from objects such as sticks and pucks from penetrating his/her skull during a collision. Helmets have four primary components: a comfort liner, an impact energy attenuating liner, a restraint system (chin strap, size adjustments), and an outer shell (Graham et al., 2014). All helmets can be differentiated by the number of impacts that they are designed to withstand. For example, helmets meant to protect the wearer in motor sports, bicycling, alpine skiing, and snowboarding are designed to attenuate only a single impact, and then be replaced. Alternatively, helmets designed for ice hockey, football, and lacrosse protect the user from many hits over multiple competitive seasons (Hoshizaki & Brien, 2004).

In ice hockey, helmets are the primary form of head protection and mandatory for players at all levels of play (Kis et al., 2013). Despite the seriousness of head/brain injuries, the head was the last location to be protected by equipment (Hoshizaki & Brien, 2004). The first head protection appeared in Sweden in the mid-1950s. It consisted of squares of leather with thin felt backing for comfort and was worn on the forehead and back of the head (Biasca et al., 2002). Subsequently, helmets began to evolve quickly, and by the early 1970s, the outer shells of the helmets were manufactured using injected polyethylene, polycarbonate, or acrylonitrile butadiene styrene (ABS) plastics, and the energy absorbing liners were made from dye-cut vinyl nitrile (VN) or ethyl vinyl acetate foams (Clement & Jones, 1989). Many of these materials are still used in ice hockey helmets today, but revisions are always being made to improve the helmet designs in terms of weight, ventilation, shape, coverage, and impact attenuation

capabilities (Hoskizaki & Brien, 2004). Current helmets designed by the manufacturers have masses ranging from 0.545 kg to 0.578 kg. The thickness of the front outer shell ranges from 2.5 mm to 2.9 mm, while the foam thickness ranges from 14.1 mm to 19.4 mm in VN helmets and 15.6 mm to 23.6 mm in expanded polypropylene (EPP) helmets (Rousseau, Post, & Hoshizaki, 2009). It also should be noted that most hockey helmet materials fall somewhere between a plastic and elastic response (Ouckama, 2013). A plastic response of a hockey helmet means that there is irreversible damage to the helmet in an impact. That is, the helmet cannot regain its original shapes (Hall, 2007). This response is most pertinent to the outer shell of the helmet, which may not fully restore its shape after many impacts. Alternatively, the foam liner of the helmet exhibits an elastic response, that is, upon contact it deforms, and then is able to regain its original shape (Hall, 2007).

Hockey helmets are mass produced due to high demand and the need to protect the head against injuries. “Consequently, more attention had been paid to the shape and size of helmets to fit an average human head and little consideration has been given to those individuals in the low and high percentiles” (Carlson, 2016, p. 29). This lack of attention can result in an ill-fitting helmet that exposes these players to a higher risk. The inadequacy of mass produced helmets to accommodate all human head sizes properly is a current limitation (Carlson, 2016) and may mitigate the hockey helmet’s ability to diminish linear accelerations (Gimbel & Hoshizaki, 2008; Graham et al., 2014). Even with this limitation, research has shown that helmets are effective at reducing the forces involved in head impacts that lead to skull fractures and traumatic head injury. Opinions are still divided, however, amongst researchers on whether helmets are effective at reducing concussions or not. Some researchers think that by wearing a helmet, athletes may be less susceptible to concussion (Benson, Hamilton, Meeuwisse, McCrory, & Dvorak, 2009) while

others do not. Helmets are designed to reduce the linear acceleration during impact, a variable associated with concussions. Therefore, it is thought that helmets can also reduce rotational acceleration (a principal cause of concussion), resulting in fewer concussions (Halstead et al., 2000; Rowson & Duma, 2011).

Outer shell. This component of the hockey helmet gives the helmet its form and ensures durability and protection using thermoplastics and composites only a few millimetres thick (Graham et al., 2014). Conventional shell materials include thermoplastics (polycarbonate), fibre reinforced plastics, ABS, and high-density polyethylene (Ouckama, 2013). The semi-rigid structure of the outer shell is deformable. This property reduces the acceleration transferred to the head by spreading the impact acceleration throughout the helmet (Di Landro, Sala, & Oliveri, 2002; Higgins, Halstead, Synder-Mackler, & Barlow, 2007). Since the deformation properties also spread the impact energy over a greater surface area, the outer shell of the helmet can reduce the incidence of focal injuries (Rousseau et al., 2009). The outer shells of current helmets consist of a front piece and rear piece (Halstead et al., 2000). The separate pieces allow the helmet to be lengthened to better fit the individual player's head. Halstead et al. (2000) noted that this design was created for better marketability of the helmets, intended to keep costs low, rather than providing a proper fit to a player's head. The geometry of the hockey helmet also plays a significant role in acceleration dissipation (Halstead et al., 2000). Helmet geometry may not be as efficient regarding reducing the impact accelerations due to certain areas of the helmet being flatter than others. The crown area, in particular, is not as effective at distributing energy away from the point of impact as other regions of the helmet (Halstead et al., 2000).

Attenuation lining. The liner is the material inside the outer shell. It ensures a snug and comfortable fit of the helmet to the player (CSA, 2015a). The primary goal of the liner, however,

is to manage the linear acceleration and absorb the kinetic energy generated by an impact to the head (Graham et al., 2014; Gimbel & Hoshizaki, 2008). Attenuation of acceleration is achieved by compression of the liner, which dissipates the energy. That is, less energy is transferred to the player's head. The inner liner does not permanently deform, but rather compresses and returns to its original dimensions (Graham et al., 2014). Liner thickness has implications for helmet manufacturers and consumers, since an increased liner density and thickness would reduce the acceleration acting on the head. Thickening the liner, however, will simultaneously increase the diameter of the helmet, leading to a greater potential for rotational accelerations, decreased aerodynamics, heavier mass, and decreased attractiveness (Di Landro et al., 2002). Current hockey helmets have liners made from either VN or EPP foams (Rousseau et al., 2009) with expanded polyethylene (EPE) and cross-linked polyethylene still being found in some older helmets. Helmets with EPP foams are typically more expensive but are thought to dissipate impacts better than VN foams (Rousseau et al., 2009).

Rousseau et al. (2009) compared the two foam types to determine which one decreased linear and rotational acceleration best. The researchers concluded that the peak linear acceleration was more efficiently reduced by EPP foam than the VN foam. VN proved, however, to be more efficient at reducing rotational acceleration than the EPP foam. Even so, it remains unclear what role the foam linings of helmets play in preventing mTBI and concussions.

Hockey helmet standards. The first types of helmets were implemented to mitigate the incidence of severe head injuries and death in hockey (Rowson et al., 2015). Hockey helmets have certification from four different organizations including the Hockey Equipment Certification Council (HECC), that follows the standards set forth by the American Society for Testing and Material (ASTM), the Canadian Standards Association (CSA), the International

Organization for Standardization (ISO) represented by a CE marking, and finally by the NOCSAE. A list of these standards can be seen below in Table 1.

Table 1

Official standards for ice hockey head protection

Standard
American Standards
ASTM Standard F1045-16 "Standard performance specification for ice hockey helmets"
Canadian Standards
CAN/CSA Standard Z262.1-15 "Ice hockey helmets"
ISO International Standards
ISO 10256-1:2016 "Protective helmets for ice hockey players"
National Operating Committee on Standards for Athletic Equipment
ND030-11m16 "Standard performance specification for newly manufactured ice hockey helmets"

The national standards organizations such as the ones mentioned above use a committee of experts from various professional fields such as health, safety, engineering, and manufacturing (Ouckama, 2013). They provide scientific reasoning to set performance requirements and specification for helmet certification (McIntosh, 2001). Hockey helmets are then designed and manufactured to pass the specific testing protocols set forth by these organizations when measuring their protective abilities (Gimbel & Hoshizaki, 2008). As mentioned previously, helmets are designed to attenuate impact energy and distribute loads over a greater area. Current models have proven effective in reducing the incidence of more traumatic injuries such as skull fractures, by reducing the peak linear acceleration transferred to the head (Kis et al., 2013). Despite helmets reducing TBIs, there is little evidence suggesting that helmets can protect against concussions. This lack of protection may be the result of standards organizations testing methods not significantly changing since their inception; even with the increasing knowledge and awareness surrounding concussion (Gwin, Chu, McAllister, & Greenwald, 2009).

Current hockey helmet testing. The performance of hockey helmets is determined through equipment testing. When a helmet manufacturer requires their helmet to be certified, the helmet is tested to ensure it meets the current criteria set forth by the standard organizations. A primary test in the certification process is the helmet's impact energy attenuation capabilities. This quality is assessed by dropping a helmeted headform at a defined height onto an anvil while measuring the peak linear acceleration of the headform (McIntosh, 2001). The peak linear acceleration is the greatest value on the acceleration-time curve encountered during an impact (CSA, 2015a). The maximum value accepted for peak linear impact acceleration for helmet ranges from 275 to 300 g depending on the organization. Researchers examining skull fractures using human cadavers determined that linear accelerations in this range likely results in fracturing (Gurdjian et al., 1966). The ice hockey helmet standards, ISO 10256, CSA Z262.1, and ASTM F-1045, all require drop test with the maximum headform acceleration criterion of 275 or 300 g. The standards differ primarily by the headform used and the impact conditions. The CSA, ISO, and ASTM utilize magnesium headforms, while the NOCSAE standard uses a biofedelic headform with a glycerin filled cavity (Ouckama, 2013). Another difference to note is that the International and Canadian standards impact helmets via a rigid anvil and headform, while the American standards, uses a deformable anvil. Helmets tested on the deformable anvil tend to produce lower peak accelerations compared to those tested on a rigid anvil with the same energy (McIntosh, 2001). Ouckama (2013) provided an in-depth comparison of the hockey helmet standards testing methods and demonstrated that the peak g value between standards is not a sufficient comparison given the multiple variables of headform size, impact velocity, and drop tower configuration (see Table 2).

Table 2

Current ice hockey standards comparison.

Standard	CSA z262.1-15	ASTM F1045-16	ISO 10256: 2003	NOCSAE ND030-11m16
Headform Type (circumference)	EN960 Half Face (575mm)	F2220/EN960 Half Face (J-570mm)	EN960 Half Face (570mm)	NOCSAE Full Face (570mm)
Headform Mass	4.7kg	4.7kg	4.7kg	4.8kg
Impact Type	Guided Monorail (uniaxial)	Guided Monorail (uniaxial)	Guided Monorail (uniaxial) or Freefall (triaxial)	Guided wire (triaxial)
Impact Velocity	4.5m/s	4.5m/s	3.96m/s	3.46, 4.88, 5.46 m/s (increasing by impact)
Impact Material	MEP60 Shore A	MEP60 Shore A	MEP60 Shore A	MEP
Acceleration Limit	275g	300g	275g	N/A
Severity Index Limit	N/A	N/A	1500	300 (3.46 m/s) 1,200 (4.46-5.46m/s)

Note. Adapted from "Time Series Measurement of Force Distribution in Ice Hockey Helmets During Varying Impact Conditions," by R. A. Ouckama, 2013, Unpublished doctoral dissertation, McGill University, Montreal, Canada. Copyright 2013 by Ryan Andrew Ouckama.

Although the helmet standards issued by the organizations mentioned above have similar performance requirements, the protocols differ between standards. The ASTM protocol utilizes a monorail drop rig system to test helmets mounted on a half face headform. The helmet strikes an impact anvil at a velocity of 4.5 m/s (Gimbel & Hoshizaki, 2008). The linear acceleration experienced by the helmeted headform cannot surpass 300 g for three consecutive trials. If this criterion is met, the helmet can be certified, meaning at an impact of 4.5 m/s the helmet can sufficiently protect the head from a skull fracture.

The standard protocols outlined in CSA Z262.1 also involves the helmet being dropped at an inbound velocity 4.5 m/s. The shock-absorbing capacity testing calls for three impacts at six different impact locations. These sites are the crown, one side, front, front boss, rear boss, and rear. The helmets are not only tested at ambient temperature but decreased and elevated

temperatures as well (CSA, 2015a). Finally, the NOCSAE has also created testing standards to evaluate helmets. Helmets are tested at six different locations including the front, right side, right front boss, right rear boss, rear, and top (NOCSAE, 2017), as depicted in Figure 2.

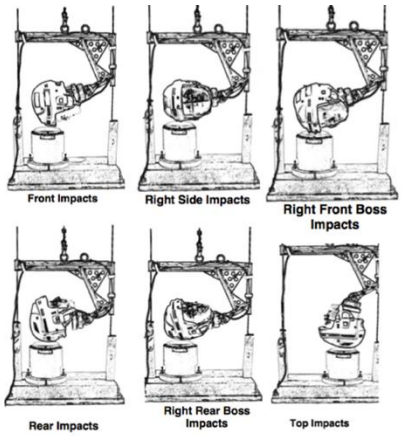

Figure 2. NOCSAE standard impact locations for ice hockey helmets (NOCSAE, 2016a). Adapted from "Standard performance specification for newly manufactured ice hockey helmet (ND 030-11m16) (2016). Overland Park, USA: NOCSAE. Copyright 2016 by the National Operating Committee on Standards for Athletic Equipment.

Each location is impacted at 3.46 m/s, 4.88 m/s, and 5.46 m/s. This organization uses derivative measures of linear acceleration to assess the helmet's ability to protect the head. No impacts should produce a SI greater than 1,200, while 3.46 m/s impact should not see a SI greater than 300 (NOCSAE, 2017). This method of assessment has been proposed to be more suited to "research, development, and the potential prediction of serious injury onset" (Halstead, 2001, p. 324). It is crucial to test helmets by impacting them how players are hit in hockey games as well as on the location of the helmets where they experience these impacts during on-ice use. When testing is completed this way, it increases the ecological validity of the inferences that can be made from the findings of a helmet impact study (Gwin et al., 2010). All of the standards organizations employ the drop testing method. The mechanism of injury that a drop test mimics is unique to a fall. Epidemiological studies have identified falls as a mechanism of injury in

hockey. Throughout the literature, however, the primary mechanism of injury (more specifically for concussion) is collision or body contact (Agel & Harvey, 2010). Impacts from a vertical impactor would simulate a low speed and high mass (body mass) impacts consistent with falls. Alternatively, a higher velocity impact with a lower mass impact would be more compatible with the types of collisions responsible for many concussion injuries in hockey. As a result, the NOCSAE also introduced the Standard Linear Impactor Testing Method and Equipment Used in Evaluating the Performance Characteristics of Protective Headgear and Faceguards document. This document was presented so researchers could more closely emulate on ice impacts believed to be responsible for mTBI (NOCSAE, 2006). The procedures for this testing method follow the specifications outlined in NOCSAE standard performance specifications mentioned above, on the impact velocities, locations, and testing conditions.

The present helmet certification and testing techniques require only a drop or linear impact test (Kis et al., 2013). A new helmet rating system unrelated to any certification organizations, however, was developed by researchers at Virginia Tech. This rating system is named the Hockey Summation of Tests for the Analysis of Risk (STAR) and evaluates the protective capabilities of helmets using differing impacts and a pendulum impactor. The evaluation components of this rating system will be explored further in Equation 1.

$$\text{Hockey STAR} = \sum_{L=1}^{4} \sum_{\theta=1}^{3} E(L, \theta) * R(a,\alpha) \quad (1)$$

where:

L = head impact location site
θ = different impact energy levels
E = number of times per season that a player is expected to experience an impact like testing conditions as a function of location and impact energy
R = the risk of concussion as a function of linear (a) and angular (α) head acceleration

When a certified helmet is rated, the STAR value represents the theoretical incidence of concussion sustained by one player over one season. This rating system is based on whether or not players experienced similar head impacts (number and magnitude) that the Hockey STAR developers used to create their equation (Rowson et al., 2015). The scientific community, however, firmly believes that concussions are under reported. Consequently, researchers decided two STAR values should be presented to consumers to account for the under-reporting rates. The first STAR value represents the frequency of concussion with no underreporting, while the larger second STAR value represents the incidence of concussion with a ten to one under reporting factor included. The overall rating is determined based on thresholds established for the larger STAR value. Regardless of under reporting, a helmet with a lower STAR value is deemed better at decreasing both linear and rotational accelerations transferred to a hockey player's brain in a range of head impact conditions.

Current standards and testing protocols such as those reviewed above have made helmets able to reduce skull fractures from head accelerations in players. Hoshizaki (1995) noted that the attenuation materials used in hockey helmets, however, were not as efficient at decreasing acceleration and energy transfer to player's head in impacts greater or less than the impacts performed during standard testing. This still leaves hockey players at risk for concussions from low and medium energy impacts as hockey helmet standards were only intended to ensure that they managed the high-energy impacts to prevent skull fractures (Gimbel & Hoshizaki, 2008). Research showed that concussions are probable at head accelerations in the 150-200 g range. Thus, the assessment criterion may not drive helmet development for a greater potential reduction in concussions (McIntosh, 2001). Additionally, Halstead et al. (2000) commented on how research has shown that the impact velocity in these standards do not reflect the upper most

impact energies sustained in hockey. These limitations of the impact standards, particularly how they do not reflect the range of impacts scenarios that a hockey player will experience during play (Gimbel & Hoshizaki, 2008), needs to be addressed to see a reduction of concussions in hockey.

Current evaluation techniques. Once an impact has been measured during helmet testing, it is necessary to have threshold values to assess the outcome values and determine the theoretical risk of injury. In the helmet testing field, research tolerance curves and injury indices are means of providing estimations of the range between fatal and non-fatal injury risk based on acceleration and time (Ouckama, 2013). Helmet manufacturers currently employ several quantitative evaluation methods to assess test performance (Caswell & Deivert, 2002). These techniques include tolerance curves such as the Wayne State Tolerance Curve (WSTC) (depicted in Figure 3) and injury indices such as the Head Injury Criterion (HIC) and SI which all stem from the work of Gurdijan (1966). These measures associate linear acceleration with severe brain injury, to quantify the risk of injury (Greenwald, Gwin, Chu, & Crisco, 2008).

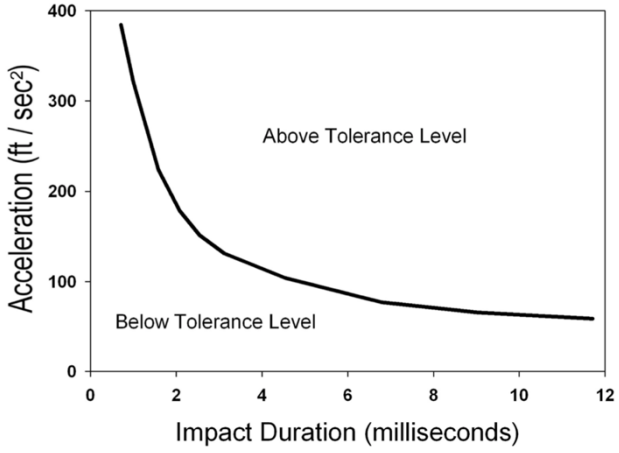

Figure 3. Wayne State Tolerance Curve. The curve shown is based off animal and cadaver data and determines risk for skull fracture during impacts at different peak linear accelerations and time duration. Adapted from "Head impact severity measures for evaluating mild traumatic brain injury risk exposure", R. Greenwald, J. Gwin, J. Chu, and J. Crisco, 2008, *Neurosurgery, 63*(4), p. 789-798. Copyright 2008 by Neurosurgery.

First, the WSTC was developed to understand head injury thresholds during automotive collisions using curves depicting linear acceleration over time (Greenwald et al., 2008). Head impact data from animals and human cadavers were used to create the tolerance curve. The likelihood of skull fracture was determined based on the magnitude of peak linear acceleration and the impact duration for any given impact period (Greenwald et al., 2008) as shown in Figure 3. Regarding intracranial pressure, this model confirmed that subjects could withstand higher accelerations, if the duration of the exposure was short. This model was then refined, with the assumption that impacts that caused a linear skull fracture also caused a moderate to severe concussion (Namjoshi et al., 2013). The WSTC's ability to determine the onset of skull fracture and concussions has led to expansions and development of other measures like the SI and HIC.

The NOCSAE and the ASTM protocols utilized the SI measure in their helmet standards, as displayed in Equation 2.

$$SI = \int_{t_0}^{t_1} A^{2.5}\, dt \qquad (2)$$

where:

A = instantaneous resultant acceleration of the headform
t_1 = impulse duration
dt = time increment

This is a measure of the instantaneous acceleration experienced by the headform in an impact, to assess the risk of injury. The logic underlying this measure is that the area under the acceleration/time curve could form the basis of an index (Ouckama, 2013). This logic means that the associated risk for certain impulse values would be the same if the impact had short duration and high acceleration characteristics, or alternatively, long duration and low acceleration

characteristics. This shortcoming is corrected for, since it is known that lower duration impacts have a decreased risk of head injury when exposed to higher acceleration. Therefore, a weighting factor of 2.5 is applied to the acceleration value (Ouckama, 2013).

A calculated SI measure cannot exceed the acceptable levels for any given impact (NOCSAE, 2016a). According to NOCSAE Test Requirements 10.1 and 10.2 in the Standard Performance Specifications for Newly Manufactured Hockey Helmets (2016a) document, "the peak SI of any impact shall not exceed 1,200 SI" (p. 5). Furthermore, impacts to any helmet location at 3.46 m/s cannot exceed 300 SI. This index is not perfect but it "can provide useful correlations to previous injuries" (Ouckama, 2013, p. 27).

The HIC, as shown in Equation 3, is a valid and accepted metric for predicting skull fracture and cerebral contusions from the linear accelerations placed on the head and brain (Kimpara & Iwamoto, 2012). This metric attempted to account for the long duration and low acceleration impact, by integrating the acceleration-time curve only over the time interval that yielded the maximum value of HIC (Ouckama, 2013). Similar issues could arise in moderate acceleration and long duration impacts, so the HIC applies a cut-off time of 36 ms.

$$\mathrm{HIC} = \left\{ (t_2 - t_1) \left[\frac{1}{t_2 - t_1} \int_{t_1}^{t_2} a(t)\,dt \right]^{2.5} \right\}_{\max} \tag{3}$$

where:

a = linear acceleration
$t_2 - t_1 \leq 36$ ms
$t_2 - t_1$ = time interval where peak acceleration occurs

Time in the formula is measured in seconds. The 2.5 weighting factor was determined by Lissner, Lebow, and Evans in 1960 as the slope of the WSTC. The threshold value for injury is

HIC = 1000 which represents approximately an 18% chance of life-threatening injury, or a 50% chance of a severe head injury (Hutchinson, Kaiser, & Lankarani, 1998).

By determining the integral of acceleration, as both the HIC and SI attempt to do, it provides researchers with an estimate of a helmet's protective ability. Other measures such as energy dissipation, energy loading, and energy unloading of a helmet may be better able to assess the injury risk during a head impact (Carlson, 2016). Furthermore, Carlson (2016) stated that "current testing methods focusing on peak linear acceleration should be improved by including other measures such as energy to provide better guidelines for helmet designers and, therefore, possibly reduce the occurrence of injuries" (p. 37).

Energy Loading Measures During Impact

Static energy loading. Static loading testing allows researchers to determine the mechanical properties of materials. Stiffness is one such material property, and is described as the amount of force needed to cause a certain amount of deformation to a material (Baumgart, 2000). When the applied forces cause deformation of the material, it means that the geometrical configuration of the structure has changed from the original unloaded structure (Baumgart, 2000). Mathematically stiffness can be represented by Equation 4, were it is the quotient of the applied load over the deformation.

$$\text{Stiffness} = \frac{\text{Load}}{\text{Deformation}} \tag{4}$$

To date only one study examined the stiffness properties of ice hockey helmets. Zerpa et al. (2016) conducted stiffness testing on helmets at the rear and side location. They concluded that a helmet being more flexible would be advantageous, as it corresponded to decreased peak linear acceleration at those locations in dynamic impact tests. Helmets fitted with facial shielding

have yet to have their stiffness properties assessed, and how they alter the mechanical properties of the helmet.

Dynamic energy loading. Current helmet testing standards do not include analysis or protocols focusing on the energy loaded onto the head. During an impact to a hockey helmet, the energy loaded onto it is absorbed primarily through the attenuation foam layer (Cui, Kiernan, & Gilchrist, 2009). This absorption of energy more correctly described as dissipation, is the conversion of mechanical energy into another form of energy, such as heat (Zerpa et al., 2016). This definition is in accordance with the first law of thermodynamics. That is, the law of conservation, in which energy is conserved over time and can neither be created nor destroyed (Zumdahl & Zumdahl, 2010). Therefore, the energy dissipated by a helmet does not remain in the helmet but is altered to another form of energy such as heat.

As seen below in Figure 4, any energy absorbing material has a characteristic loading and unloading curve.

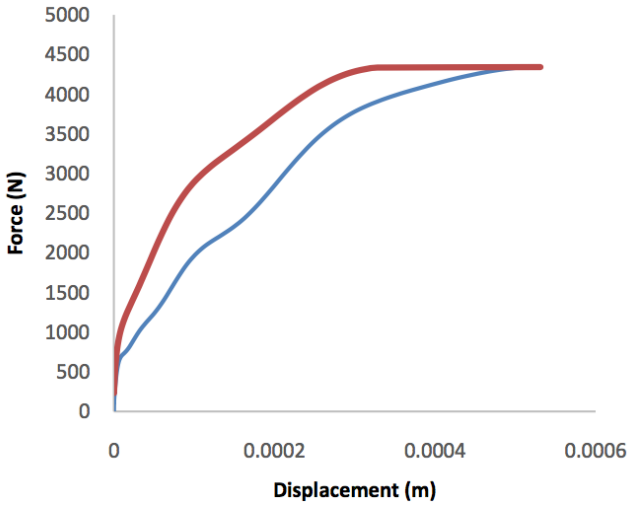

Figure 4. Characteristic loading and unloading curve for a helmet impact. The red line represents the loading, the blue line represents the unloading of the helmet, while the area in between represents the total energy dissipated by the helmet. Adapted from "Energy Dissipation Measures on a Hockey Helmet across Impact Locations", C. Zerpa, S. Carlson, S. Elyasi, E. Przysucha, & T. Hoshizaki, 2016, *Journal of Safety Engineering*, *5*(2), p. 28.

The figure also illustrates the energy dissipated by the foam upon impact as the area between the loading and unloading curves (Zerpa et al., 2016). Ideally, the helmet's "foam would be loaded with the entirety of the incoming impact energy, and all this energy would dissipate out of the system during the unloading phase. This concept would suggest that all incoming energy generated during an impact would be absorbed and directed away from the head and brain" (Zerpa et al., 2016, p. 28). Helmets, however, are not currently able to do this.

A helmet's ability to dissipate energy can be represented by a force versus displacement loading curve or the work being applied to the helmet (Carlson, 2016). Work is equated with the change in kinetic energy of the impact system to simplify the relationship. This then allows the researcher to determine the kinetic energy (KE) transferred to the helmet or energy loading in a helmet impact using Equation 5 (Carlson, 2016).

$$KE = \frac{1}{2}mv^2 \tag{5}$$

where:

m = mass of system
v = velocity

Figure 4 displays the energy loading portion of the impact using a red line. The blue line in the illustration signifies the energy unloading characteristic of an impact. After the loading phase, some energy returns from the impactor to the helmet, which the researcher can also calculate using Equation 5 (Carlson, 2016). The final feature of this figure, of interest to the researcher, is the area between the two curves. This is energy dissipated during a helmet impact. Mathematically, it is the initial input energy loaded onto the helmet subtracted from the energy returning from the helmet to the impactor and is represented by Equation 6 (Carlson, 2016).

$$E_{dissipated} = E_{loading} - E_{unloading} \tag{6}$$

Next, the ability of the helmet to absorb energy (E_{ab}) loaded on the helmet can be calculated using Equation 7. Mathematically this is represented by the quotient of energy dissipated by the helmet from an impact compared to the energy initially inputted into the system (Carlson, 2016).

$$E_{ab} = \frac{\text{Energy}_{\text{dissipated}}}{\text{Energy}_{\text{input}}} \times 100\% \quad (7)$$

The degree to which energy absorption properties of an attenuation liner perform will have direct implications for the amount of energy loaded directly to the head from an impact. Liners that have greater energy dampening abilities will produce a lower rebound velocity and minimize further risk of secondary impact mechanism and countercoup injuries (Barth, Freeman, Broshek, & Varney, 2001; Monthatipkul et al., 2012).

Researchers examined how the energy dissipation characteristics of protective equipment can potentially reduce injury when exposed to an impact. Energy dissipation analysis has been used to investigate the protective potentials of bicycle face protection (Monthatipku et al., 2012), soccer headgear (Marsh, McPherson, & Zerpa, 2008), and most recently hockey helmet performance (Carlson, 2016; Zerpa et al., 2016).

Zerpa et al. (2016) measured energy absorption during impacts of hockey helmets and paired these measures to the traditional linear acceleration tests. Hockey helmets were impacted according to NOCSAE protocols using a drop rig. Accelerometers in the headform measured the acceleration upon impact. The impact force could then be calculated using the known impactor mass and acceleration. Force versus displacement curves for each impact could then be created, like the one depicted in Figure 4, providing insight on the loading and unloading of the attenuation foam during impacts. Researchers reported that these hockey helmets dissipated 10.47 to 22.01% of the energy loaded into the helmet. The percent dissipation varied depending on the impact location. For instance, the side location provided the greatest energy dissipation,

while the front boss location performed poorest in terms of energy dissipation. The energy analysis conducted in this study also supported the findings obtained via traditional measures of peak linear acceleration. Researchers reported that the front boss site did not dissipate as much energy as the other impact sites (Zerpa et al., 2016). Additionally, the peak linear accelerations corresponded with the energy analysis, with the front boss location allowing the most acceleration to pass to the head (Zerpa et al., 2016). Furthermore, Zerpa and colleagues also found that the loading energy was more efficiently dissipated at the side location, which related to lower peak linear acceleration when compared to the other impact areas. Furthermore, this study concluded that helmets with greater energy dissipation properties minimized the likelihood of brain injury (Barth et al., 2001).

Most studies that conducted energy dissipation analyses have not attempted to measure the energy dissipation in sports-specific simulations. Energy studies have often overlooked the influence that the neck has on energy dissipation in an impact. Carlson (2016) included neck stiffness as an independent variable and examined helmet energy dissipation measures using a drop test. He found that there was no significant difference in the amount of energy loaded onto the head and neckform when the neck stiffness was manipulated. Theoretically, the energy loading onto the helmet should be reduced with increased neck stiffness as this would decrease impact forces, leading to greater energy dispersion (Cantu, 1992). Therefore, future research is needed to determine whether or not neck stiffness can influence energy transferred to a player's head in simulated helmet impacts.

Examining energy loading and dissipation may allow for more accurate assessments of impact severity and the total amount of energy transferred to a player in a collision (Carlson, 2016). Carlson (2016) also examined this relationship by comparing the energy loaded onto a

helmet to SI measures. The analysis revealed a moderate correlation, suggesting higher energy loadings are associated with higher SI measures. By examining the energy loaded onto the system, the impact severity can be determined using the entire impact as opposed to traditional measuring techniques, which rely on a single peak linear acceleration value. These findings are promising since an energy loading analysis method may offer a new avenue to assess hockey helmets impact, better than the current pass and fail criteria, and provide a better understanding of how helmet materials perform when trying to minimize head trauma (Carlson, 2016).

The present use of measures of linear acceleration for helmet testing is recognized to be a useful prediction tool for risk related to skull fractures and other severe head traumas. This avenue of testing remains, however, a poor predictor of risk related to mTBI (Post et al., 2011). Using an energy analysis to study helmet performance would be advantageous compared to current evaluations because it allows the determination of dynamic responses of the helmet's material properties in dissipating energy across impact locations (Zerpa et al., 2016). Specifically, "this approach accounts for the force generated during an impact and the deflection of the helmet material to withstand this force at each location" (Zerpa et al., 2016, p. 34). This information will be useful for understanding the injury mechanism (Namjoshi et al., 2013) and the behaviour of the helmet material, as an avenue to possibly improve the protective ability of the helmet (Zerpa et al., 2016).

Currently, no literature exists examining if and how full facial shields affect energy loading and dissipation in hockey helmets. Furthermore, all studies conducted their energy analyses using drop rigs. Using a horizontal impactor will allow for post impact kinetics and kinematics of the head and neck to occur. The influence of these two variables needs to be examined further to build upon the existing literature in this area.

Facials Shields Relationship to Injury and Concussions

Face shields. A face shield in ice hockey is described as a protective device made of impact-resistant plastic or metal that is attached to a player's helmet designed to reduce the risk of injury to his/her face (Graham et al., 2014). The first face protectors were developed in 1972 as a method of ensuring adequate eye protection for hockey players (Biasca et al., 2002). These offered inadequate protection since hockey stick blades could still penetrate them. Therefore, the CSA technical committee was charged with investigating standards for ice hockey visors and face protectors. It was not long after, that both American and Canadian hockey players were required to wear a certified face shield attached to a certified helmet (Biasca et al., 2002).

Currently, there are two primary categories of facial protection including full-face shields and half-face shields (or visors) as illustrated in Figure 5.

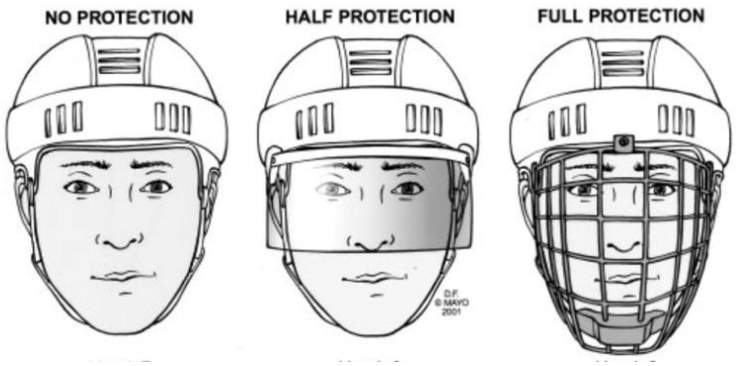

Figure 5. Different types of facial protection. Depending on the level of play and age level players can wear no facial protection, half protection, or full protection. Adapted from "A Comparison of Facial Protection and the Incidence of Head, Neck, and Facial Injuries in Junior A Hockey Players. A Function of Individual Playing Time," by M. J. Stuart, A. M. Smith, S. A. Malo-Ortiguera, T. L. Fischer, & D. R. Larson, 2002, *American Journal of Sports Medicine*, *30*(1), p. 42. Copyright 2002 by the American Journal of Sports Medicine.

The protection offered by each is self-evident; full-facial shields cover the entire face, whereas, half-face shields only cover the upper portion of the face. Half-face shields are constructed out of high impact polycarbonate. They come in several different sizes, profiles, and differ in terms of

how they attach to the helmet. Full-face shields can also be constructed of high impact polycarbonate plastics. This material is chosen for both types of face shields because of its inherent ability to withstand significant forces (Kaplan, Driscoll, & Singer, 2000). More commonly used full facial shields are often referred to as cages. These types of facial shields cover the entire face and are constructed of titanium or stainless steel.

Full-face shields are mounted to the brim on the front of the helmet in the mid sagittal plane. Screws hold the cage in place here and act as the pivot point and allow the facial protection to be moved away from the face so that the player can remove his/her helmet. A chin cup is another important aspect of facial protection. The chin cup is made of energy absorbing foams and can help attenuate impacts directed to the facial shield. This feature is attached to the bottom of the cage and is positioned against the chin. It was designed to keep the helmet in place during an impact, as well as reduce the forces transmitted from the player's mandible to the brain (Lemair, 2007). Two snap clips on webbing straps are secured to grommets on the rear of the helmet to keep the chin cup in place during play and prevent the cage from swinging open. Finally, to prevent lateral and superior displacement J-clips are attached to the helmet just in front of the ear pieces. Figure 6 shows where each of these features is located on a helmet with a full facial shield.

1 – Chin cup
2 – Webbing straps with snap clips
3 – J-clip
4 – Screws and hinges
5 – Stainless steel cage

Figure 6. Components of full facial protection for an ice hockey cage. The various components keep the cage in contact with the player's chin, as well as prevent the cage from displacing laterally and superiorly. Adapted from "CCM Resistance 110 Ice Hockey Helmet Combo," by Dick's Sporting Goods, 2017. Copyright 2017 by Dick's Sporting Goods.

Facial shield standards. The current standards (ASTM, CSA, ISO, and NOCSAE) for facial protection specify the performance requirements and test methods deemed appropriate for face protectors. The main areas focused on in these standards documents are construction, puck impact resistance, penetration, and field of view. For example, the puck impact tests subject's facial protection to pucks being projected at the mask or visor at speeds ranging from 15-36 m/s. When the puck hits the mask, it may contact the headform. Contact is indicated by pressure sensitive gels. A puck has a mass of approximately 170 g and when propelled at 36 m/s has considerable momentum, which would translate into significant force and acceleration to the head and brain. There is no mention of the influence that facial protection may have on mitigating forces during head impacts for direct blows to the facial shields or to other areas of the helmet when a facial shield is attached to the helmet. This is a gap in the current standards and certification procedures that should be addressed since there is some evidence that facial shields can protect players from concussions.

Facial shields and concussion. Facial protection has been found to reduce the incidence of ocular, facial, and dental injuries by 70% (Asplund, Bettcher, & Borchers, 2009; Stuart et al., 2002). In addition, economic studies have shown that if every hockey player received facial shielding for free, the cost would be less than the medical expenses from injuries that could have been prevented by wearing a facial shield (Cook, Cusimano, Tator, & Chipman, 2003). Some researchers, however, still believed that additional mass added by facial shielding to player's head, would leave the player susceptible to cervical spine trauma (Lemair, 2007). Smith, Bishop, and Wells (1985) tested this hypothesis using a Hybrid III head and neck and found that addition of the facial protection increased the angular displacement. This however, did not result in a significant increase in the angular acceleration of the head. Therefore, the researchers concluded that the addition of a facial shield, did not increase the risk of a player sustaining trauma to the cervical spine.

From a practical perspective, it is thought by many that players that cages "obstruct the field of view which impedes play" (Lemair, 2007, p. 26), while polycarbonate shields tend to fog up which also alters the player's ability to see (Lemair, 2007). Moreover, hockey analysists also think that full facial shields will never be adopted in professional leagues for several different reasons. Bob McKenzie of The Sports Network (TSN), said in a podcast, that from a business prospective they will reduce the marketability of the players. He stated that "the game is not the same when you cannot see the player's faces" as "it takes away their personality". Furthermore, McKenzie also stated that he thinks players will not want to wear this additional protection as it with make others perceive them as weak and could subject them to ridicule.

More recently, it has been suggested that facial protection may also play a role in reducing the number and severity of brain injuries by aiding helmets in decreasing head

acceleration after an impact (Lemair & Pearsall, 2007). Benson et al. (2009) reviewed four clinical studies and one biomechanical study concerning the use and non-use of face shields in ice hockey. The first clinical study by Benson et al. (1999) was a large prospective cohort study investigating the risk of injury among 642 Canadian intercollegiate ice hockey players wearing full versus half face shields (visors). This study revealed that the risk of sustaining a concussion was not significantly different between the two cohorts. Benson et al. (2002) then conducted a multivariate analysis using the same group's data and revealed that players who wore visors missed more practices and games per concussion than those who wore full facial protectors. Another study by Stuart et al. (2002), assessed the concussion rates of Junior A hockey players wearing different types of facial protection (full, visor, and none). No significant differences in concussion rates were found between the three cohorts. The final clinical study found no statistically significant differences in concussion rates between NHL players who wore visors and those who did not (Stevens et al., 2006). The players who wore visors, however, did not miss as many games as the players who did not wear facial protection.

Currently, there is no substantial scientific evidence from clinical studies to suggest an association between face shield use and a reduced concussion risk (Benson et al., 2009). There is scientific evidence; however, that supports the use of ice hockey full facial shields in protecting athletes from more severe concussions, as measured by time lost from competition (Benson et al., 2009). Benson et al. (2009) concluded by stating that "future research should focus on sport-specific, analytical studies of sufficient power to determine the true relative risk of concussion associated with specific types of protective equipment use" (p. 66).

Clinical research studies offer valuable information on the protective abilities of face shields in a game or practice setting. Research conducted in game and practice settings, however,

have confounding variables that the researcher cannot control. Alternatively, biomechanical studies use laboratory research to exert control over such variables to focus on relationships free from nuisance variables. For instance, in a theoretical study examining the number of concussions received by players with and without facial protection, there are many variables such as the magnitude of the impact, neck stiffness, where the player is struck, and how many impacts each group receives, that could influence the number of concussion each group receives thereby affecting the findings of the study. All of these confounding variables, however, can be accounted for in a laboratory research setting.

Currently, in the literature, there is only one laboratory study examining how visors and full facial protection affected the peak acceleration in a helmeted headform. Lemair and Pearsall (2007) compared three different types of visors and three different facial cages on two different types of helmets (VN and EPP). The researchers found that the use of cages and visors substantially and significantly reduced the peak acceleration. The reduction can be demonstrated by the fact that impacts on an uncovered headform ranged from 380 to 420 g. When the surrogate head was fitted with a helmet, the peak acceleration was reduced by up to 100 to 130 g. Finally, the attachment of the face protectors reduced the peak acceleration in a range of 10 to 100 g. The researchers also concluded that facial protection decreased the peak acceleration from facially directed impacts which may, in turn, decrease the severity or incidence of head injuries.

Lemair and Pearsall (2007) provided valuable information that facial protection can theoretically aid in the reduction of concussions. Even with these promising results, there are areas in the methodologies that can be improved in future research. The researchers of this study utilized a vertical drop impactor to impact the headform. As previously mentioned, this type of impactor would simulate a falling mechanism of injury but the majority of concussions occurring

in hockey are attributed to collisions or body-to-head impacts (Hutchison, 2011). Therefore, these types of impacts could be better represented by using a horizontal impactor. Gwin et al. (2010) stated that it is crucial to test helmets as they are used in sport. Better testing means subjecting helmets to impacts and simulating them using the primary mechanism of injury and in the same locations as the players get hit when they are in a game or practice situation. Consequently, this approach increases the ecological validity of the inferences that can be made from the findings of a helmet impact study.

Chapter 3 - Method

Purpose

This study had three purposes. The first purpose was to assess the durability of the helmet when exposed to multiple impacts during helmet testing protocols. The second purpose was to test the helmets in a static setting to investigate the effect of facial shielding and helmet location on measures of helmet stiffness. The third purpose was to examine the effect of impact location, type of facial protection, and neckform stiffness on peak linear acceleration, severity index (SI), and energy loading properties of the hockey helmet during dynamic simulated horizontal impacts.

Instruments

Pneumatic linear impactor. This impactor was designed under collaboration between the Lakehead University School of Kinesiology and Mechanical Engineering Department. This impactor consists of a main frame, an impacting rod, and headform assembly as depicted in Figure 7. The main frame of the impactor consists of a welded steel frame, which is secured to the floor. The main frame also houses a compressed air tank and the impacting rod. The impactor is designed to propel the impact rod between 0 – 7 m/s from the pressure released from a 3-gallon compressed air tank. The pressure can be manipulated using a MGA-100-A digital pressure gauge from Sintered Specialties Inc. (SSI) with an accuracy of ± 1% full scale. The impact rod, has a mass of 13.1 kg, and is propelled horizontally by compressed air. The tip of the impact arm has a cap consisting of a 7.4 cm (diameter) by 2.7 cm (thick) cylindrical nylon pad covering a 7.4 cm long metal disc.

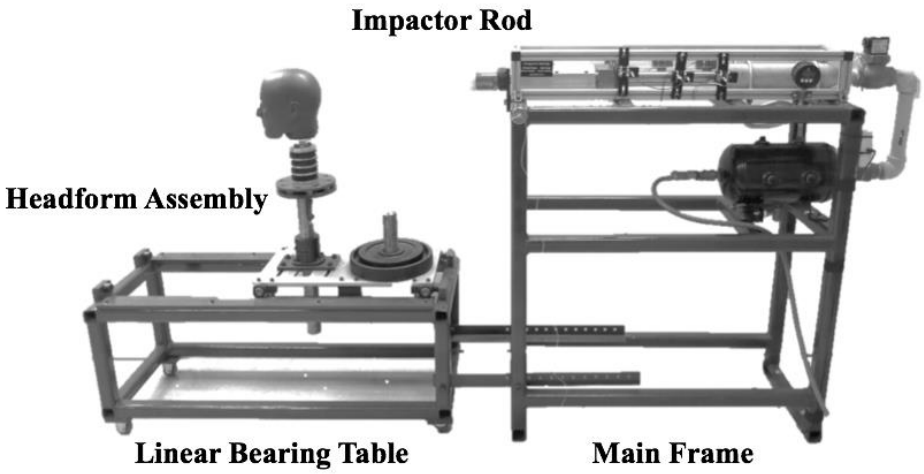

Figure 7. Pneumatic linear impactor. This figure displays the various components that comprise the impactor.

Another component of the impactor is the headform assembly which enables the plate to move backward 0.49 m on rollers after an impact and then it is stopped by rubber bumper blocks. The shuttle plate allows the operator to load plate weights onto it to simulate the inertia of a person's body mass subjected to an impact. For the purpose of this study, the same mass of 16.3 kg was used for all impact trials. The headform assembly attachment plate is designed to allow for the head to be positioned with precision. Headform positioning adjustments can be made in five degrees of freedom, forward and backward (x), laterally (y), up and down (z), tilting forward and backwards, and laterally rotating. Once adjustments are made, the headform assembly is secured and remains fixed throughout the procedures. The shuttle table has a mass of 46.6 kg and when the NOCSAE headform is attached, the total mass of the system increases to 56.1 kg.

Evidence of reliability and concurrent-related validity for the linear impact acceleration measures of Lakehead University's horizontal head impacting system were determined through a pilot study (Jeffries, Zerpa, Przysucha, Sanzo, & Carlson, 2017). Concurrent validity is the degree to which instrument measurements are correlated with another appropriate instrument measure or standard as the primary test of interest (Furr & Bacharach, 2008). The horizontal

impactor used in this study, was compared to the Lakehead University impact drop system previously validated by (Carlson et al., 2016) to provide concurrent–related evidence of validity for the use of the horizontal impactor in the current research. The results indicated strong intraclass correlation (ICC) between both systems; ICC = .949, $p < .001$ for front impacts; ICC = .852, $p < .001$, for side impacts; and finally, an ICC = .876, $p < .001$ for rear impacts.

Reliability, more specifically in this case the stability, refers to the consistency of a test or measurement across repeated trials (Charkrabratty, 2013). To provide evidence of reliability for the use of the horizontal impactor in the current study, 100 identical impacts were administered to the helmeted headform at 4.39 m/s at the front, side, and rear impact locations. Strong evidence of reliability was found across replications of the protocol with correlation values between the system measures of ICC = .875, $p < .001$; ICC = .787, $p < .001$; and ICC = .809, $p < .001$ when using the split-half technique (Jeffries et al., 2017). This technique assesses the consistency of the measures via comparison of even and odd number impacts. The ICC results obtained from the pilot study provided satisfactory evidence of consistency of the horizontal impact and the acceleration measures across identical trials.

Instron 1000 mechanical device. A modified Instron device was used to study static material properties of helmets with and without facial shield by compressing the front, rear, and side locations. The hardware of this device was upgraded by connecting the instrument to a data acquisition board from National Instruments and interfaced to the Labview software as a means of measuring compressive and tensile forces as well as material deflection. This instrument is featured in Figure 8.

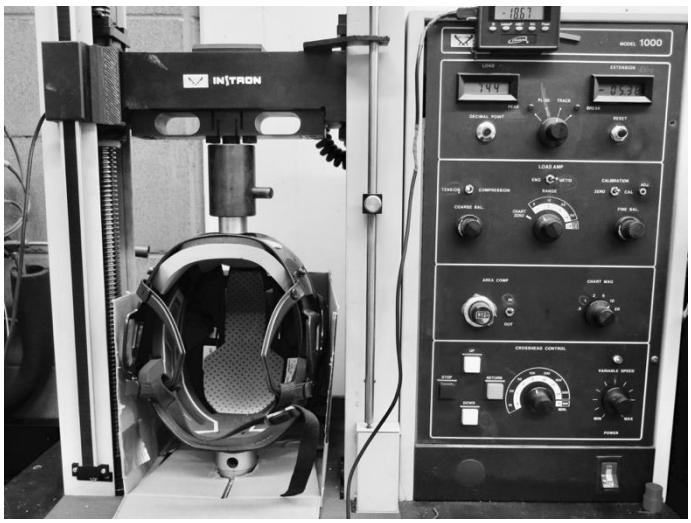

Figure 8. Instron 1000 Mechanical Device. This instrument was used to assess the stiffness properties of the helmet by compressing the helmet between the two cylinders.

Headform. A NOCSAE headform, as depicted in Figure 9, was used for all impact trials. This medium sized headform has been used in many published research studies to simulate the dynamic response of impacts when measuring both linear and rotational accelerations (Carlson, 2016; Rowson et al., 2015; Rowson & Duma, 2011; Zerpa et al., 2016). Designed by Hodgson (1975), the biofidelic headform with a glycerin filled cavity simulates the dynamic responses that a human head experiences during impact (McAllister, 2013; Ouckama, 2013). The headform has a mass of 4.90 kg and is representative of a 50th percentile adult human head. This headform is also considered to be anatomically representative due to the inclusion of appropriate facial features and bone structure (McAllister, 2013). It is important to have an anatomically representative headform when conducting helmet testing as stated by Hodgson (cited in Ouckama, 2013, p. 33) "unless the surrogate head has the same weight, mass distribution and deformation qualities as a human head, one cannot relate the data directly to human tolerance."

Another feature of the NOCSAE headform is an array of accelerometers to quantify the acceleration felt at impact in the anterior-posterior, superior-inferior, and the left-right directions (Zerpa et al., 2016). Traditionally, NOCSAE headforms are designed to be mounted on a rigid

arm rather than on a surrogate neck and, therefore, cannot be used to examine the influence of neck strength and anisotropic bending of the neck on head acceleration (McAllister, 2013). The headform used in this study, however, was modified so that it could be mounted on a custom mechanical neckform.

Figure 9. NOCSAE headform fitted with an ice hockey helmet.

Mechanical neckform. The neckform depicted in Figure 10, was also designed by the Lakehead University Faculty of Engineering. It was designed to mimic a 50th percentile human neck. The neckform consisted of four neoprene rubber discs fitted between circular steel discs with end plates at the top and bottom. To prevent displacement of the steel and rubber discs, the rubber discs protrude past the metal ones slightly allowing for the metal and rubber discs to be compressed tightly together. A top plate and base bracket hold the components of the neck together. This neckform can simulate inertial effects experienced by the neck during loading since it was designed with two characteristics of the human neck in mind. The first feature included a hole through the centre of the discs. The second feature included are large cut-outs in each of the rubber discs on the back of the neck as depicted in Figure 9. These two design

elements try to mimic the vertebral and cervical spine muscle's loading response that a human neck would experience during the impact.

Figure 10. Mechanical neckform. This custom neckform can be attached to a NOCSAE headform and together simulate the dynamic response human experience upon impact.

To keep the components firmly pressed together, a wire cable ran longitudinally through the centre of the neckform, shown in Figure 11. "The cable is constructed of galvanized stainless steel, ultra-flexible 7 x 19 strand right lay rope with a machined end-shank made from 303 stainless steel welded to the top of the wire and press-fit into the top plate of the neckform" (Carlson, 2016, p. 48). This feature also allows the stiffness of the neckform to be adjusted. Tightening a nut at the base of the neck, allows the researcher to manipulate the degree to which the neck rotates and flexes during impacts. The neck and headform are secured to a circular steel plate with four bolts that thread into the base bracket. Eight holes around the edge of the plate allow the bolts to mount the headform assembly on the linear bearing table on the horizontal impactor.

Figure 11. Wire-rope cable. This is a depiction of the wire-rope cable that runs longitudinally through the centre of the neckform.

The neckform stiffness levels, used in this study were determined by Carlson (2016). He accomplished this by tightening the neck to different torque values, then conducted flexion loading tests to examine the stiffness of the headform for flexion, extension, and lateral flexion. Carlson took the force and neck length through a range of motion to create moment-angle of flexion curves fit to a regression model.

Accelerometers, power supply, and software interface. Similar to Carlson (2016), piezoelectric sensors were fastened inside the surrogate headform and were used to measure the magnitude of the impact. The sensors were interfaced to a PCB model 482A04 integrated circuit piezoelectric sensor (ICP) amplifier/power supply unit. The analog output signals from the accelerometers were amplified and converted to digital signals via an analog to digital converter from AD Instruments PowerLab26T. For this study, acceleration measures were collected in the x, y, and z axes at a sampling frequency of 20 kHz and converted to units of gravity expressed as g. To obtain this conversion, each channel output in the x, y, and z direction was divided by 0.01041 in an arithmetic function as depicted in Equation 8 using the Power Lab Chart version 7.3.1 software.

$$g = Ch/0.01041 \tag{8}$$

These three channels were then combined using Equation 9 to compute a resultant acceleration to represent the total magnitude of the impact. A low-pass filter with a cut-off frequency of 1000 Hz was also applied to the resultant acceleration data to eliminate high frequency noise generated due to vibrations induced to the headform during the impacts.

$$\text{Resultant Acceleration} = \sqrt{a_x^2 + a_y^2 + a_z^2} \tag{9}$$

where:

a_x = linear acceleration in the x-direction
a_y = linear acceleration in the y-direction

a_z = linear acceleration in the z-direction

Helmets. Five medium sized identical helmets with VN attenuation liners were used for the impact testing. The number of helmets needed for this study was determined using a similar approach to Carlson's (2016) study. The helmets were medium sized (54 to 59 cm head circumference) and contained a dual density VN liner along with a lightweight ventilated outer shell and were certified by CSA, HECC, and ISO standards. The helmet also features a tool-free adjustment system located on both sides of the helmet. The helmets were adjusted to their fourth largest size, using the adjustment system (best fitted on this headform) before each impact as per helmet fitting instructions defined by NOCSAE standards.

Facial shielding. In addition to the headform being fitted with helmets, some of the helmets were also outfitted with facial shielding. Two different types of facial protectors were used in this study. The first type was a metal facial shield; which was constructed out of thin and strong stainless steel. The second type was a full-face shield made of high impact polycarbonate. Both types of facial shields were mounted to the brim of the helmet in the mid sagittal plane. Two screws held the cage in place and acted as the pivot point and allowed the helmet to be taken on and off the headform. The free-floating, dual-density chin cup that is attached to the bottom of the cage was positioned against the chin as specified by the manufacturer. J-clips were also attached to the helmet just anterior to the earpieces to prevent the cage from displacing laterally and superiorly. Finally, to prevent the facial shields from opening, two snap clips on webbing straps were secured to grommets on the rear of the helmet.

Procedures

Before the static and dynamic responses of the helmets were tested, one helmet was subjected to a durability test to determine if the helmet's attenuation properties were

compromised due to the large number of impacts per location. Similar to the protocol implemented by Carlson (2016), a helmet was impacted in the front and rear locations to measure deterioration over the proposed number of impacts per helmet impact location. A pneumatic repetitive impactor with a Biokinetics magnesium half headform was fitted with the helmet. It was secured using the chin restraint on the helmet and additional cord to prevent any helmet movement during impacts. The helmet contacted an AMTI force platform in a blunt collision at a velocity of 1.04 m/s. The force platform measured the horizontal force of each impact. A total of 200 impacts were administered to the helmet at the front and rear impact sites. Figure 12 illustrates how the helmet was positioned when striking the force platform. The peak force data was taken once the impactor had stabilized.

Rear testing site **Front testing site**

Figure 12. Rear and front helmet durability testing sites.

Next, the stiffness properties of a helmet were tested at Lakehead University's Thunder Bay campus in an engineering laboratory. A technologically updated Instron 1000 device was used to assess the stiffness properties of the helmet at the front, rear, and side locations as seen in Figure 13. This procedure was conducted first at each location with just the helmet and then repeated subsequently with the metal facial shield and high impact polycarbonate facial shield. Force was applied by the Instron at each location using a 31.67 cm^2 cylinder with a diameter of

31.75 mm. Before data was collected, calibration curves were created for both force and displacement data, using known loads and displacements. During helmet testing the force and deflection data were sent to the computer via a custom Labview script and finally exported to Microsoft Excel software. The data for each testing condition were then adjusted to accurately reflect the force and deformation before analysis.

Side testing site **Front testing site** **Rear testing site**

Figure 13. Static stiffness testing sites. The helmet was positioned under the compression cylinder on the Instron 100 at these three locations.

All data collected for the final portion of the procedure was collected at the Thunder Bay Lakehead University campus in the Multipurpose Laboratory located in the Sanders Building, room 1028. For safety reasons, the research lab was only occupied by the researcher while data collection occurred. The researcher also wore ear protection during impact testing. The horizontal impact testing procedure for this study was conducted following the NOSCAE standard protocols (ND001-15m17 and ND081-14m15) that apply to horizontal impact testing (NOCSAE, 2017; NOCSAE, 2016b). The NOCSAE protocols were chosen to comply with testing standards for helmets sent to the market. These protocols state that "A headgear is positioned on a headform that is mounted onto a 50th percentile Hybrid III neck assembly which is rigidly mounted to a linear bearing table to achieve post impact kinematics. The impactor is propelled at the headgear such that the velocity is within 2% of the specified level when

measured over a distance no more than two inches. The impact must occur with one inch of velocity capture. At impact, the resultant peak linear acceleration, SI, and resultant peak rotational acceleration shall be captured" (NOCSAE, 2016b, p. 2). The NOCSAE protocols were modified slightly for this study. That is, the NOCSAE headform was secured to a custom mechanical neckform instead of a 50^{th} percentile Hybrid III neck assembly and only the peak linear acceleration was captured.

For all simulated impacts in this study, the resultant linear acceleration over time was collected and imported into a Microsoft Excel file, where it was subsequently integrated to compute SI using Equation 2. Data recording on LabChart was initiated manually by the researcher before discharging the impactor rod. The peak linear acceleration was taken as the greatest value on the acceleration-time curve encountered during the impact (CSA, 2015a). For SI, the acceleration-time data was trimmed to exclude all values before the signal rose above 4 g as well as when the signal fell below 4 g, after it had peaked (NOCSAE, 2017). The remaining acceleration-time data was put to the exponent of 2.5 then integrated to produce the SI for each impact. These calculations were performed in Microsoft Excel. The linear acceleration data were captured from the centre of mass of the headform, and represented the acceleration of the entire system (linear bearing table, headform, neck, and helmet/facial shield). Therefore, these variables were considered when determining the energy loaded onto the system during each dynamic impact. Each impact data were again imported into Microsoft Excel where computations of energy loading were performed using the following set of equations as described in the Zerpa et al. (2016) study.

$$F = m \cdot a \tag{10}$$

where:

F = force due to the impact
m = mass of the shuttle plate, headform, neck, and helmet
a = resultant acceleration measured by accelerometers

Next velocity during the impact was calculated using Equation (11)

$$V_f(t) = V_i + \frac{1}{m}\int_0^t F \cdot dt \tag{11}$$

where:

$V_f(t)$ = final velocity during the impact
V_i = initial velocity during the impact
m = mass of the shuttle plate, headform, neck, and helmet
F = force due to the impact
t = time duration of the impact
dt = sampling time

Following the calculations of velocity for each impact, the change in displacement for the duration of impact was calculated using Equation (12).

$$s(t) = s(t_0) + \int_{t_0}^t V_f(t) \cdot dt \tag{12}$$

where:

$s(t)$ = change in position
$s(t_0)$ = initial positon
t_0 = time at beginning of interval
t = time at end of interval
V_f = velocity
dt = sampling time

Finally, the loading during the impact was calculated based on Equation 13.

$$E_{Loading} = \int_0^s F_1 \cdot ds \tag{13}$$

where:

$E_{Loading}$ = energy produced due to the deformation of material shape at impact
F_1 = force of action to deform the material shape at impact
ds = compression interval
s = total displacement of material due to deformation

The dynamic helmet testing required the helmets to be properly fitted to the surrogate headform. The instructions provided by the manufacturer were followed to ensure an appropriate fit. This fit was further standardized by ensuring the foam liner was in contact with the headform, as well as, consistently measuring 50 mm from the brim of the helmet to the bridge of the nose, following each impact. Similarly, facial shields were also attached to the helmets complying with the manufacturer's instructions. The distance from the headform to the facial shield at the level of the brow and philtrum were also standardized. The standards for testing in Canada state that these distances should not exceed 60 mm (CSA, 2015b), see Figure 14.

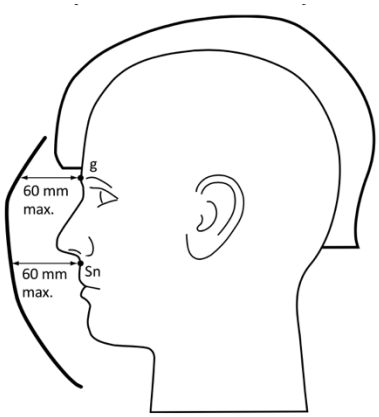

Figure 14. Maximum allowed distance from headform to facial protector. Retrieved from "Face protectors for use in ice hockey," (Z262.2-15). (2015). Toronto, Canada: CSA. Copyright 2015 by Canadian Standards Association.

The helmet was impacted one single time (Post et al., 2011) for each combination of magnitude (variable impact velocities), neckform stiffness level, impact location, and facial shielding condition. The magnitude of the impact was based on 18 different impact velocities. This approach was used to simulate 18 hockey players being hit at different impact velocities, resulting in a total of 810 impacts for 45 different impact conditions (see Appendix A). This study impacted five of the six locations as defined by NOCSAE testing standards (NOCSAE, 2017). These locations were: the front, front boss, side, rear boss, and rear. The top impact

location was not tested in this study as the horizontal impactor could not strike this location. Figure 2 displays the impact conditions used by NOCSAE and the ones used in this study. The front location was situated “in the median plane approximately 25 mm above the anterior intersection of the median and reference plane” (NOCSAE, 2017, p. 26). The front boss was defined as “a point approximately in the 45-degree plan from the median plane measured clockwise and located approximately 25 mm above the reference plane” (NOCSAE, 2017, p. 26). The side location was located “approximately at the intersection of the reference and coronal planes on the right side of the headform” (NOCSAE, 2017, p. 26). The rear boss was found “approximately at the posterior intersection of the median and the reference planes” (NOCSAE 2017, p. 26). Finally, the rear was located “approximately at the intersection of the median and reference planes” (NOCSAE, 2017, p. 26). These locations were marked on the headform. The centre of impactor rod was then lined up with these reference points each time before the helmet was fitted and, subsequently, impacted.

In addition to impact location, neckform stiffness was also manipulated to examine the effect neck strength has in a dynamic response. Like the protocols used by Carlson (2016) and Rousseau and Hoskizaki (2009), neckform stiffness was altered to represent three different neck strengths. Carlson (2016) determined the exact neckform stiffness torques for the mechanical neckform and these torque values were used in this study. These stiffness levels are described as medium (50^{th} percentile adult human neck), low (30% below medium), and high (30% above medium). Their corresponding torque requirements can be seen in Table 3 and were adapted from Carlson (2016). To achieve these various stiffness conditions, a Chatillon DFE II and a torque wrench were used to obtain the appropriate torque measurement. During the calibration of

neckform stiffness, the headform was placed in a custom-built jig. The jig ensured the head was secured as well as the torque was applied perpendicularly to the nut as depicted in Figure 15.

Table 3

Mechanical neckform stiffness conditions and torques requirements

Stiffness	Torque (in-lb)	Torque (Nm)
Low	8.4	0.95
Medium	12.0	1.36
High	15.6	1.76

Note. Retrieved from "The Influence of Neck Stiffness, Impact Location, and Angle on Peak Linear Acceleration, Shear Force, and Energy Loading Measures on Hockey Helmet Impacts," by S. Carlson, (Unpublished masters thesis). Lakehead University, Thunder Bay, Canada. Copyright 2016 by Lakehead University Knowledge Commons.

Figure 15. Custom jig built by Brittany Pennock, School of Kinesiology Master Student for adjusting the stiffness of the mechanical neckform. The jig ensures that the headform does not rotate and that the torque wrench applies the force perpendicular to the neck.

When performing the actual helmet impact testing procedure, each helmet location was impacted by the pneumatic horizontal impacting system. All impacts to each facial shielding condition were completed before moving to the next. Therefore, the impacts at each different neckform stiffness level were completed before moving on to the subsequent facial shielding condition. For each of these different impact conditions, the helmet was exposed to 18 impacts at the different incremental velocities to all the relevant impact sites. The order of impacts was as

follows: front, front boss, side, rear boss, and rear (following NOCSAE standards). This procedure continued until all the impact conditions were tested. The impact velocities were determined in a pilot study based on average measures taken from high speed video analysis at each of the tank pressures that were used in this study. The pilot testing began at a pressure of 14 psi and it was increased by 2 psi until a pressure of 60 psi was reached. This resulted in 24 impact trials. Peak Motus video analysis software was used to digitize a reflective marker at the end of the impact rod to determine the impact velocity. These velocities then allowed the researcher to model this relationship. Equation 14 was used to determine the speed based on the pressure of the tank. The equation has a small root mean square error (RMSE = 0.179) and coefficient of determination of ($R^2 = 0.99449$). Eighteen pressures were used in this study to generate the impact velocities using the regression model in Equation 14. The pressures were increased in increments of 2 psi with the pressure beginning at a lower limit of 24.0 psi and concluding at an upper limit of 58.0 psi as shown in Table 4. This corresponds to impact velocities beginning at 2.01 m/s and increased by an average of 0.2 m/s to a corresponding final impact velocity of 5.13 m/s.

$$\text{Velocity} = 0.00005(\text{psi})^3 - 0.0063(\text{psi})^2 + 0.3307(\text{psi}) - 2.9423 \quad (14)$$

Table 4

Tank pressure of the Lakehead University horizontal impactor and corresponding contact velocity

Simulee Number	Pressures (psi ± 1%)	Impact Velocity (m/s)
1	24.0	2.01
2	26.0	2.14
3	28.0	2.42
4	30.0	2.62
5	32.0	2.83
6	34.0	3.12
7	36.0	3.25
8	38.0	3.47
9	40.0	3.61
10	42.0	3.64
11	44.0	3.86
12	46.0	3.94
13	48.0	4.11
14	50.0	4.26
15	52.0	4.48
16	54.0	4.56
17	56.0	4.65
18	58.0	5.13

Dependent and Independent Variables

This study used several dependent and independent variables when addressing the third purpose. The dependent measures were peak linear acceleration, SI, and energy loading. The independent variables manipulated by the researcher in this study were the location on the headform where it was impacted (impact location), the type of facial shield attached to hockey helmet (facial shielding condition), and the stiffness of the neckform in which the headform was attached to (neckform stiffness).

Data Analysis

A combination of descriptive and inferential statistical analyses were used to address each of the research purposes for this study. For the first purpose of this study, regarding the

helmet's durability to repetitive impacts, a least squares linear interpolation function was used to determine any changes in durability of the material from repetitive impacts across locations.

For the second purpose pertaining to the stiffness measures of a hockey helmet with and without facial protection at the various locations, another least squares linear interpolation function was used. This procedure allowed the slopes of the force-deformation regression line (also known as the stiffness) to be determined and compared to other conditions. That is, the slopes for each of the facial shielding conditions (no facial shield vs. metal facial shield vs. polycarbonate facial shield) and static testing locations (front vs. rear vs. side) were compared using ratios. The ratio used were structured to expressed the condition with the higher slope (stiffness) as a multiple of the other condition in the comparison.

For the third purpose which aimed at examining the influence of hockey helmet impact location, helmet facial shielding, and neckform stiffness on measures of peak linear acceleration, SI, and energy loading, three separate 3 (Neckform Stiffness [low vs. medium vs. high] x 5 Impact Location [front vs. front boss vs. side vs. rear boss vs. rear] x 3 Facial Shield Conditions [no facial shield vs. metal facial shield vs. polycarbonate facial shield]) mixed Factorial ANOVAs with repeated measures on the last two factors were conducted for each of the dependent variables.

Three-way interactions were examined among the independent variables, for each dependent variable. If a significant three-way interaction was present, then to explain the three-way interaction, three, 3 (Facial Shield Conditions [no facial shield vs. metal facial shield vs. polycarbonate facial shield] x 5 Impact Location [front vs. front boss vs. side vs. rear boss vs. rear]) two-way Factorial ANOVAs were conducted for each level of neckform stiffness [low vs. medium vs. high]. Any two-way interactions that were revealed, subsequently led to the

examination of the interaction using simple main effects with one-way ANOVAs (Keppel, 1991). This was completed for each facial shielding condition, and impact location.. The Bonferroni procedure was used for the post hoc comparison. This is a conservative analysis appropriate for pairwise mean comparisons (Keppel, 1991). Only the statistically significant comparisons were then reported. Finally, the effect sizes were calculated for all significant interaction and main effects. The partial eta squared (η_p^2) statistic was reported, with small, medium, and large effect sizes corresponding to η_p^2 values of .0099, .0588, and .1379, respectively (Richardson, 2011).

Chapter 4 – Results and Discussions

Purpose 1: Assessment of Helmet Durability

Repetitive impacts on two helmet locations (front and side) were conducted to assess the durability of the helmet. This test was necessary to minimize any errors in the measurements due to wear and tear of the helmet material. Any changes detected in the force absorption properties of the material due to repetitive impacts indicated when to switch the helmet for a new one to maintain the integrity of the dynamic impact testing data. The results of this durability test at the front and rear locations are depicted in Figure 16 and Figure 17.

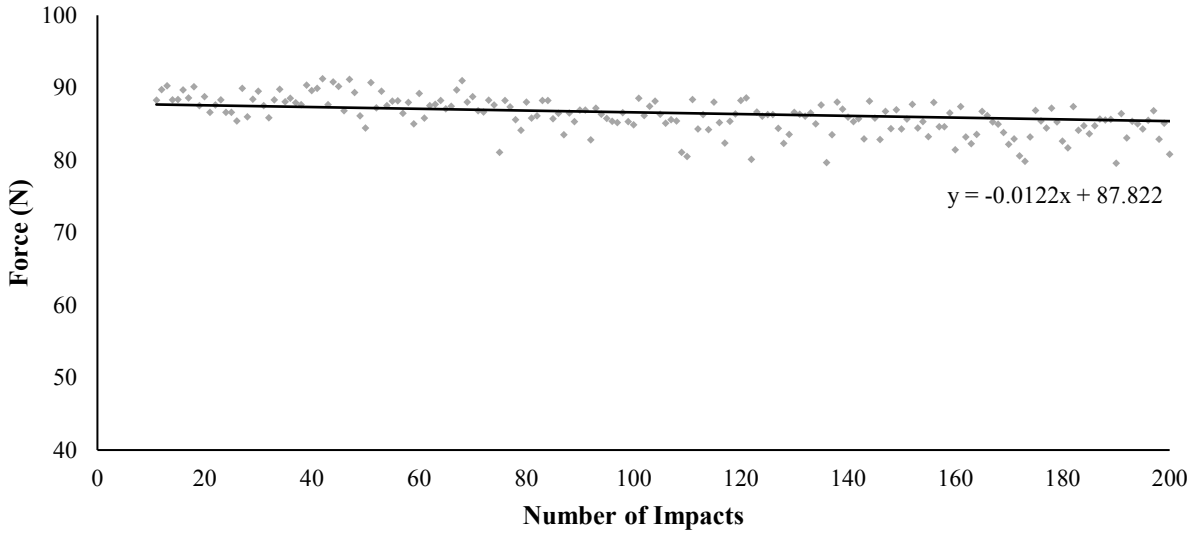

Figure 16. Durability testing of the helmet at the front impact site. This figure displays the maximum impact force in the horizontal direction for the first 200 impacts of the helmet using a repetitive impactor.

A least square linear interpolation was added to front location force data to show the general trend of the peak force transferred from the headform through the helmet to the force platform. The force data, however, remained relatively stable at the front impact site.

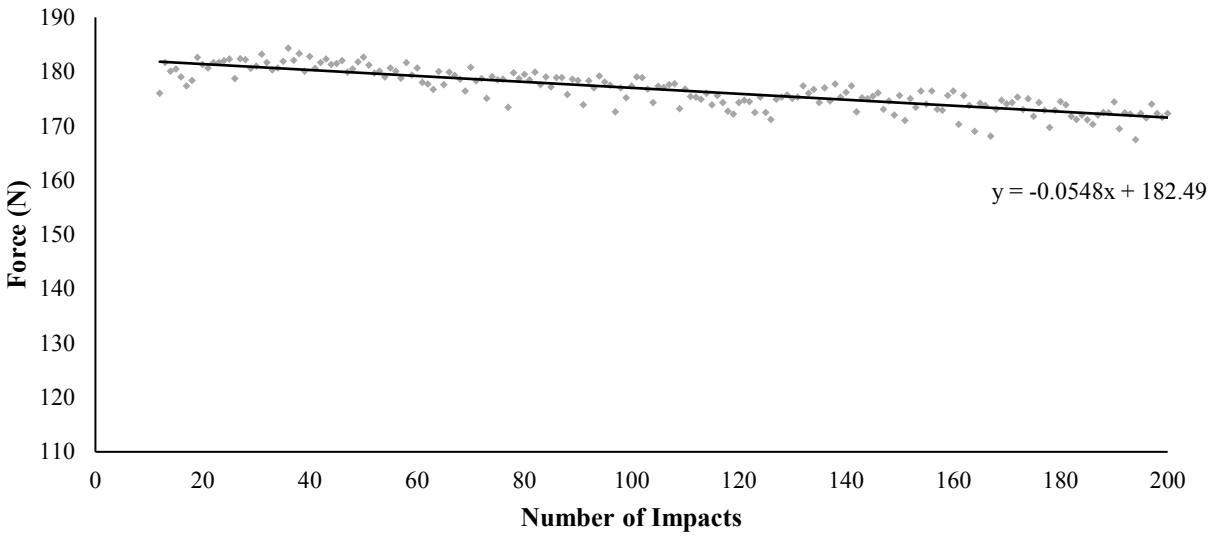

Figure 17. Durability testing of the helmet at the rear impact site. This figure displays the maximum impact force in the horizontal direction for the first 200 impacts of the helmet using a repetitive impactor.

Like the durability analysis at the front location, the peak force transferred from the headform through the helmet to the force platform at the rear impacting site remained stable over the course of 200 impacts, as displayed by the least squares linear interpolation fitted to the data.

Discussion

Hockey helmets have been shown to behave differently when being subjected to repeated impacts (Hakim-Zadeh, 2002). That is, the attenuation properties of a helmet begin to degrade after numerous impacts. The rate at which the attenuation properties diminish also varies with the impact site, the model of helmet, and related factors such as liner padding materials, shape, thickness, and outer shell geometry (Hakim-Zadeh, 2002).

Since the helmets used in this study were impacted multiple times it was vital to test their durability. Carlson (2016) used this procedure in his study and stated that this approach allowed "researchers to predict helmet deterioration and give insight into how often the helmet should be replaced to maintain the integrity of the results" (p. 54).

Initially, in the current study, less expensive helmets with a surpassed expiration date were used for the testing. The outer shell of these helmets, however, fractured during testing at the front site. These observations highlighted that cheaper helmets or helmets that had expired could leave the wearer more vulnerable to a head injury. Based on this outcome, new and more expensive helmets were obtained to conduct this study.

The new helmets used in this study underwent the same testing procedures as Carlson (2016). These repetitive impacts allowed the cushioning effect of the helmet to be examined over the course of 200 impacts. As the liner and/or outer shell's attenuation properties deteriorated, the peak force transferred through the helmet to the force platform was expected to increase. As Figures 16 and 17 displayed, the force did not increase as expected illustrating the attenuation properties of the helmet remained intact. Furthermore, the impact conditions experienced by the helmet in this testing scenario would never be experienced in a hockey game and, therefore, represents a severe evaluation of the helmet. Based on the results of this durability assessment, it was deemed appropriate that one helmet could receive 54 impacts at each location before being replaced. Additionally, the helmets were only impacted 18 times per location before the next location was tested. Finally, a rest period between each impact allowed the material properties of the helmet to restore before administering the next impact.

Purpose 2: Helmet Stiffness Testing Results

This study also investigated the influence that facial shielding and helmet location had on measures of static helmet stiffness. Figure 18 depicts the helmet stiffness measures at the front, rear and side locations, at each of the three facial shielding conditions: no facial shielding, metal facial shield, and high impact polycarbonate shield.

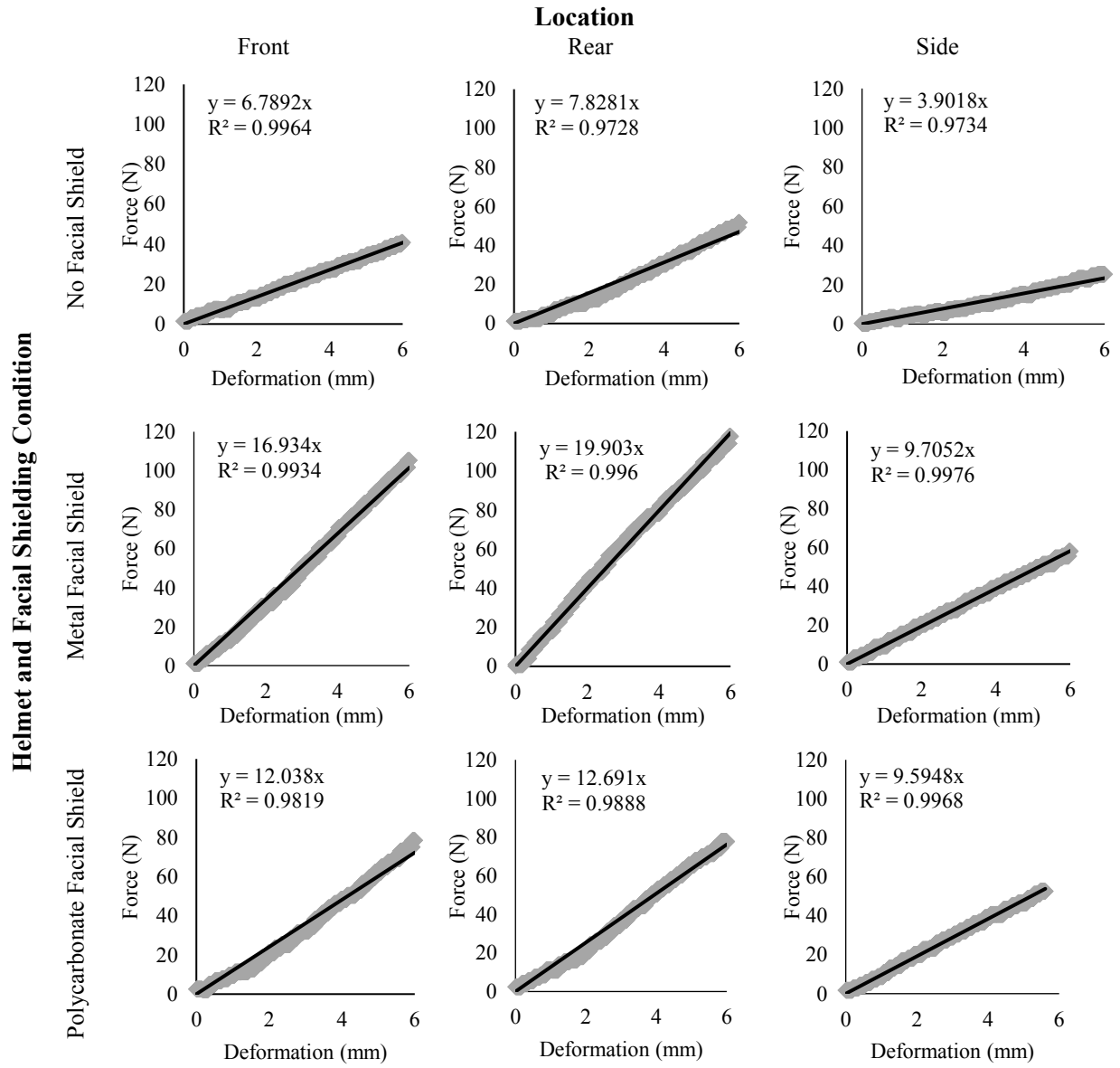

Figure 18. Stiffness of a hockey helmet with varying facial shielding conditions at the front, rear, and side locations.

The stiffness measures of the different conditions were compared using ratios of the slopes of the different linear interpolation lines. The nine unique stiffness testing conditions allow a total of 72 comparisons to be made. The comparisons that seemed most relevant were those that revealed how the facial shield condition changed the stiffness properties of the helmet across locations of the helmet.

At the front location, the ratio for the stiffness of the metal facial shield and no facial shield conditions (ratio = 16.93/6.79) indicated that the helmet with metal facial shield required 2.49 times more force to acquire the same deformation as when the helmet had no facial shield. Similarly, the ratio calculations revealed that the polycarbonate shielding requires 1.77 times more force to deform the helmet when compared to no facial shield (ratio = 12.04/6.79). Finally, the ratio comparing the helmets with metal and polycarbonate shielding (ratio = 16.93/12.04) indicated that the metal facial shielding condition required 1.41 times more force to produce an identical deformation as the helmet with the polycarbonate shielding.

When facial shields were added to the rear and side locations, it also increased the amount of force required to produce identical deformations. At the rear location, force requirements to deform the helmet were increased by 2.54 times by the metal facial shield (ratio = 19.90/7.83) and 1.53 times by the polycarbonate shielding (ratio = 12.04/7.83). At the side location, the force requirements for identical helmet deformation were 2.5 times more in a helmet with the metal facial shield (ratio = 9.71/3.90) and 2.46 more for the helmet with the polycarbonate shield (ratio = 9.59/3.90). Finally, the metal facial shielding condition increased the force requirements for equal deformation by 1.57 and 1.01 times at the rear and side locations, respectively, compared to the polycarbonate shields (ratio = 19.90/12.69; ratio = 9.71/9.59).

When comparing the slopes of the three compression locations on the helmet with respect to the three facial shielding conditions, it was determined that the rear location required the most force for deformation, followed by the front and side locations. To quantify the magnitude of the difference, ratios were once again used. On the helmet with no facial shielding, the rear was 2.01, and 1.15 times stiffer than the side and front respectively (ratio = 7.83/3.90; ratio = 7.83/6.79). Furthermore, the front was also 1.74 times stiffer than the side (ratio = 6.79/3.90). Similarly, the helmet with the metal facial shield, made the rear location 2.05 and 1.18 times stiffer than the side and front locations, respectively (ratio = 19.90/9.71; ratio = 19.90/16.93). Whereas, the front was 1.74 times stiffer than the side (ratio = 16.93/9.71). Finally, the helmet with the polycarbonate shield required 1.32 and 1.05 times more force to deform the rear location as compared to the side and the front locations (ratio = 12.69/9.59; ratio = 12.69/12.04). While, this facial shielding condition also caused the front to be 1.26 times stiffer than the side (ratio = 12.04/9.59).

Discussion

Stiffness is a material property described as the amount of force needed to cause a certain amount of deformation to a material (Baumgart, 2000). This study assessed the stiffness properties of helmets at different locations on the helmet for each of the three facial shielding conditions. The force and deformation data for each condition was captured using an Instron 1000 device. Mathematically the stiffness of a material is the quotient of the load divided by deformation (Baumgart, 2000). Therefore, the slope of the linear interpolation lines for force and deformation represented the average stiffness of the helmet conditions (Baumgart, 2000).

This study found several trends when comparing the stiffness of helmets with and without facial shielding at the various locations. The first was that the helmet outfitted with the

metal facial shield had the greatest stiffness when compared to the plastic facial shield and to the no facial shielding condition. It should be noted that the hockey helmet tested in this study consisted of an outer shell made of ABS plastic and an inner liner of VN. The metal facial shield used was constructed from stainless steel, while the plastic shield was constructed from high impact polycarbonate. Each of these materials had their own unique mechanical properties (Hearn, 1997). One of these properties is the strength of the material. This property is a measure of the extension or strain of the material at increasing loads or stress (Hearn, 1997). Materials used in helmet construction generally behave elastically at first when the stress is proportional to the strain (i.e., Hooke's Law). There comes a point, however, where the elastic limit of the material has been reached and plastic deformation occurs meaning the material does not fully recover (Hearn, 1997). These mechanical concepts are important when discussing the stiffness properties of the helmet, and can aid in the explanation of the results. The literature shows that material properties of metal and polycarbonate facial shields are different under load (Lemair & Pearsall, 2007). Researchers directly impacted similar types of facial shields to the ones in this study and stated that the metal facial shields permanently deformed when impacted, while the polycarbonate shields deformed and rebounded to its original geometric configuration (observed using high speed motion capture). Lemair and Pearsall's observations along with the varying tensile test curves for these materials (Hearn, 1997), supports that these facial shields have different mechanical properties as well as strengths.

The stainless steel of the metal facial shield is more resistant to the load (stiffer) than the polycarbonate of the plastic facial shield. When either shield was attached, it reduced the flexibility of the helmet, meaning the helmet deformed less under the same load; as the stiffer material of the facial shields aided the helmet's ability to resist force. Mechanically speaking, the

addition of the facial shield increased the elastic limit of helmet, leading to a greater resistance of load before the elastic limit was reached and plastic deformation could occur. The load applied by the Instron was great enough for the researcher to visibly observe that the ABS outer shell of the helmet deformed for all facial shielding conditions. It should also be stated, that when the cage was added to the helmet, J-clips were also added just in front of the ear pieces on the helmet. Compressing the helmet now meant that the facial shield pushed against the J-clips and, therefore, some of the load was likely transferred to other areas of the helmet, meaning the deformation now required a greater load.

In terms of helmet locations, the rear location exhibited the greatest stiffness compared to the front and side locations at all facial shielding conditions. The geometry of the human head and helmet may provide some explanation for these results. The human head is ellipsoidal in nature, with the head length being greater than the head breadth (Young, 1993). Helmets must, therefore, accommodate this, meaning their geometry is subsequently affected. The compression sites where the cylinders were placed on the helmet before compression are further apart at the front and rear compression sites (semi-major axis of an ellipse) compared to the side location (semi-minor axis of an ellipse). Geometrically, this means that the curvature at the side location is not as pronounced as it is at the front and rear locations and the helmet is unable to spread the load as effectively. Halstead (2000) stated that these flat surfaces on hockey helmets are ineffective at spreading and deflecting impact energies. The ellipsoid geometry also supports why the front and rear locations exhibited similar stiffness properties. The orientation of the helmet at these two sites was opposite, meaning the front of the helmet was positioned up when tested at the front compression site, and down when tested at the rear compression site. The helmet is also designed with two separate components at the front and back with the pieces

attaching at the side. The interaction between the two components also influences the stiffness. When loaded at the front and rear sites the aperture of the helmet becomes more circular in nature, whereas when compressed at the side the helmet becomes more ellipsoidal.

Higher stiffness in motorcycle helmets have been shown to lead to higher accelerations (Kostopoulos, Markopoulos, Giannopoulos, & Vlachos, 2002). Although not stated in the literature, less flexibility means less elasticity of the material, meaning a reduced distance that the helmet is able to decelerate the force. More of the force is transferred to the head leading to greater accelerations. Alternatively, it is noted that if impact force is spread over a greater area it can be a protective property of the helmet (Graham et al., 2014). Facial shields, increase the area over which forces transferred to the helmet can be spread, even though they do increase the stiffness properties of the helmet. This could mean there is an optimal zone where, the flexibility and the efficiency to spread the energy load is best. This is an area where further research is needed.

The findings of the static stiffness testing for the current study supported the research work of Zerpa et al. (2016) when testing the stiffness of helmets with no facial shield. Their study revealed that the rear location was 2.48 times stiffer than the side. The helmet used in this study was also found to be stiffer at the rear compared to the side by 2.01 times. The difference between these studies is likely due to differences in the material properties of the individual helmets used in each study (model, brand, and construction). Helmets from Zerpa's study and the one used for this study were made by different manufacturers. This means that different materials were likely used in their construction resulting in different mechanical properties. The geometry and thickness of the outer shell as well as how the front and back pieces interacted would also likely have been different. Examining the Hockey STAR helmet ratings may further

explain why there is a difference between the stiffness properties of the helmets. The rating of the helmet used in Zerpa's study had a STAR Value of 0.613 – 6.13 concussions per season and a rating of two stars, whereas, the helmet used in this study had a STAR Value of 1.210 – 12.10 concussions per season and a rating of not recommended. These values reinforce that the construction and design of the helmet used by Zerpa et al. is likely superior to the helmet used in this study.

The results of the current study add to existing literature (Zerpa et al., 2016) on helmet stiffness testing. Future studies should examine the stiffness differences between helmets with VN liners and EPP liners. Furthermore, the front and rear boss positions have not been tested extensively regarding their specific stiffness properties. This type of testing may also have applications for determining the wear and tear on helmet materials. Since new helmets exhibit certain mechanical properties, static stiffness testing can help reveal differences on static loading across helmet locations when the elastic response of the helmet begins to significantly differ from a new helmet.

Purpose 3: Dynamic Helmet Testing Results

The third purpose of this study was to examine the influence of facial shielding, impact location, and neckform stiffness on the dynamic response of a NOCSAE headform when measuring peak linear acceleration, severity index (SI), and energy loading for different impact velocities using a pneumatic horizontal impactor. A total of 810 impacts were completed for all combinations of the five helmet impact locations, three facial shielding conditions, and three neckform stiffness levels. The results are displayed in Appendix B, and categorized in terms of neckform stiffness (low, medium, and high). The results are expressed in mean values and standard deviations (shown in parentheses) for each dependent variable.

As the third purpose of this research study involved examining the influence of the independent variables on the three separate dependent variables, the results from the inferential statistical analyses and their subsequent discussions are presented according to each dependent variable. Peak linear acceleration is presented first, followed by SI, and energy loading.

Peak Linear Acceleration Analysis Results

Three-way interaction. A three-way mixed factorial ANOVA, with repeated measures on facial shielding and impact location factors was conducted for the peak linear acceleration measures of the NOCSAE headform. Statistical significance was tested at $p < .05$. This analysis revealed a statistically significant three-way interaction between facial shielding, impact location, and neckform stiffness, F (3.40, 86.77) = 6.31, $p < .001$, $\eta_p^2 = .19$.

Two-way interactions. Statistically significant two-way interactions between facial shielding and location for peak linear acceleration were observed at the low neckform stiffness condition, F (1.44, 24.49) = 31.11, $p < .001$, $\eta_p^2 = .64$, (Figure 19).

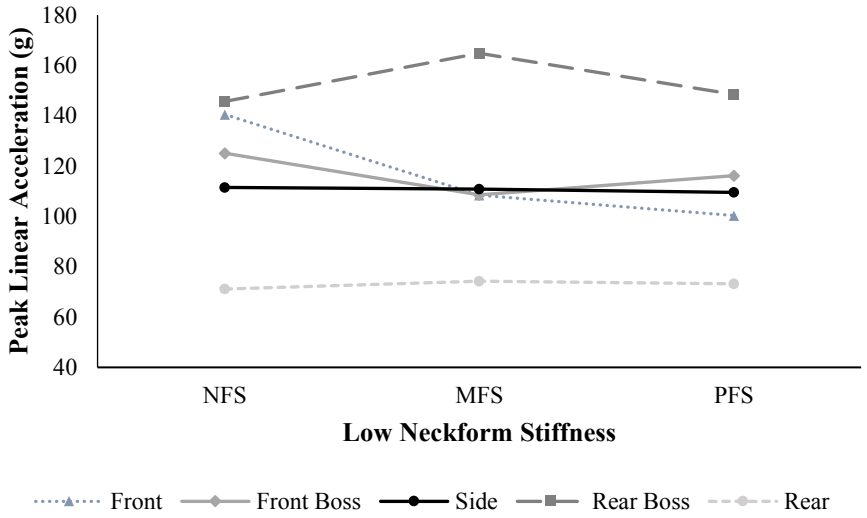

Figure 19. Peak linear acceleration at low neckform stiffness. The five impact locations are represented by the various lines, and the facial shielding conditions are represented by the grouping labels: no facial shielding (NFS), metal facial shielding (MFS), and by polycarbonate facial shielding (PFS).

For the medium neckform stiffness condition, a significant two-way interaction between impact location and facial shielding condition was also found; F (1.53, 26.05) = 18.60, $p < .001$, $\eta_p^2 = .52$ (Figure 20).

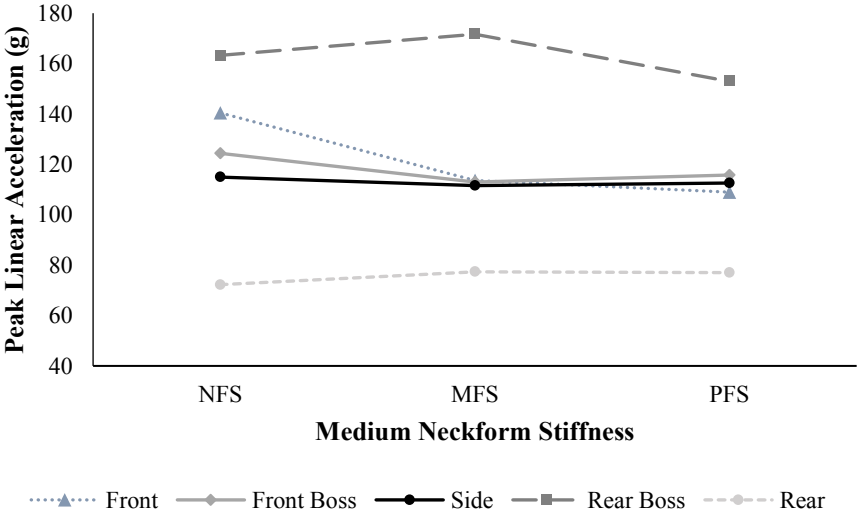

Figure 20. Peak linear acceleration at medium neckform stiffness. The five impact locations are represented by the various lines, and the facial shielding conditions are represented by the grouping labels: no facial shielding (NFS), metal facial shielding (MFS), and by polycarbonate facial shielding (PFS).

For the highest neckform stiffness, a two-way interaction between facial shielding and impact location, was again observed (Figure 21); F (1.42, 24.18) = 24.44, $p < .001$, $\eta_p^2 = .59$.

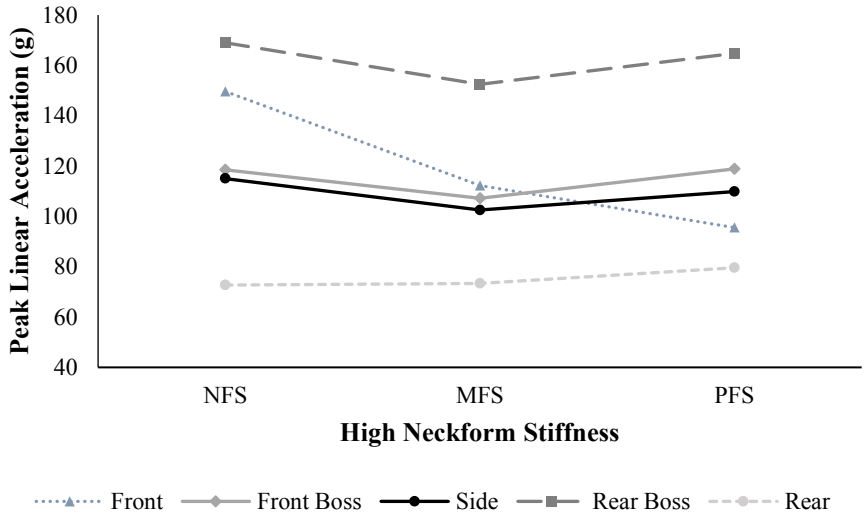

Figure 21. Peak linear acceleration at the high neckform stiffness. The various lines represent the different impact locations, while facial shielding conditions are represented by no facial shielding (NFS), metal facial shielding (MFS), and by polycarbonate facial shielding (PFS).

Simple main effects of impact location at low neckform stiffness.

No facial shielding. First, a significant simple main effect of impact location on helmets without facial shields at the lowest neckform stiffness was revealed, F (1.10, 18.74) = 26.91, $p < .001$, $\eta_p^2 = .61$. The mean peak linear acceleration for each impact location at the low neckform stiffness with no facial shielding were as follows: rear boss (M = 145.68 g, SD = 91.11); front (M = 140.51 g, SD = 68.93); front boss (M = 125.11 g, SD = 68.50); side (M = 111.50 g, SD = 65.24); and rear (M = 71.14 g, SD = 91.11). The front location was significantly greater than the front boss ($p < .001$); the side location ($p < .001$); and the rear location ($p < .001$). Next, the front boss location was also statistically significantly greater than the side ($p < .001$); and the rear location ($p < .001$). The side location was only statistically significantly greater than the rear

location (p = .005). Finally, the mean peak linear acceleration, at the rear boss was significantly greater than the front boss (p = .023); side (p < .001); and the rear location (p = .002).

Metal facial shielding. A significant simple main effect of impact location on helmets with metal facial shields at the lowest neckform stiffness was also observed, F (1.05, 17.91) = 25.21, p < .001, η_p^2 = .60. The mean peak linear acceleration for each impact location at this condition were as follows: rear boss (M = 164.81 g, SD = 103.83); front boss (M = 108.56 g, SD = 60.67); front (M = 108.46 g, SD = 52.63); side (M = 110.89 g, SD = 61.60); and rear (M = 74.25 g, SD = 30.24). The mean peak linear acceleration for the front location was significantly greater than the rear location (p < .001). The front boss was also significantly greater than the rear location (p = .003); as was the side location (p = .002). Lastly, the mean peak linear acceleration at the rear boss was significantly greater than all the other sites. The rear boss was statistically greater than the front, (p = .003); front boss (p < .001); the side ($p \leq .001$); and the rear location ($p \leq .001$).

Polycarbonate facial shielding. The final facial shielding condition also had a significant simple main effect of impact location when the neckform was at its lowest neck stiffness level, F (1.13, 19.21) = 17.54, p < .001, η_p^2 = .51. The mean peak linear acceleration, at each impact location, for the lowest neck stiffness condition with polycarbonate shielding were as follows: rear boss (M = 148.50 g, SD = 97.67); front boss (M = 116.12 g, SD = 64.34); side (M = 109.54 g, SD = 63.19); front (M = 100.33 g, SD = 42.32); and rear (M = 73.16 g, SD = 29.31). The average peak linear acceleration for the front location was significantly greater than the rear location (p < .001). The front boss location was significantly greater than the side location ($p \leq$ .001) and the rear location ($p \leq .001$). Next, the side location was significantly greater than the

rear location, (p = .004). Finally, the rear boss location was significantly greater than the front, (p = .031); front boss (p = .008); side (p = .002); and rear locations, (p = .003).

Simple main effects of impact location at medium neckform stiffness.

No facial shielding. At this level of neck stiffness, there was also a significant simple main effect of impact location on helmets with no facial shields, F (1.06, 17.98) = 31.83, p < .001, η_p^2 = 65. The mean peak linear acceleration at each of the impact locations at the medium neck stiffness with no facial shielding were as follows: rear boss (M = 163.20 g, SD = 99.23); front (M = 140.43 g, SD = 70.24); front boss (M = 124.38 g, SD = 69.47); side (M = 114.94 g, SD = 66.17); and rear (M = 72.25 g, SD = 30.41). The front location was again significantly greater than the front boss (p < .001); the side location, (p < .001); and the rear location, (p < .001). While the mean peak linear acceleration for the front boss location was significantly greater than the side, (p < .001); and the rear location, (p < .001). Next, the side location was significantly greater than the rear location, (p = .005). Finally, the rear boss location was significantly greater than the front (p = .049); front boss (p < .001); the side ($p \leq .001$); and the rear location (p < .001).

Metal facial shielding. There was a statistically significant simple main effect of impact location, when the neck was at its medium stiffness F (1.14, 19.37) = 31.062, p < .001, η_p^2 = .65. The mean peak linear acceleration at each of the impact locations at the medium neck stiffness with metal facial shielding were as follows: rear boss (M = 171.65 g, SD = 104.68); front (M = 113.63 g, SD = 53.12); front boss (M = 112.98 g, SD = 64.63); side (M = 111.57 g, SD = 61.75); and rear (M = 77.34 g, SD = 41.11). The peak linear acceleration at front location was significantly greater than the rear location (p < .001). The front boss was also significantly greater than the rear location (p < .001); as was the side location (p < .001). Finally, the rear boss

was significantly greater than front ($p = .002$); front boss ($p < .001$); the side ($p < .001$); and the rear location ($p < .001$).

Polycarbonate facial shielding. A statistically significant simple main effect of impact location, at a medium neck stiffness was also found for this facial shielding condition F (1.23, 20.84) = 20.90, $p < .001$, $\eta_p^2 = .52$. The mean peak linear acceleration at each of the impact locations at the medium neck stiffness condition with polycarbonate shielding were as follows: rear boss (M = 152.92 g, SD = 96.09); front boss (M = 115.73 g, SD = 65.17); side (M = 112.54 g, SD = 65.17); front (M = 108.96 g, SD = 42.90); and rear (M = 76.97 g, SD = 38.56). The front location received significantly more peak linear acceleration than the rear location, ($p < .001$). The linear acceleration for the front boss location was again significantly greater than the rear location, ($p \leq .001$). The side location was significantly greater compared to the rear location ($p = .004$). While the rear boss was significantly greater than the front ($p = .046$); front boss ($p \leq .001$); the side ($p \leq .001$); and the rear location ($p < .001$).

Simple main effects of impact location at high neckform stiffness.

No facial shielding. There was a statistically significant simple main effect for impact location at this condition when the neck stiffness was at its greatest F (1.07, 18.16) = 36.50, $p < .001$, $\eta_p^2 = .68$. The mean peak linear acceleration at each of the impact locations at the high neck stiffness condition with no facial shielding were as follows: rear boss (M = 168.99 g, SD = 100.76); front (M = 149.64 g, SD = 72.07); front boss (M = 118.55 g, SD= 64.14); side (M = 115.00 g, SD = 65.87); and rear (M = 72.71 g, SD = 31.47). The front location was again significantly greater than the front boss ($p < .001$); the side location ($p < .001$); and the rear location ($p < .001$). The front boss location was significantly greater than the rear location ($p < .001$). The side location was significantly greater than the rear location ($p \leq .001$). Finally, the

peak linear acceleration at the rear boss location was significantly greater than the front boss ($p <$ .001); the side ($p < .001$); and the rear location, ($p < .001$).

Metal facial shielding. Next, a statistically significant simple main effect of impact location on helmets with metal facial shields, when the neck was at its greatest stiffness F (1.12, 19.09) = 21.343, $p < .001$, $\eta_p^2 = .56$. The mean peak linear acceleration of each impact location for this testing condition were as follows: rear boss (M = 152.48 g, SD = 100.60); front (M = 112.29 g, SD = 53.85); front boss (M = 107.19 g, SD = 62.34); side (M = 102.54 g, SD = 60.34); and rear (M = 73.40 g, SD = 32.76). The mean peak linear acceleration for the front location, ($p < .001$); front boss, ($p = .004$); and side, ($p = .006$), were all significantly greater than the rear location. The rear boss was significantly greater than the front ($p = .026$); front boss ($p \leq .001$); the side ($p \leq .001$); and the rear ($p = .002$).

Polycarbonate facial shielding. There was a statistically significant simple main effect of impact location when the headform was fitted with a helmet with polycarbonate facial shields, at the high neck stiffness F (1.16, 19.74) = 25.17, $p < .001$, $\eta_p^2 = .60$. The mean peak linear acceleration at the highest neck stiffness condition were as follows: rear boss (M = 164.83 g, SD = 100.18); front boss (M = 118.87 g, SD = 64.71); side (M = 109.89 g, SD = 61.13); front (M = 95.55 g, SD = 34.05); and rear (M = 79.59 g, SD = 43.24). The front location was significantly greater than the rear location ($p = .031$). The mean peak linear acceleration for the front boss location was significantly greater than the side ($p = .008$); and the rear location ($p < .001$). The mean peak linear acceleration for the side location was significantly greater than the rear location ($p < .001$). Finally, the rear boss was significantly greater than the front ($p = .005$); front boss ($p \leq .001$); the side ($p < .001$); and the rear location ($p < .001$).

Simple main effects of facial shielding at the low neckform stiffness.

Front location. The first statistically significant simple main effect for facial shielding on peak linear acceleration was at the front impact location at low neckform stiffness F (1.10, 18.72) = 36.22, $p < .001$, $\eta_p^2 = .68$. The mean peak linear acceleration for each of the different facial shielding combinations were as follows: helmets with no facial shield (M = 140.51 g, SD = 68.93); the metal facial shield combination (M = 108.46 g, SD = 52.63); and the polycarbonate facial shield combination (M = 100.33 g, SD = 42.32). The peak linear acceleration at the front location at a low neckform stiffness was statistically significantly higher in the helmet with no facial shield compared to the helmet with the metal, ($p < .001$); and high impact polycarbonate shield ($p < .001$).

Front boss location. Next, the front boss impact location at low neckform stiffness also had a significant simple main effect of facial shielding on peak linear acceleration F (1.40, 23.83) = 57.97, $p < .001$, $\eta_p^2 = .77$. The peak linear acceleration for each of the different facial shielding combinations were as follows: helmets with no facial shield (M = 125.11 g, SD = 68.50); the polycarbonate facial shield combination (M = 116.12 g, SD = 64.33); and the metal facial shield combination (M = 108.56 g, SD = 60.67). The front boss location showed statistically significantly higher peak linear acceleration in the helmet with no facial shield compared to the helmet with the metal ($p < .001$); and high impact polycarbonate shield ($p < .001$). There was also a statistically significant difference between the helmet with metal and polycarbonate facial shielding ($p < .001$).

Side location. This location did not show a statistically significant simple main effect for facial shielding on peak linear acceleration at the side impact location at low neckform stiffness F (2, 34) = 1.44, $p = .252$, $\eta_p^2 = .08$.

Rear boss location. A statistically significant simple main effect for facial shielding on peak linear acceleration at the rear boss impact location at low neckform stiffness was also found F (2, 34) = 24.83, $p < .001$, $\eta_p^2 = .59$. The different facial shielding combinations resulted in different mean peak linear accelerations, which were: (M = 164.81 g, SD = 103.83) for the metal facial shield combination; (M = 148.50 g, SD = 97.67) for the polycarbonate facial shield combination; and (M = 145.68 g, SD = 91.11) for helmets with no facial shield. The peak linear acceleration at the rear boss location at a low neckform stiffness was statistically significantly higher in the helmet with a metal shield compared to the helmet with the none ($p < .001$); and high impact polycarbonate shield ($p < .001$).

***Rear location*.** Finally, a statistically significant simple main effect for facial shielding on peak linear acceleration at the rear impact location at low neckform stiffness was found F (1.43, 24.38) = 5.55, $p = .017$, $\eta_p^2 = .25$. The mean peak linear acceleration for each of the different facial shielding combinations were as follows: the metal facial shield combination (M = 74.25 g, SD = 30.24); the polycarbonate facial shield combination (M = 73.16 g, SD = 29.31); and the helmet with no facial shield (M = 71.14 g, SD = 26.27). The mean peak linear acceleration at the side location on a low neckform stiffness, revealed that were no significant differences between any of the facial shielding conditions.

Simple main effects of facial shielding at the medium neckform stiffness.

Front location. There was a statistically significant simple main effect for facial shielding on peak linear acceleration at the front impact location at medium neckform stiffness F (1.07, 18.23) = 21.66, $p < .001$, $\eta_p^2 = .56$. The mean peak linear acceleration for each of the different facial shielding combinations were as follows: helmets with no facial shield (M = 140.43 g, SD = 70.24); the metal facial shield combination (M = 113.62 g, SD = 53.12); and the

polycarbonate facial shield combination (M = 108.96 g, SD = 42.90). The peak linear acceleration at the front location at a medium neckform stiffness was statistically significantly higher in the helmet with no facial shield as compared to the helmet with the metal ($p < .001$); and high impact polycarbonate shield ($p < .001$).

Front boss location. There was a statistically significant simple main effect for facial shielding on peak linear acceleration at the front boss impact location at medium neckform stiffness F (2, 34) = 29.60, $p < .001$, $\eta_p^2 = .64$. The mean peak linear acceleration for each of the different facial shielding combinations were as follows: helmets with no facial shield (M = 124.38 g, SD = 69.47); the polycarbonate facial shield combination (M = 115.73 g, SD = 65.17); and the metal facial shield combination (M = 112.98 g, SD = 64.63). The peak linear acceleration at the front boss location at a medium neckform stiffness was statistically significantly higher in the helmet with no facial shield compared to the helmet with the metal ($p < .001$); and to the high impact polycarbonate shield ($p < .001$).

Side location. There was a statistically significant simple main effect for facial shielding on peak linear acceleration at the side impact location at medium neckform stiffness F (1.63, 27.75) = 4.01, $p = .037$, $\eta_p^2 = .19$. The mean peak linear acceleration for each of the different facial shielding combinations were as follows: helmets with no facial shield (M = 114.94 g, SD = 70.24); the polycarbonate facial shield combination (M = 112.54 g, SD = 63.77); and the metal facial shield combination (M =111.57 g, SD = 61.75). All simple pairwise comparisons were run between the different facial shielding conditions with a Bonferroni adjustment. The mean peak linear acceleration at the side location on a medium neckform stiffness revealed that were no significant differences between the facial shielding conditions.

Rear boss location. There was a statistically significant simple main effect for facial shielding on peak linear acceleration at the rear boss impact location at medium neckform stiffness F (1.29, 22.00) = 36.42, $p < .001$, $\eta_p^2 = .68$. The mean peak linear acceleration for each of the different facial shielding combinations were as follows: the metal facial shield combination (M = 171.65 g, SD = 104.68); helmets with no facial shield (M = 163.20 g, SD = 99.23); and the polycarbonate facial shield combination (M = 152.91 g, SD = 96.09). The peak linear acceleration at the rear boss location at a medium neckform stiffness was statistically significantly higher in the helmet with no metal facial shield as compared to the helmet with none ($p < .001$); and to the high impact polycarbonate shield ($p < .001$). There was also a significant difference between the helmet with no facial shielding and the helmet with polycarbonate facial shielding ($p < .001$).

Rear location. There was not a statistically significant simple main effect for facial shielding on peak linear acceleration at the rear impact location at medium neckform stiffness F (1.32, 22.35) = 3.67, $p = .058$, $\eta_p^2 = .18$.

Simple main effects of facial shielding at the high neckform stiffness.

Front location. A statistically significant simple main effect for facial shielding on peak linear acceleration at the front impact location at a high neckform stiffness was found F (1.05, 17.85) = 34.58, $p < .001$, $\eta_p^2 = .67$. Each different facial shielding combination resulted in altered peak linear accelerations which were as follows: helmets with no facial shield (M = 149.64 g, SD = 72.07); the metal facial shield combination (M =112.29 g, SD = 53.85); and the polycarbonate facial shield combination (M = 95.55 g, SD = 34.05). The pairwise comparison revealed that the front location at a high neckform stiffness was statistically significantly higher in the helmet with no facial shield as compared to the helmet with the metal shield ($p < .001$); as

well as to the high impact polycarbonate shield ($p < .001$). A statistically significant difference was found between metal facial shield and the polycarbonate facial shield combination ($p < .001$).

Front boss location. There was a statistically significant simple main effect for facial shielding at the front boss impact location at this neckform stiffness F (1.51, 25.59) = 23.71, $p < .001$, $\eta_p^2 = .58$. The mean peak linear acceleration for each of the different facial shielding combinations were as follows: the polycarbonate facial shield combination (M = 118.87 g, SD = 64.71); helmets with no facial shield (M = 118.55 g, SD = 64.14); and the metal facial shield combination (M = 107.19 g, SD = 62.34). The peak linear acceleration at the front boss location was statistically significantly higher in the helmet with no facial shield compared to the helmet with the metal facial shielding ($p < .001$). There was also a statistically significant difference between the helmet with metal and polycarbonate facial shielding ($p < .001$).

Side location. Next, a statistically significant simple main effect for facial shielding on peak linear acceleration at the side location was observed F (1.70, 28.91) = 25.41, $p < .001$, $\eta_p^2 = .60$. Helmets with no facial shields received the greatest peak linear acceleration (M = 115.00 g, SD = 65.87), followed by the polycarbonate facial shield combination (M = 109.89 g, SD = 61.13) and the metal facial shield combination (M = 102.54 g, SD = 60.33). The peak linear acceleration at the side location at a high neckform stiffness was statistically significantly higher in the helmet with no facial shield as compared to the helmet with the metal facial shielding ($p < .001$); and the polycarbonate shield ($p = .007$). There was also a statistically significant difference between the helmet with metal and polycarbonate facial shielding ($p = .002$).

Rear boss location. A significant simple main effect was also found for facial shielding at the rear boss impact location F (1.42, 24.18) = 33.81, $p < .001$, $\eta_p^2 = .67$. The mean peak

linear acceleration for each of the different facial shielding combinations were as follows: helmets with no facial shield (M = 168.99 g, SD = 100.76); the polycarbonate facial shield combination (M = 164.83 g, SD = 100.18); and the metal facial shield combination (M = 152.48 g, SD = 100.60). The peak linear acceleration on the rear boss of the helmet was statistically significantly higher in the helmet with no facial shielding compared to the helmet with metal facial shielding ($p < .001$); and the high impact polycarbonate shield ($p < .001$). There was also a significant difference between the helmet with metal and polycarbonate facial shielding ($p < .001$).

Rear location. Finally, there was a statistically significant simple main effect for facial shielding on peak linear acceleration at the rear impact location at a high neckform stiffness $F(1.10, 18.74) = 4.91$, $p = .036$, $\eta_p^2 = .22$. The mean peak linear acceleration for each of the different facial shielding combinations were as follows: the polycarbonate facial shield combination (M = 79.59 g, SD = 43.24); the metal facial shield combination (M = 73.40 g, SD = 32.76); and the helmet with no facial shield (M = 72.72 g, SD = 31.47). All simple pairwise comparisons were run between the different facial shielding conditions with a Bonferroni adjustment. The mean peak linear acceleration at the side location on a high neckform stiffness, revealed that there were not any significant mean differences between the peak linear accelerations at various facial shielding conditions.

Discussion

Peak linear acceleration is a vector quantity, which represents the rate of change of linear velocity over time. International helmet standards organizations such as the ASTM, CSA, and ISO use this measure as a determinant for head injuries and concussion risk (Gimbel & Hoshizaki, 2008; Zhang et al., 2004). The peak linear accelerations for all 45 dynamically tested

helmet impact conditions tested in the current study are displayed in Tables 5, 6, and 7 (Appendix B). To analyze these outcomes and determine if the impacts posed a risk of sustaining a mTBI through the simulation, concussive threshold measures for peak linear acceleration in the 25th, 50th, and 80th percentiles were used to compare the data of this study, based off the research work of Zhang et al. (2004). More specifically, the resultant peak linear acceleration values of 66 g, 82 g, and 106 g, respectively, were used in the current study to represent the threshold percentiles as proposed by Zhang et al. (2004). The mean acceleration values in the current study, apart from the rear location, were greater than 106 g, meaning a probability of a concussion in the 80th percentile. The average acceleration values for the rear impact site fell between 66 and 82 g, corresponding to a probability of concussion risk between the 25th and 50th percentiles, based on the research work of Zhang et al., (2004).

While studies and helmet testing protocols measure peak linear accelerations across helmet impact locations to determine helmet protective characteristics as an avenue to minimize the risk of concussions (ASTM, 2016; CSA, 2015a; NOCSAE, 2016a; Walsh et al., 2011), few studies have examined the interaction effect of neckform stiffness and location on measures of peak linear acceleration to assess helmet safety and minimize risk of head injuries (Carlson, 2016; Zerpa, Carlson, Sanzo, Przysucha, Hoshizaki, & Kivi, 2017; Walsh et al., 2011). The current study builds on existing literature (Carlson, 2016; Lemair & Pearsall, 2007; Rousseau & Hoskizaki, 2009) by examining the extent to which impact location, facial shielding, and neckform stiffness affect one another on measures of peak linear impact acceleration when assessing helmet material properties in preventing brain injuries and concussions. The current study revealed a significant three-way interaction among impact location, facial shielding, and neckform stiffness on peak linear acceleration measures. Two-way factorial ANOVA

interactions between impact location and facial shielding at various levels of neckform stiffness revealed that peak linear acceleration was different across impact locations. For example, the rear boss location experienced the greatest mean peak linear acceleration (M = 159.10 g, SD = 97.12); followed by the front (M = 118.88 g, SD = 57.57); front boss (M = 116.62 g, SD = 63.50); side (M = 110.93 g, SD = 61.76); and finally, at the rear location at (M = 74.53 g, SD = 33.40). Since this interaction was influenced by the impact location and the type of facial shielding attached to the helmet, a more in-depth examination was required.

Helmet impact locations with no face shielding. An examination of the three levels of neckform stiffness without face shielding on measures of peak linear acceleration, demonstrated similar trends. Comparisons of the five impact sites revealed that certain areas of the helmet allowed greater linear accelerations to pass through to the head. The rear boss location always received the highest linear accelerations compared to all other impact sites. Following the rear boss, the headform experienced the greatest peak linear accelerations at the front, front boss, side, and rear locations, respectively. The helmets were inspected visually to help explain possible reasons why acceleration values were greater in some areas as compared to others. It was noted that the rear boss had less attenuation lining on the area of impact for this location, meaning the force was not sufficiently dissipated and was, therefore, transferred to the headform. Conversely, the rear location had the lowest acceleration values, and correspondingly had the thickest lining. The geometry of the outer shell of the hockey helmet may also contribute to the differences observed in the linear accelerations at the different locations. Halstead (1998) stated that helmets used by today's players are geometrically "square" and have many external ridges; as a result, there are many flatter areas of the helmet. These portions of the helmet are not as efficient at spreading and reducing impact accelerations. In the current study, four impact

locations (front, front boss, side, and rear boss) of the helmet were relatively flat, the front boss location of the helmet also had ridges, which were the primary contact point for the impactor head. This helmet structure may explain the elevated peak linear acceleration at the front boss location. Stated differently, the presence of ridges and the plastic response properties of the helmet might have become compromised after numerous impacts. Furthermore, this location of the helmet showed visible signs of stress in the outer shell, including miniature fractures in the plastic, which might have caused the site to fail to rebound to its original geometry after the repeated impacts.

Helmet impact location with facial shielding. When the helmet was fitted with a metal facial shield, the results revealed significant simple main effects on measures of peak linear acceleration for impact location at each level of stiffness. Helmets with metal facial shielding closely resembled the pattern observed in the helmet tested with no facial shields across impact locations, except at the lowest neckform stiffness. Here the front boss location had a higher peak linear acceleration than the front location. This study also found that the helmet with a polycarbonate shield had statistically significant simple main effects at each level of neckform stiffness. The comparisons of the impact locations revealed that this facial shielding combination resulted in different trends in terms of which impact location experienced the greatest peak linear acceleration. Once again with the polycarbonate facial shielding condition, the rear boss location consistently experienced the highest peak linear acceleration as compared to the front boss, side, and then front sites. The current study revealed that helmets with facial shielding still have areas where the greater amounts of linear acceleration can pass to the head and brain. The outcome of this data, however, revealed that when the helmet was fitted with facial protection, a greater ability to reduce the peak linear acceleration at the front, front boss, and side location was

demonstrated. Some of the reasons for this outcome may be that the geometry of both facial shields formed a hemisphere over the face which has been found in other research studies to reduce linear impact acceleration (Lemair & Pearsall, 2007). The shape of the shield may have also helped spread some of the force received radially and away from the centre of mass of the headform, which was the point where the accelerometers were located and, consequently, decreased the peak linear acceleration recorded by the headform. This theoretical rationale can be supported by the research work of Lemair (2007) who found substantial reductions in the peak linear acceleration when directly impacting facial shields of helmeted headforms. Lemair and Pearsall (2007) also stated that chin support offered by the facial protectors helped with force distribution above and below the basic plane.

Upon consideration of all impact sites collectively, facial shields on average, were able to reduce the peak linear acceleration transferred to the headform by 9.02 g and 10.17 g in metal and polycarbonate facial shielded helmets, respectively. Some of the mean differences, however, were as great as 54.08 g (front impact location at high neckform stiffness level). Large differences in peak linear acceleration and even the relatively small differences (i.e., 9 to 10 g) could be the difference between a hockey player sustaining or avoiding a concussion. The Wayne State Tolerance Curve (WSTC) supports this notion, as a resultant linear acceleration of 80 g is below the concussive threshold while an increase of 10 g to 90 g may produce a concussion (Gurdijuan, 1964). More recently Zhang et al. (2004) attempted to determine concussive thresholds by recreating football impacts. It was determined that the probability of concussion for peak resultant linear accelerations at the centre of gravity of the head was estimated to be 66, 82, and 106 g for the 25^{th}, 50^{th}, and 80^{th} percentiles. The differences between the 25^{th} and 50^{th} percentiles is only 16 g, while the difference between the 50^{th} and 80^{th}

percentiles is 24 g. These relatively small differences in peak accelerations translate to a substantially increased risk of sustaining a concussion.

In the current study, the addition of the facial shielding was beneficial at some locations, but created problems at others. It was also noticed that when the helmets were tested at the front location with the polycarbonate shield, the screws used to attach the facial shield to the helmet were pushed back into the helmet. This helmet configuration may have increased the distance in which the helmet could decelerate the forces at impact and may explain why the front location had such a large difference between facial shielding conditions. Finally, it was observed that the screws that held the facial shields in place tore through the VN foam beneath the screws. That is, when the impactor struck this location, the foam was not thick enough to stop the screws from coming into contact with the headform, leaving contact marks. This outcome poses a safety concern because if an impact to the front location of a helmet with a facial shield were to occur to a human player, it could potentially lead to the screw penetrating an athlete's skin.

Concerning the facial shielding conditions, the results also revealed that after administering 270 impacts to each facial shielding condition, the helmets with no facial protection were the least efficient at reducing the peak linear acceleration transferred to the headform (M = 122.41 g, SD = 74.04), when compared to the helmet with the metal facial shielding (M =113.39 g, SD = 70.85), and the helmet with the polycarbonate facial shielding (M = 112.24 g, SD = 67.86). According to the second law of Newtonian physics, facial shields should, theoretically, reduce the linear accelerations acting on the head, independent of the location on which the helmet was struck (Hall, 2007). As stated by Graham et al. (2014), the added mass of the shielding increases the total mass of the system and, therefore, the inertia or the ability of the system to resist motion. Stated differently, if two identical forces acted on a

helmet without facial protection, one with less mass and the other one with a greater mass, than the one with facial protection will experience decreased head acceleration. This outcome, however, comes with a trade-off. That is, adding a facial shield will also increase the radius of the helmet (Graham et al., 2014). An increased radius translates into increased angular acceleration acting on the head. The current study, however, did not examine angular acceleration as its aim was to examine linear acceleration. The results of the peak linear acceleration analysis of this study revealed that facial shields did not always reduce the peak linear acceleration as expected. At the three different neckform stiffness levels, helmets with some form of facial shielding resulted in greater peak linear accelerations at some locations. One possible explanation for this observation was that the addition of the 0.5 kg shield did not significantly increase the mass, and, therefore, did not change the system's ability to reduce the acceleration. This outcome can be supported by examining the rear impact location in which there were no significant pairwise comparisons at any level of neckform stiffness.

Impact location and neckform stiffness. At the highest neckform stiffness level, all impact locations had significant simple main effects. The impact locations, however, exhibited a different trend with facial shielding combination, which was most effective at reducing the peak linear acceleration. Helmets with no facial shields received the highest peak linear acceleration at the front, side, and rear boss locations. They differed slightly as the metal facial shield was more effective at reducing the acceleration compared to the polycarbonate shield at the side and rear boss locations. Alternatively, the polycarbonate shield reduced the linear acceleration better than the metal shield at the front location. Another interesting finding at this neckform stiffness was that at the front boss and rear impact sites, the polycarbonate facial shielding condition received the greatest peak linear accelerations. The metal facial shielding combination was slightly more

effective at reducing the linear acceleration at the front boss location while no facial shield resulted in the lowest acceleration values observed at the rear impact location.

Comparing the outcome of this study to previous research. This study used a similar testing protocol to Carlson (2016) who also found a main effect across helmet impact locations. In Carlson's study, the greatest peak linear acceleration occurred at the front boss location (M = 132.03 g, SD = 65.76); followed by the front (M = 119.22g, SD = 42.51); side (M = 117.41 g, SD = 33.40); rear (M = 113.07 g, SD = 27.29); and the rear boss (M = 107.46 g, SD = 31.78). Although the impact speeds used were very similar, and the same head and neckform were used, the current study used a horizontal impacting method while Carlson's study used a drop testing method. The alterations in design likely led to differences in the dynamic response of the headform. These outcomes indicate that helmets may behave differently depending on the injury mechanisms. In the comparison of the horizontal and vertical impact simulations, the difference may be attributed to the impactors having different inbound momentums due to the mechanism of impact and the surface area over which the impact was delivered. Another key difference between the studies was that different helmets were used. Helmets differ in the types of foam used to line the inside of the helmet, the placement and thickness of these foams, as well as their outer shell geometry; all elements play a critical role on the performance of the helmet in minimizing the risk of injury (Rousseau et al., 2009). In addition, the quality of the helmet design and construction would also play a role in the rate at which the helmets deteriorate and attenuate forces as rated by Hockey STAR (Rowson et al., 2015). Other causes of discrepancies in the comparison may result from the use of different surrogate headforms such as the NOCSAE and the Hybrid III, which have been shown to respond differently to the same dynamic impact (Cobb, Zadnik, & Rowson, 2016; Kendall, Walsh, & Hoshikazi, 2012). This is not the case when

comparing Carlson's (2016) research findings to the current study, however, as the same surrogate headform was used for both studies. When comparing the findings of the current study to Walsh et al. (2011) during horizontal impacting using a similar protocol, Walsh et al. (2016) found that the side of the hockey helmet location (M = 132.8 g, SD = 3.8), allowed the most acceleration to be transferred to the head, followed by the front (M = 121.3 g, SD = 5.6); rear (M = 116.9 g, SD = 2.0); front boss (M = 102.1 g, SD = 5.1); and rear boss (M = 92.8 g, SD = 6.2) locations. The lack of consistency between these studies may more likely be due to factors relating to helmet differences and surrogate headform differences as previously stated by Cobb et al. (2016) and Kendall et al. (2012). The results do, however, illustrate that certain areas of the helmet are not as effective as others at reducing the linear accelerations and, therefore, are associated with a higher risk of injury. Additionally, this data emphasizes, the need to improve helmet design to better reduce the peak linear acceleration that a player's head will experience at all helmet impact locations.

When comparing the results of the current study to previous research in relation to neckform stiffness, the researcher found that the results mirrored the findings of Rousseau and Hoshizaki (2009), when the helmet was impacted without any facial protection. As the stiffness of the neckform was increased so did the peak linear acceleration transmitted to the headform. When all impacts with facial shielding were taken into account (impacts with facial shielding), the medium neckform stiffness level produced the highest mean peak linear accelerations, followed closely by the stiffest neckform condition, and then the least stiff condition.

The trend observed in the peak linear acceleration by Rousseau and Hoshizaki (2009) were also observed in the other facial shielding conditions of this study. The addition of the facial shield, however, may have altered this trend, but it is more likely that the greatest torque

setting on the neckform may not have been maintained after a given number of times impacted. Changes to the torque may have been caused by the rotation of the wire cable and possibly from changes to the material properties of the neckform. Using different neckforms at set stiffness levels when testing the effects of neckform stiffness would reduce the variability that is introduced when manually tightening a single neck. Finally, it is also possible that the neckforms used by Rousseau and Hoshizaki (2009) had greater differences between their neck stiffness levels than in the current study, which also could have contributed to the differences between the studies. Alternatively, Carlson (2016) used the same neckform as the one used in this study and reported that no interaction or main effects were found between the variables.

The Hybrid III neckform is currently the standard neckform used in most helmet testing research. The custom neckform was first used in a pilot study and tested on a drop impactor against a standardized impactor with a Hybrid III neckform (Carlson et al., 2016). Furthermore, the structure of these neckforms also differ. The Hybrid III is symmetrical in that discs are notched equally around the entire neckform. This configuration may not accurately simulate the responses that a human neck would display upon impact, as the neck has been shown to respond differently based on its anatomical movement (Ashrafiuon et al., 1996). To compensate for this, the custom neckform was designed with asymmetries, caused by the slits in the neoprene discs on the anterior side of the neckform and the indentations on the posterior portion (Carlson, 2016). Carlson (2016) performed static testing on the neckform and determined the resulting torques to bend the neck. The results of this testing revealed that the neckform had asymmetries in the torque required to bend the neckform. The lateral flexion movement of the neckform required the greatest amount of torque to cause the same amount of bending as compared to flexion and extension movements. These asymmetries could alter kinematic data produced by the

headform. The neck's greater ability to bend at the front and rear locations means that there is a greater distance in which deceleration can occur. This idea can be supported by the work of Foreman (2010), who demonstrated that neck asymmetries may change the peak linear acceleration response at various locations.

Currently, only the Hybrid III neckforms and the custom designed neckform used in this study are discussed in the literature. Some headforms are still tested when mounted on rigid arms but then the dynamic responses of the neckforms are lost (MacAllister, 2013). These neckforms do add to helmet impact simulation, but with technological advancements such as three-dimensional printing, the designs of neckforms can be further improved with printed components that simulate the bones, ligaments, and muscles within the cervical spine.

Severity Index (SI) Analysis Results

Three-way interaction. A three-way mixed factorial ANOVA, with repeated measures on facial shielding and impact location factors was conducted for SI measures. Statistical significance was tested at $p < .05$. This analysis revealed a statistically significant three-way interaction between facial shielding, impact location, and neckform stiffness on SI measures, $F(3.28, 83.72) = 4.51$, $p = .004$, $\eta_p^2 = .15$.

Two-way interactions. Statistically significant two-way interactions between facial shielding and location for SI were observed at the low neckform stiffness level, $F(1.18, 20.12) = 17.15$, $p < .001$, $\eta_p^2 = .50$, (Figure 22).

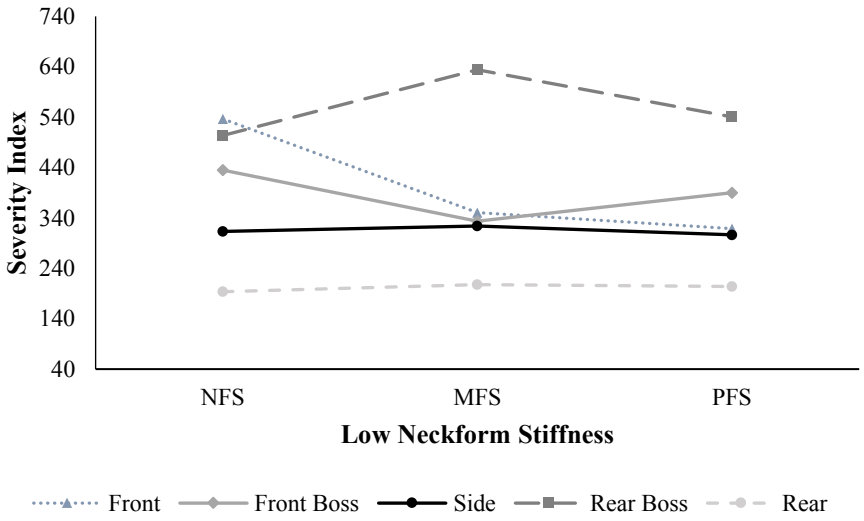

Figure 22 .Severity index at low neckform stiffness. The five impact locations are represented by the various lines, and the facial shielding conditions are represented by the grouping labels: no facial shielding (NFS), metal facial shielding (MFS), and by polycarbonate facial shielding (PFS).

For the medium neckform stiffness, a two-way interaction between impact location and facial shielding condition was found, F (1.36, 23.14) = 12.77, $p \leq .001$, $\eta_p^2 = .43$ (Figure 23).

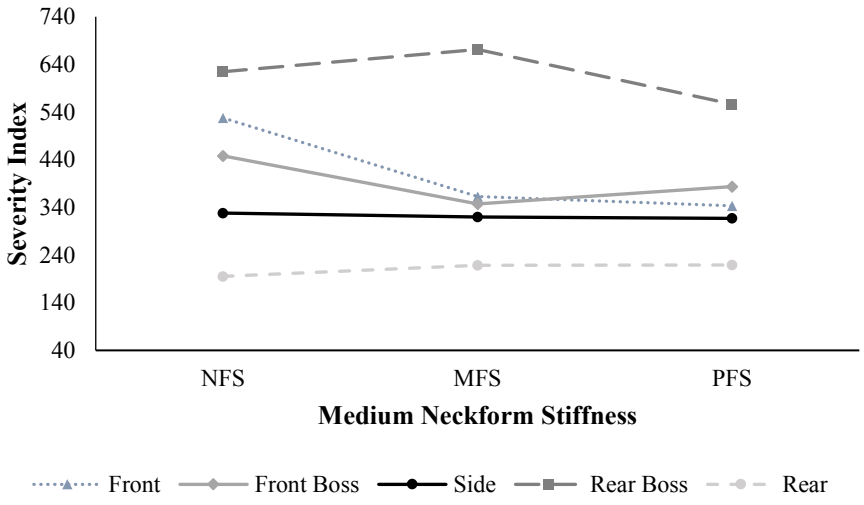

Figure 23. Severity index at medium neckform stiffness. The five impact locations are represented by the various lines, and the facial shielding conditions are represented by the grouping labels: no facial shielding (NFS), metal facial shielding (MFS), and by polycarbonate facial shielding (PFS).

For the high neckform stiffness level, a two-way interaction between impact location and facial shielding condition was also found, F (1.26, 21.38) = 16.26, $p < .001$, $\eta_p^2 = .59$, (Figure 24).

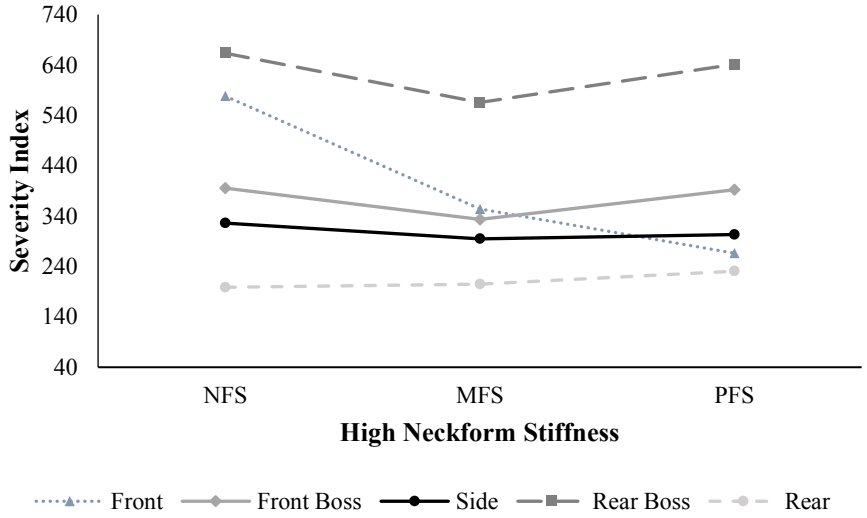

Figure 24. Severity index at the high neckform stiffness. The various lines represent the different impact locations, while facial shielding conditions are represented by no facial shielding (NFS), metal facial shielding (MFS), and by polycarbonate facial shielding (PFS).

Simple main effects of impact location at low neckform stiffness.

No facial shielding. A statistically significant simple main effect of impact location on helmets with no facial shields when the neckform was at its lowest stiffness, F (1.11, 18.84) = 18.53, $p < .001$, $\eta_p^2 = .52$. The mean SI at each impact location at the low neckform stiffness with no facial shielding were as follows: front (M = 536.58, SD = 444.05); rear boss (M = 503.73, SD = 477.55); front boss (M = 434.92, SD = 382.93); side (M = 313.19, SD = 292.58); and rear (M = 193.61, SD = 138.34). The front location was significantly greater than the front boss ($p < .001$); the side location ($p < .001$); and the rear location ($p = .002$). Next, the front boss location was significantly greater than the side ($p \leq .001$); and the rear location ($p = .007$). While the side location was only significantly greater than the rear location ($p = .05$). Finally, the mean

SI at the rear boss was significantly greater than the side (p = .008); and the rear location (p = .013).

Metal facial shielding. Next a statistically significant simple main effect of impact location on helmets with metal shields at the lowest neckform stiffness was observed, F (1.03, 17.45) = 15.13, $p < .001$, $\eta_p^2 = .47$. The mean SI for each impact location at this condition were as follows: rear boss (M = 634.11, SD = 611.78); front (M = 350.56, SD= 286.37); front boss (M= 333.56, SD= 296.66); side (M= 324.00, SD= 284.80); and rear (M = 207.73, SD = 150.79). The front location was significantly greater than the rear location (p = .004). Next, the front boss location was significantly greater than the rear location (p = .022). The side location was only significantly greater than the rear (p = .02). Finally, the mean SI at the rear boss was significantly greater than the front (p = .021); front boss (p = .009); side (p = .009); and the rear location (p = .011).

Polycarbonate facial shielding. Next a statistically significant simple main effect of impact location for helmets with polycarbonate facial shielding when the neckform stiffness was at the lowest stiffness was found F (1.06, 18.01) = 11.97, p = .002, $\eta_p^2 = .41$. The mean SI at each impact location at the low neckform stiffness with polycarbonate facial shielding were as follows: rear boss (M = 540.46, SD = 540.10); front boss (M = 389.92, SD = 350.10); front (M = 318.78, SD = 233.33); side (M = 306.55, SD = 279.10); and rear (M = 203.84, SD = 145.82). The front location was significantly greater than the rear ($p \leq .001$). Next, the front boss location was significantly greater than the side (p = .002); and the rear location (p = .014). Finally, the mean SI at the rear boss was significantly greater than the front boss (p = .041); the side (p = .015); and the rear location (p = .022).

Simple main effects of impact location at medium neckform stiffness.

No facial shielding. There was also a statistically significant simple main effect of impact location for helmets with no facial shields when the neckform stiffness was at the medium stiffness F (1.03, 17.48) = 17.88, $p < .001$, $\eta_p^2 = .51$. The mean SI at each impact location at the medium neckform stiffness with no facial shielding were as follows: rear boss (M = 624.36, SD = 594.47); front (M = 527.67, SD = 450.00); front boss (M = 448.07, SD = 409.19); side (M = 328.08, SD = 296.00); and rear (M = 195.30, SD = 149.57). The mean SI for the front location was again significantly greater than the front boss ($p < .001$); the side location ($p < .001$); and the rear location ($p = .002$). Next, the mean SI for the front boss location was significantly greater than the side ($p < .001$); and the rear location ($p = .007$). The SI for the side location was significantly greater than the rear location ($p = .014$). Finally, the mean SI at the rear boss location was significantly greater than the front boss ($p = .01$); the side ($p = .006$); and the rear location ($p = .008$).

Metal facial shielding. There was also a statistically significant simple main effect of impact location for helmets with metal shields when the neckform stiffness was at its medium stiffness F (1.04, 17.66) = 17.30, $p \leq .001$, $\eta_p^2 = .50$. The mean SI at each impact location at the medium neckform stiffness with metal facial shielding were as follows: rear boss (M = 671.28, SD = 634.78); front (M = 362.82, SD = 289.56); front boss (M = 347.27, SD = 319.30); side (M = 319.57, SD = 281.00); and rear (M = 218.58, SD = 188.62). The mean SI for the front location was again significantly greater than the side location ($p = .009$); and the rear location ($p = .002$). Next, the mean SI for the front boss location was significantly greater than rear location ($p = .009$); while the SI for the side location was significantly greater than the rear location ($p = .005$). Finally, the mean SI at the rear boss location was significantly greater than the front ($p = .017$); front boss ($p = .005$); the side ($p = .006$); and the rear location ($p = .005$).

Polycarbonate facial shielding. There was also a statistically significant simple main effect of impact location for helmets with polycarbonate shields when the neckform stiffness was at the medium neckform stiffness F (1.13, 19.21) = 12.76, $p \leq .001$, $\eta_p^2 = .43$. The mean SI at each impact location at the medium neckform stiffness with polycarbonate facial shielding were as follows: rear boss (M = 556.68, SD = 540.52); front boss (M = 383.36, SD = 346.93); front (M = 343.30, SD = 228.87); side (M = 316.93, SD = 285.14); and rear (M = 219.13, SD = 183.55). The mean SI for the front location was again significantly greater than the rear location ($p < .001$). Next, the mean SI for the front boss location was significantly greater than the side ($p = .008$); and rear location ($p = .007$). The SI for the side location was significantly greater than the rear location ($p = .012$). Finally, the mean SI at the rear boss location was significantly greater than the front boss ($p = .018$); the side ($p = .01$); and the rear location ($p = .01$).

Main effects of impact location at high neckform stiffness.

No facial shielding. A statistically significant simple main effect of impact location for helmets with no facial shields when the neckform stiffness at its highest stiffness was observed F (1.04, 17.63) = 19.20, $p < .001$, $\eta_p^2 = .53$. The mean SI at each impact location at a high neckform stiffness with no facial shielding were as follows: rear boss (M = 663.16, SD = 628.88); front (M = 578.12, SD = 470.99); front boss (M = 395.41, SD = 343.38); side (M = 326.03, SD = 293.04); and rear (M = 198.68, SD = 153.73). The SI for the front location was again significantly greater than the front boss ($p < .001$); the side location ($p < .001$); and the rear location ($p \leq .001$). The front boss location was significantly greater than the side location ($p = .001$); as well as the rear location ($p \leq .001$). The side location was also significantly greater than the rear location ($p = .013$). Finally, the mean SI at the rear boss location was significantly greater than the front boss ($p = .011$); the side ($p = .005$); and the rear location ($p = .007$).

Metal facial shielding. Another statistically significant simple main effect of impact location for helmets with metal facial shields when the neckform stiffness at its highest stiffness was observed F (1.06, 17.95) = 12.29, p = .002, η_p^2 = .42. The mean SI at each impact location at a high neckform stiffness with no facial shielding were as follows: rear boss (M = 565.50, SD = 586.43); front (M = 354.32, SD = 289.75); front boss (M = 333.40, SD = 311.14); side (M = 294.79, SD = 279.45); and rear (M = 205.11, SD = 157.99). The SI for the front location was again significantly greater than the side location ($p \leq .001$); and the rear location (p = .003). The front boss location was significantly greater than the side location (p = .047); and the rear location (p = .03). Finally, the mean SI at the rear boss location was significantly greater than the front boss (p = .027); the side (p = .017); and the rear location (p = .024).

Polycarbonate facial shielding. Finally, a statistically significant simple main effect of impact location for helmets with polycarbonate shields when the neckform stiffness at its highest stiffness was observed F (1.06, 18.05) = 15.22, $p \leq .001$, η_p^2 = .47. The mean SI at each impact location at a high neckform stiffness with polycarbonate shielding were as follows: rear boss (M = 641.25, SD = 605.34); front boss (M = 392.01, SD = 350.83); side (M = 303.17, SD = 264.89); front (M = 266.36, SD = 169.06); and rear (M = 230.65, SD = 204.09). The SI for the front boss location was significantly greater than the side location (p = .01); and the rear location (p = .003). The side location was significantly greater than the rear location (p = .005). Finally, the mean SI at the rear boss location was significantly greater than the front (p = .024); the front boss (p = .008); side (p = .006); and the rear location (p = .005).

Simple main effects of facial shielding at low neckform stiffness.

Front location. There was a statistically significant simple main effect for facial shielding on SI at the front impact location at low neckform stiffness F (1.03, 17.53) = 19.42, p <

.001, η_p^2 = .53. The mean SI for each of the different facial shielding combinations were as follows: the helmet with no facial shield (M = 536.58, SD = 444.04); the metal facial shield combination (M = 350.56, SD = 286.37); and the polycarbonate facial shield combination (M = 318.78, SD = 233.33). The SI experienced by the headform at the front location at a low neckform stiffness was statistically significantly higher in the helmet with no facial shield compared to the helmet with the metal facial shielding ($p < .001$); and high impact polycarbonate shield ($p = .002$).

Front boss location. There was a statistically significant simple main effect for facial shielding on SI at the front boss impact location at low neckform stiffness F (1.40, 17.82) = 22.56, $p < .001$, $\eta_p^2 = .57$. The mean SI for each of the different facial shielding combinations were as follows: the helmet with no facial shield (M = 434.92, SD = 382.93); the polycarbonate facial shield combination (M = 389.91, SD = 350.10); and the metal facial shield combination (M = 333.56, SD = 296.67). The SI at the front boss location at a low neckform stiffness was statistically significantly higher in the helmet with no facial shield compared to the helmet with the metal ($p < .001$); and high impact polycarbonate shield ($p < .001$). There was also a statistically significant difference in the mean SI between the helmet with polycarbonate and metal facial shielding. ($p = .002$).

Side location. There was statistically significant simple main effect for facial shielding on SI at the side impact location at low neckform stiffness F (2, 34) = 4.12, $p = .025$, $\eta_p^2 = .20$. The mean SI for each of the different facial shielding combinations were as follows: the metal facial shield combination (M = 324.00, SD = 284.80); the helmet with no facial shield (M = 313.19, SD = 292.58); and the polycarbonate facial shield combination (M = 306.56, SD =

279.10). The simple comparison of the different facial shielding conditions revealed that at the side location the risk of injury (p = .008), then the polycarbonate facial shield.

Rear boss location. There was a statistically significant simple main effect for facial shielding on SI at the rear boss impact location at low neckform stiffness F (1.34, 22.77) = 12.68, $p \leq .001$, $\eta_p^2 = .43$. The mean SI for each of the different facial shielding combinations were as follows: the metal facial shield combination (M = 634.11, SD = 611.78); the polycarbonate facial shield combination (M = 540.46, SD = 540.10); and the helmet with no facial shield (M = 503.72, SD = 477.55). The mean SI at the rear boss location at a low neckform stiffness was statistically significantly higher in the helmet with a metal shield compared to the helmet with the none (p = .005); and high impact polycarbonate shield (p < .001).

Rear location. There was a statistically significant simple main effect for facial shielding on SI at the rear impact location at low neckform stiffness F (2, 34) = 9.09, $p \leq .001$, $\eta_p^2 = .35$. The mean SI for each of the different facial shielding combinations were as follows: the metal facial shield combination (M = 207.72, SD = 150.79); the polycarbonate facial shield combination (M = 203.84, SD = 145.81); and the helmet with no facial shield (M = 193.61, SD = 138.34). The mean SI at the rear location was statistically significantly greater in the metal facial shield (p = .008); and polycarbonate facial shielding (p = .015), as compared to a helmet with no facial shield.

Simple main effects of facial shielding at medium neckform stiffness.

Front location. There was a statistically significant simple main effect for facial shielding on SI at the front impact location at medium neckform stiffness F (1.06, 18.04) = 12.20, p = .002, $\eta_p^2 = .42$. The mean SI for each of the different facial shielding combinations were as follows: the helmet with no facial shield (M = 527.67, SD = 450.00); the metal facial

shield combination (M = 362.82, SD = 289.56); and the polycarbonate facial shield combination (M = 343.30, SD = 228.87). The SI at the front location at a medium neckform stiffness was statistically significantly higher in the helmet with no facial shield compared to the helmet with the metal facial shields (p = .002); and high impact polycarbonate shields (p = .013).

Front boss location. There was a statistically significant simple main effect for facial shielding on SI at the front boss impact location at medium neckform stiffness F (1.18, 19.99) = 16.81, p < .001, η_p^2 = .50. The mean SI for each of the different facial shielding combinations were as follows: the helmet with no facial shield (M = 448.07, SD = 409.19); the polycarbonate facial shield combination (M = 383.36, SD = 350.10); and the metal facial shield combination (M = 347.27, SD = 319.30). The SI at the front boss location at a medium neckform stiffness was statistically significantly higher in the helmet with no facial shield compared to the helmet with the metal facial shield (p = .002); and high impact polycarbonate shield (p = .002). There was also a significant difference in the SI between the helmet with polycarbonate and metal facial shielding (p = .018).

Side location. There was not a statistically significant simple main effect for facial shielding on SI at the side impact location at medium neckform stiffness F (2, 34) = 2.16, p = .13, η_p^2 = .11.

Rear boss location. There was a statistically significant simple main effect for facial shielding on SI at the rear boss impact location at medium neckform stiffness F (1.25, 21.28) = 17.58, p < .001, η_p^2 = .51. The mean SI for each of the different facial shielding combinations were as follows: the metal facial shield combination (M = 671.28, SD = 540.52); the helmet with no facial shield (M = 624.36, SD = 594.47); and the polycarbonate facial shield combination (M = 556.68, SD = 540.52). The mean SI at the rear boss location at a medium neckform stiffness

was statistically significantly higher in the helmet with a metal facial shield compared to the helmet with none ($p = .008$); and high impact polycarbonate shield ($p \leq .001$). There was also a statistically significant difference in the mean SI between the helmet no facial shielding and polycarbonate facial shielding ($p < .001$).

Rear location. There was a statistically significant simple main effect for facial shielding on SI at the rear impact location at medium neckform stiffness F (1.30, 22.18) = 5.50, $p = .021$, $\eta_p^2 = .24$. The mean SI for each of the different facial shielding combinations were as follows: the polycarbonate facial shield combination (M = 219.13, SD = 183.55); the metal facial shield combination (M = 218.58, SD = 188.62); and the helmet with no facial shield (M = 195.30, SD = 149.57). The only statistically significant simple comparison for this condition was found between helmets with polycarbonate facial shields and the helmet without facial shielding ($p = .047$).

Simple main effects of facial shielding at high neckform stiffness.

Front location. There was a statistically significant simple main effect for facial shielding on SI at the front impact location at a high neckform stiffness F (1.02, 17.30) = 19.12, $p < .001$, $\eta_p^2 = .53$. The mean SI for each of the different facial shielding combinations were as follows: the helmet with no facial shield (M = 578.12, SD = 470.98); the metal facial shield combination (M = 354.32, SD = 289.75); and the polycarbonate facial shield combination (M = 266.36, SD = 169.06). The SI at the front location at a high neckform stiffness was statistically significantly higher in the helmet with no facial shield compared to the helmet with the metal facial shield ($p < .001$); and high impact polycarbonate shield ($p < .001$). There was also a statistically significant difference in the mean SI between the helmet with metal and polycarbonate facial shielding ($p = .032$).

Front boss location. There was a statistically significant simple main effect for facial shielding on SI at the front boss impact location at a high neckform stiffness F (1.37, 23.30) = 16.00, $p < .001$, $\eta_p^2 = .49$. The mean SI for each of the different facial shielding combinations were as follows: the helmet with no facial shield (M = 395.41 SD = 343.93); the polycarbonate facial shield combination (M = 392.01, SD = 350.83); and the metal facial shield combination (M = 333.40, SD = 311.14). The mean SI at the front boss location at a high neckform stiffness was statistically significantly higher in the helmet with no facial shield compared to the helmet with the metal facial shield ($p < .001$). There was also a statistically significant difference in the SI between the helmet with polycarbonate and metal facial shielding, ($p = .005$).

Side location. There was a statistically significant simple main effect for facial shielding on SI at the side location at a high neckform stiffness F (2, 34) = 8.56, $p \leq .001$, $\eta_p^2 = .34$. The mean SI for each of the different facial shielding combinations were as follows: the helmet with no facial shield (M= 326.03, SD= 293.04); the polycarbonate facial shield combination (M = 303.17, SD = 264.89); and the metal facial shield combination (M = 294.79, SD = 264.89). The mean SI at the side location at a high neckform stiffness was statistically significantly higher in the helmet with no facial shield compared to the helmet with the metal facials ($p = .001$); and polycarbonate shield ($p = .043$).

Rear boss location. There was a statistically significant simple main effect for facial shielding on SI at the rear boss impact location at a high neckform stiffness F (1.44, 24.71) = 17.69, $p < .001$, $\eta_p^2 = .51$. The mean SI for each of the different facial shielding combinations were as follows: the helmet with no facial shield (M = 663.16, SD = 628.88); the polycarbonate facial shield combination (M = 641.25, SD = 605.34); and the metal facial shield combination (M = 565.50, SD = 586.43). The mean SI at the rear boss location at a medium neckform

stiffness was statistically significantly higher in the helmet with no metal facial shield compared to the helmet with metal facial shield ($p < .001$). There was also a statistically significant difference in the mean SI between the helmet with metal and polycarbonate facial shielding ($p = .006$).

Rear location. There was a statistically significant simple main effect for facial shielding on SI at the rear impact location at a high neckform stiffness F (1.08, 18.28) = 5.71, $p = .026$, $\eta_p^2 = .25$. All pairwise comparisons were run between the different facial shielding conditions with a Bonferroni adjustment. The mean SI at the side location on a high neckform stiffness, revealed that were not significant difference between the facial shielding conditions.

Discussion

Simulating helmet impacts in the lab is an approach meant to mimic how helmets are impacted in a game to better understand injury mechanisms. In Canada, over 475,000, about 75% of all hockey players are required to wear full facial shielding (Hockey Canada, 2015). Consequently, most hockey players who receive contact to the head will be wearing a helmet with full facial protection. Given this situation, it is critical to understand the extent to which helmet facial shielding minimizes injuries to the head upon impact.

To assess the severity of the risk of head injury, the SI measure is used to determine the probability of head injuries or skull fractures for any given impact (Greenwald et al., 2008). This measure was used in the current study to assess the interaction among impact location, facial shielding protection, and neckform stiffness on risk of head injury (Ouckama, 2013). The results revealed that the facial shielding variable interacted with both neckform stiffness and impact location on the SI measures. More specifically, SI measures were dependent on the facial shielding condition and specific location where the helmet was impacted.

Facial shielding and risk of injury. Lemair and Pearsall (2007) also reported differences in SI measures when directly impacting different facial shields. Comparisons of the present study to theirs, however, are challenging as Lemair and Pearsall used modified impact locations to ensure that the facial shield would be directly impacted at the level of the basic plane. Furthermore, the risk of injury data is not sufficiently discussed by the authors. Lemair and Pearsall (2007) did, however, report that the different locations tested on the facial shield led to various SI measures, possibly suggesting that contact to certain areas of the facial shield may lead to a greater likelihood of injury.

The results of the current study, build on the research work of Lemair and Pearsall (2007) by providing new information on how facial shielding alters SI when the facial shield is not directly impacted, but still present on a helmet. That is, the outcome of the current study now provides a more comprehensive picture of how the helmet facial shielding combination cooperates with the helmet, and which facial shielding conditions leave players more vulnerable to injury.

Other sporting helmets such as lacrosse helmets have been tested by Caswell and Deivert (2002) using SI as an outcome variable. The lacrosse helmets were tested with metal facial shielding and were also not directly impacted in the study (Caswell & Deivert, 2002). The current research adds to the literature as it is the first studies to test both polycarbonate and metal full facial shields attached to the hockey helmet when measuring SI.

Caswell and Deivert's (2002) work was also built upon by comparing different facial shielding conditions without direct impact on the facial shield. When considering the impacts administered to each facial shielding condition independent of the location and neckform stiffness level, helmets with no facial protection typically demonstrated the highest SI measures.

This condition also had the greatest number of instances (17) where the SI exceeded 1,200 SI, a value that should never be exceeded in helmet testing as a severe brain injury is likely to occur (Biasca et al., 2002; NOCSAE, 2016a). The helmet with metal facial shielding combination, produced the next greatest mean SI value with some impacts (11) exceeding the accepted threshold values. Lastly, the polycarbonate facial shielding condition on average received the lowest SI measure, and had the lowest occurrence of impacts (10) producing SI values surpassing 1,200.

The rationale used to explain why the peak linear acceleration was greater in helmets with facial shields also applies to the findings concerning SI. As previously stated, the added mass of the facial shielding increases the inertia of the system resulting in lower acceleration values (Hall, 2007). The results of the current study supported this rationale and indicated that the helmets with facial shields produced lower SI values. The results, however, revealed that the helmet with no facial shielding did not always produce the greatest SI measures across the three different neckform stiffness levels. Similar to the peak linear acceleration measures, the addition of the 0.5 kg shield might not have sufficiently increased the mass of the helmet to change the system's ability to reduce the SI values.

Impact location and risk of injury. Other factors such as impact location contributed to the significant interaction with facial shielding at different levels of neckform stiffness on measures of SI. Helmets with no facial shields and metal facial shields displayed significant simple main effects for impact location at each level of neckform stiffness on SI measures. The rear boss, for example, produced the greatest risk of injury followed by the front, front boss, side, and rear location. Helmets with polycarbonate shields also had statistically significant simple main effects at each level of neckform stiffness. For this type of shield, however, the rear boss

and rear locations experienced the highest and lowest SI measures respectively, but the other impact locations (i.e., front boss, side, and front) did not follow any trends across the different neckform stiffness.

These findings further confirm that helmet performance in terms of impact severity reduction is non-uniform across impact locations. These outcomes can be corroborated with previous research findings. For example, Caswell and Deivert (2002) reported differences between the front and rear boss locations on lacrosse helmets. Carlson (2016) also reported a significant main effect of the impact location on SI. There are, however, several key differences between the current research work and Carlson's (2016). The first difference is the brand and model of the helmets used. The geometry of each type of helmet differs, as well as, the areas where the attenuation liners are positioned (Rousseau et al., 2009). The second key difference was that the helmets in this study were impacted using a horizontal pneumatic system, while Carlson's study tested helmets using a vertical drop testing system. Finally, Carlson's study did not consider facial shielding and instead focused on the angle of impact. Both studies, however, do support that an athlete could be exposed to an increased risk of injury depending upon where on the helmet, they are contacted. Nonetheless, the current study builds on Carlson's findings and suggests that the risk of injury is also dependent on the type of facial shielding attached to the helmet.

To further support these findings, a total of 38 instances were recorded in the current study across locations to assess the number of impacts exceeding the NOCSAE threshold value of 1,200 SI, which is an indication of head injury. Thirty of these impacts occurred at the rear boss exceeding the threshold value of 1,200 SI. From the remaining 8 impacts, 6 at the front location and 2 at the front boss location exceeded the threshold value of 1,200 SI. Several factors

may contribute to exceeding these SI threshold levels across impact locations. These factors may be related to neckform asymmetry (Ashrafiuon et al., 1996), as well as, the geometry of the helmet with and without facial shielding (Halstead, 1998; Lemair & Pearsall, 2007). Based on the location at which the helmet was struck, these factors might influence the acceleration and/or duration of the impact leading to greater SI measures.

Impact location is thought to be associated with the player's susceptibility to receiving a concussion (Greenwald et al., 2008). Lateral impacts are often thought to be associated with the greatest risk of receiving a concussion (Hodgson et al, 1983). In this study, however, the side impact location on the helmet did not have the highest SI values. In fact, the rear boss location had the greatest likelihood of injury across impact conditions. The front and front boss locations were consistently the next highest in terms of risk of injury. This outcome is similar to the findings of Carlson (2016), who reported that highest risk of injury at these locations. Although the findings support the literature that differences do exist on SI measures when impacting helmets at the various testing locations, it is unclear exactly why this is the case and this concern highlights the need for further investigation (Carlson, 2016; Lemair & Pearsall, 2007; Walsh et al., 2011).

Neckform stiffness and risk of injury. In terms of the main effects for neckform stiffness levels on measures of SI, this study did not produce any statistically significant results. This outcome parallels the findings of both Carlson (2016) and Rousseau and Hoshizaki (2009), which found that SI measures did not differ for the three different neckform stiffness levels used. Rousseau and Hoshizaki (2009) did report, however, that the least stiff neckform condition resulted in the greatest SI measures at all speeds in which the headform was impacted. Additionally, as the stiffness increased, a general trend observed was that the SI decreased, just

as it did with the peak linear acceleration. The lack of statistically significant main effects of neckform stiffness in each study implies that the impact duration may not have been sufficiently altered by the different levels of neckform stiffness.

The trends concerning the SI measures in this study were congruent with the peak linear acceleration trends discussed above. The trends for which neckform stiffness level had the highest risk of injury, however, were different between the current study and previous research work (Carlson, 2016; Rousseau & Hoshizaki, 2009), but these differences may also be explained by the factors related to different types of injury mechanisms such as vertical or horizontal impacts.

Finally, no simulation study has yet produced statistically significant results that suggest an increase in neckform stiffness aids in head injury protection. Furthermore, neckforms such as the Hybrid III, have been criticized for their inability to respond as a human head would in an impact (Ono et al., 2003). The neckform used in the current study, however, is thought to be able to be adjusted for different neckform stiffness or compliance levels. It is important to highlight that there is a need to develop better mechanical neckforms to simulate human neck strength as this is the only ethical and viable way to conduct head impact testing using procedures with repeated impacts (Walsh et al., 2011).

Energy Loading Analysis Results

Three-way interaction. A three-way mixed factorial ANOVA, with repeated measures on facial shielding and impact location was conducted for energy loading measures. The results, of this analysis revealed a statistically significant three-way interaction between facial shielding, impact location, and neckform stiffness on energy loading measures, F (16, 408) = 2.25, p = .004, η_p^2 = .08.

Two-way interactions. Statistically significant two-way interactions between facial shielding and location for energy loading was observed at the lowest neckform stiffness, F (8, 136) = 13.74, $p < .001$, $\eta_p^2 = .45$ (Figure 25).

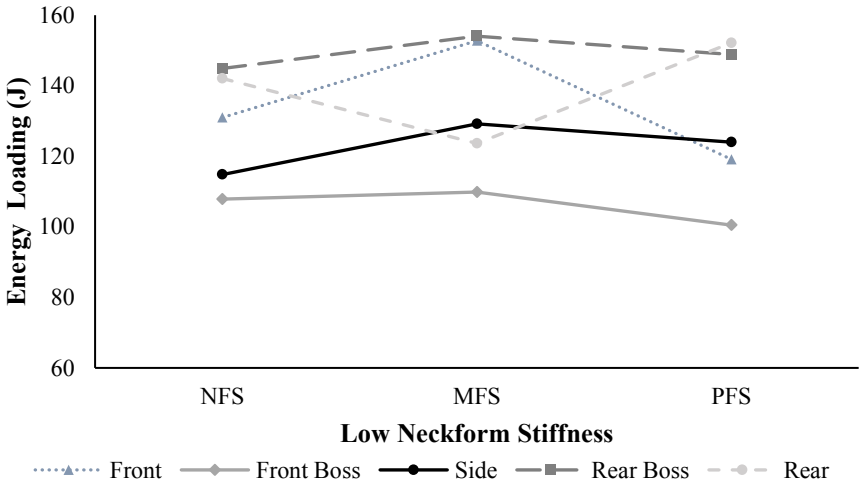

Figure 26. Energy loading at low neckform stiffness. The five impact locations are represented by the various lines, and the facial shielding conditions are represented by the grouping labels: no facial shielding (NFS), metal facial shielding (MFS), and by polycarbonate facial shielding (PFS).

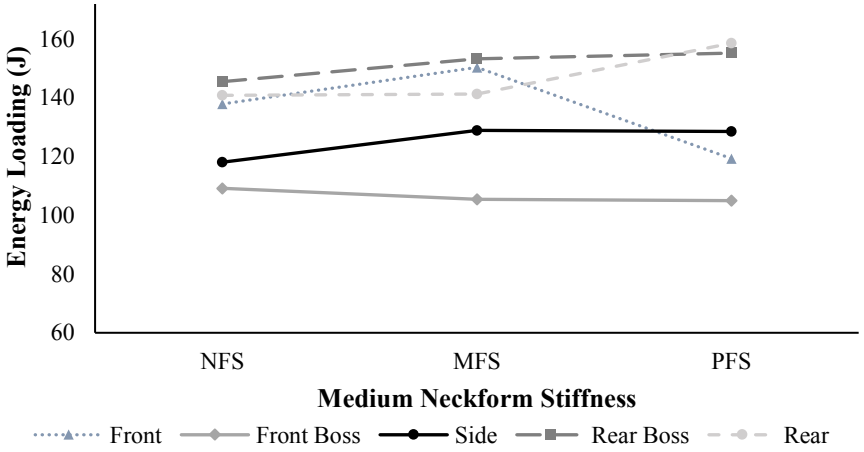

Figure 25. Energy loading at medium neckform stiffness. The five impact locations are represented by the various lines, and the facial shielding conditions are represented by the grouping labels: no facial shielding (NFS), metal facial shielding (MFS), and by polycarbonate facial shielding (PFS).

For a medium neckform stiffness, a two-way interaction between impact location and facial shielding condition was also observed; F (8, 136) = 10.51, $p < .001$, $\eta_p^2 = .38$ (Figure 26).

Finally, for the high neckform stiffness level, a two-way interaction between impact location and facial shielding condition was found, F (4.15, 70.54) = 8.36, $p < .001$, $\eta_p^2 = .33$., (Figure 27).

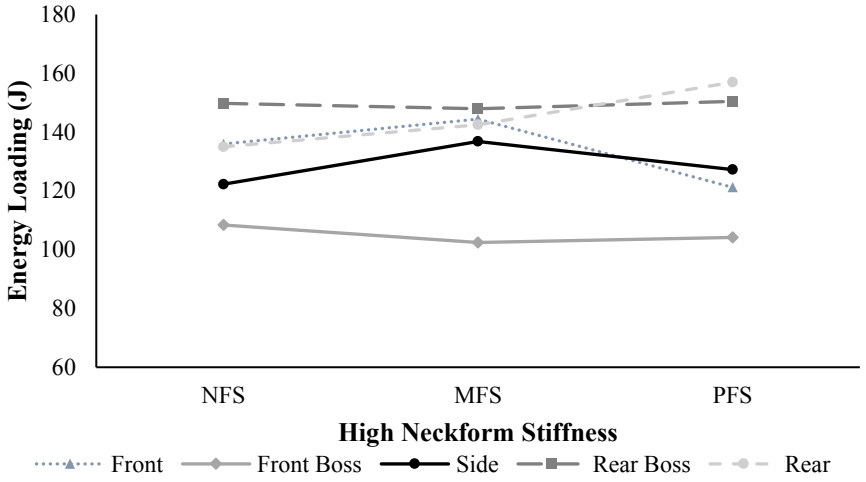

Figure 27. Energy loading at the high neckform stiffness. The various lines represent the different impact locations, while facial shielding conditions are represented by no facial shielding (NFS), metal facial shielding (MFS), and by polycarbonate facial shielding (PFS).

Simple main effects of impact location at low neckform stiffness.

***No facial shielding*.** A statistically significant simple main effect of impact location for helmets with no facial shields was found for the lowest neckform stiffness, F (1.53, 26.09) = 12.65, $p < .001$, $\eta_p^2 = .43$. The mean energy loaded onto each impact location at the low neckform stiffness with no facial shielding were as follows: rear boss (M = 144.89 J, SD = 75.01); rear (M = 142.08 J, SD = 73.01); front (M = 131.03 J, SD = 56.04); side (M = 114.81 J, SD = 58.48); and front boss (M = 107.84 J, SD = 36.10). The energy loaded onto the front location was significantly greater than the front boss ($p = .016$); and the side location ($p \leq .001$). Next, the mean energy loading at the rear boss was significantly greater than the front boss ($p = .017$); and side locations ($p < .001$). The rear was also significantly greater than the front boss ($p = .042$); and side locations ($p \leq .001$).

Metal facial shielding. A statistically significant simple main effect of impact location for helmets with metal shields when the neckform stiffness was at the lowest stiffness was found F (2.00, 33.99) = 16.04, $p < .001$, $\eta_p^2 = .50$. The mean energy loading at each impact location at the low neckform stiffness with metal facial shielding were as follows: rear boss (M = 154.05 J, SD = 77.91); front (M = 152.77 J, SD= 73.03); side (M = 129.19 J, SD = 61.76); rear (M = 123.64 J, SD = 70.70); and front boss (M = 109.86 J, SD = 38.29). The energy loaded onto the front location was significantly greater than the front boss ($p \leq .001$); the side location ($p < .001$); and the rear location ($p < .001$). Next, the mean energy loading at the rear boss was also significantly greater than the front boss *(*$p = .003$); side ($p \leq .001$); and rear locations ($p \leq .001$).

Polycarbonate facial shielding. Next a statistically significant simple main effect of impact location for helmets with polycarbonate shields when the neckform stiffness was at the lowest stiffness was found F (2.14, 36.35) = 12.10, $p < .001$, $\eta_p^2 = .42$. The mean energy loading at each impact location at the low neckform stiffness with polycarbonate facial shielding were as follows: rear (M = 152.17 J, SD = 79.71), rear boss (M = 148.86 J, SD= 78.49); side (M = 124.04 J, SD = 59.72); front (M = 119.13 J, SD = 62.79); and front boss (M = 100.48 J, SD = 34.93). First, the side location was significantly greater than the front boss location ($p = .029$). Next, the rear boss location was significantly greater than the front ($p = .04$); the front boss location ($p = .004$); and the side ($p \leq .001$). Lastly, the mean energy loading at the rear location was significantly greater than the front boss ($p = .007$); and side ($p = .018$).

Simple main effects of impact location at medium neckform stiffness.

No facial shielding. A statistically significant simple main effect of impact location for helmets with no facial shields when the neckform stiffness was at the medium stiffness was a found upon analysis, F (1.38, 23.37) = 9.40, $p = .003$, $\eta_p^2 = .36$.The mean energy loaded at each

impact location at the medium neckform stiffness with no facial shielding were as follows: rear boss (M = 145.44 J, SD = 70.04); rear (M = 140.76 J, SD = 85.96); front (M = 137.03 J, SD = 59.68); side (M = 118.03 J, SD = 60.26); and front boss (M = 109.16 J, SD = 38.79). The mean energy loading for the front location was significantly greater than the front boss ($p = .009$); as well as the side location ($p < .001$). The mean energy loading for the rear boss location was also significantly greater than the front boss ($p = .008$); and side location ($p < .001$).

Metal facial shielding. Next, a statistically significant simple main effect of impact location for helmets with metal shields when the neckform stiffness was at the medium stiffness was observed F (1.68, 28.58) = 12.84, $p < .001$, $\eta_p^2 = .43$. The mean energy loaded onto each impact location at the medium neckform stiffness with metal facial shielding were as follows: rear boss (M = 153.17 J, SD = 70.79); front (M = 150.30 J, SD = 69.87); rear (M = 141.25 J, SD = 89.29); side (M = 128.86 J, SD = 63.59); and front boss (M = 105.36 J, SD = 40.96). The mean energy loading for the front location was again significantly greater than the front boss location, ($p < .001$); and the side location ($p = .002$). While the mean energy loading for the side location was significantly greater than the front boss location ($p = .012$). Finally, the energy loading onto the rear boss location was significantly greater than the front boss ($p < .001$); and the side ($p < .001$).

Polycarbonate facial shielding. There was also a statistically significant simple main effect of impact location for helmets with polycarbonate facial shielding when the neckform stiffness was at the medium stiffness F (1.47, 24.97) = 17.03, $p < .001$, $\eta_p^2 = .50$. The mean energy loading at each impact location at the medium neckform stiffness with polycarbonate shielding were as follows: rear (M = 158.51 J, SD = 84.81); rear boss (M = 155.15 J, SD = 79.90); side (M = 128.52 J, SD = 63.22); front (M = 1.34 J, SD = 0.66); and front boss (M =

104.95 J, SD = 41.12). The mean energy loaded onto the side location was statistically significantly greater than the front boss location ($p = .016$). While the mean energy loading for the rear boss location was significantly greater than the front ($p = .019$); the front boss location ($p \leq .001$); and the side location ($p < .001$). Finally, the mean energy loaded onto the rear location was also significantly greater than the front ($p = .022$); front boss ($p = .002$); and side ($p \leq .001$).

Simple main effects of impact location at high neckform stiffness.

No facial shielding. A statistically significant simple main effect of impact location for helmets with no facial shields when the neckform stiffness at its highest was observed F (1.18, 20.03) = 7.50, $p = .01$, $\eta_p^2 = .31$. The mean energy at each impact location at a high neckform stiffness with no facial shielding were as follows: rear boss (M = 149.78 J, SD = 68.38); front (M = 135.94 J, SD = 52.90); rear (M = 135.02 J, SD = 88.34); side (M = 122.28 J, SD = 55.59); and front boss (M = 108.40 J, SD = 35.75). The mean energy loading for the front location was significantly greater than the front boss ($p = .002$); as well as the side location ($p < .001$). The mean energy loading for the rear boss location was also significantly greater than the front boss ($p = .004$); and side location ($p < .001$).

Metal facial shielding. A statistically significant simple main effect of impact location for helmets with metal facial shields when the neckform stiffness at its highest stiffness was observed F (1.46, 24.73) = 10.83, $p \leq .001$, $\eta_p^2 = .39$. The mean energy loading at each impact location at a high neckform stiffness with metal facial shielding were as follows: rear boss (M = 147.94 J, SD = 83.27); front (M = 144.43 J, SD= 69.33); rear (M = 142.50 J, SD = 87.49); side (M = 136.80 J, SD = 65.80); and front boss (M = 102.42 J, SD = 40.31). The energy loading for the front location was again significantly greater than the front boss location ($p = .004$). The side location was significantly greater than the front boss location by ($p = .005$). Finally, the mean

energy loading at the rear boss location was also significantly greater than the front boss (p = .011).

Polycarbonate facial shielding. Finally, a statistically significant simple main effect of impact location for helmets with polycarbonate facial shielding when the neckform stiffness at its highest stiffness was observed F (1.96, 33.31) = 15.39, $p < .001$, $\eta_p^2 = .48$. The mean SI at each impact location at a high neckform stiffness with polycarbonate facial shielding were as follows: rear (M = 156.97 J, SD = 87.92); rear boss (M = 150.45 J, SD = 71.46); side (M = 127.29 J, SD = 56.03); front (M = 121.21 J, SD = 64.89); and front boss (M = 104.14 J, SD = 43.16). The energy loading for the side location was significantly greater than the front boss location ($p \leq .001$). Next the rear boss location was significantly greater than the front (p = .004); the front boss location ($p < .001$); and side location ($p \leq .001$). Finally, the mean energy loading at the rear location was also significantly greater than the front (p = .009); the front boss (p = .004); and side (p = .023).

Simple main effects of facial shielding at low neckform stiffness.

***Front location*.** There was a statistically significant simple main effect for facial shielding on energy loading at the front impact location at low neckform stiffness F (1.51, 25.59) = 9.70, p = .002, $\eta_p^2 = .36$. The mean energy loading on helmets differed for each facial shielding condition. The metal facial shield resulted in the greatest energy loading (M = 152.77 J, SD = 73.01); followed by no facial shielding (M = 131.03 J, SD = 56.04); and polycarbonate shielding (M = 119.13 J, SD = 62.79). The energy loading experienced by the headform at the front location at a low neckform stiffness was statistically significantly higher in the helmet with metal facial shield compared to the helmet with the no facial shielding (p = .002); and high impact polycarbonate shield (p = .005).

Front boss location. There was a statistically significant simple main effect for facial shielding on energy loading at the front boss impact location at low neckform stiffness F (1.48, 25.19) = 6.58, p = .009, η_p^2 = .28. The mean energy loading for the different facial shielding combinations were as follows: metal facial shield combination (M = 109.86 J, SD = 38.29); helmets with no facial shield (M = 107.84 J, SD = 36.10); and polycarbonate facial shield combination (M = 100.48 J, SD = 34.93). The energy loading at the front boss location at a low neckform stiffness was statistically significantly higher in the helmet with no facial shield compared to the high impact polycarbonate shield (p = .002). There was also a statistically significant difference in the mean energy loading on the helmet with metal facial shielding as compared to the helmet with the polycarbonate cage combination (p = .026).

Side location. There was statistically significant simple main effect for facial shielding on energy loading at the side impact location at low neckform stiffness F (2, 34) = 17.50, p < .001, η_p^2 = .51. The mean energy loading for the different facial shielding combinations were as follows: metal facial shield combination (M = 129.19 J, SD = 61.76); polycarbonate facial shield combination (M = 124.04 J, SD = 59.72); followed by helmets with no facial shield (M = 114.81 J, SD = 58.48). The simple comparison revealed that at the side location, had more energy loaded onto them then in the helmet with no facial shields compared to metal facial shields (p < .001) and polycarbonate facial shields (p = .002).

Rear boss location. There was a statistically significant simple main effect for facial shielding on energy loading at the rear boss impact location at low neckform stiffness F (2, 34) = 7.66, p = .002, η_p^2 = .31. The mean energy loading for the different facial shielding combinations were as follows: metal facial shield combination (M = 154.05 J, SD = 77.91); polycarbonate facial shield combination (M = 148.86 J, SD = 78.49); and helmets with no facial shield (M =

144.89 J, SD = 75.01). The pairwise comparison for this condition revealed that the energy loading on helmet with metal shield statistically significant greater than the helmet with no facial shielding (p = .002).

Rear location. There was a statistically significant simple main effect for facial shielding on energy loading at the rear impact location at low neckform stiffness F (2, 34) = 22.34, p < .001, η_p^2 = .57. The mean energy loading for the different facial shielding combinations were as follows: polycarbonate facial shield combination (M = 152.17 J, SD = 79.71); helmets with no facial shield (M = 142.08 J, SD = 73.01); and metal facial shield combination (M = 123.64 J, SD = 70.70). The mean energy loaded onto the rear impact location for this neckform stiffness was statistically significantly different on helmets with no facial shielding as compared to helmets with metal shielding (p < .001). Additionally, the polycarbonate facial shield had more energy loaded onto it then the metal facial shield helmet combination (p < .001).

Simple main effects of facial shielding at medium neckform stiffness.

Front location. There was a statistically significant simple main effect for facial shielding on energy loading at the front impact location at medium neckform stiffness F (2, 34) = 11.41, p < .001, η_p^2 = .40. The mean energy loading on helmets differed for each facial shielding condition. The metal facial shield resulted in the greatest energy loading (M = 150.30 J, SD = 69.87); followed by no facial shielding (M = 137.03 J, SD = 59.68); and polycarbonate shielding (M = 119.27 J, SD = 49.82). The energy loading at the front location at a medium neckform stiffness was statistically significantly higher in both the helmet with no facial shield *(p* = .022), and with the metal shield (p = .004) compared to the helmet with the polycarbonate shielding condition

Front boss location. There was not a statistically significant simple main effect for facial shielding on energy loading at the front boss impact location at medium neckform stiffness F (2, 34) = 1.21, p = .312, η_p^2 = .07.

Side location. A statistically significant simple main effect for facial shielding on energy loading at the side impact location at medium neckform stiffness F (2, 34) = 14.11, p < .001, η_p^2 = .45. The mean energy loading for the different facial shielding combinations were as follows: metal facial shield combination (M = 128.86 J, SD = 63.59); polycarbonate facial shield combination (M = 128.52 J, SD = 63.22); followed by helmets with no facial shield (M= 118.03 J, SD= 60.26). The simple comparison, again revealed that at the side location, helmets with metal had more energy loaded onto them then helmets with no facial shields (p = .002). Similarly, polycarbonate facial shields also had more energy loaded onto them then helmets with no facial shields ($p \leq .001$).

Rear boss location. There was a statistically significant simple main effect for facial shielding on energy loading at the rear boss impact location at medium neckform stiffness F (2, 34) = 5.55, p = .008, η_p^2 = .25. The mean energy loading for the different facial shielding combinations were as follows: polycarbonate facial shield combination (M = 155.15 J, SD = 79.90); metal facial shield combination (M = 153.17 J, SD = 70.79); and helmets with no facial shield (M = 145.44 J, SD = 70.04). The mean energy loading at the rear boss location at a medium neckform stiffness was statistically significantly higher in the helmet with a metal shield (p = .037); and in the helmet with high impact polycarbonate shield (p = .030), as compare to the helmet with no facial protection.

Rear location. There was a statistically significant simple main effect for facial shielding on energy loading at the rear impact location at medium neckform stiffness F (1.46, 24.89) =

8.02, $p = .004$, $\eta_p^2 = .32$. The mean energy loading for the different facial shielding combinations were as follows: polycarbonate facial shield combination (M = 158.51 J, SD = 84.81); metal facial shield combination (M= 141.25 J, SD= 89.29); and helmets with no facial shield (M = 140.76 J, SD = 85.96). The simple comparison revealed that at the rear location, helmets with polycarbonate facial shields had more energy loaded onto them then helmets with no facial shields ($p < .001$); as well as, metal facial shields ($p = .010$).

Simple main effects of facial shielding at high neckform stiffness.

Front location. There was a statistically significant simple main effect for facial shielding on energy loading at the front impact location at a high neckform stiffness F (2, 34) = 7.66, $p = .002$, $\eta_p^2 = .31$. The mean energy loading on helmets differed for each facial shielding condition. The metal facial shield resulted in the greatest energy loading (M = 144.43 J, SD = 69.33); followed by no facial shielding (M = 135.94 J, SD = 52.90); and polycarbonate shielding (M = 121.21 J, SD = 64.89). The energy loading at the front location at a high neckform stiffness was statistically significantly higher in the helmet with the metal shield compared to the helmet with high impact polycarbonate shield, ($p = .002$).

Front boss location. There was not a statistically significant simple main effect for facial shielding on energy loading at the front boss impact location at a high neckform stiffness F (2, 34) = 1.07, $p = .353$, $\eta_p^2 = .06$.

Side location. There was a statistically significant simple main effect for facial shielding on energy loading at the side location at a high neckform stiffness F (2, 34) = 8.35, $p = .001$, $\eta_p^2 = .33$. The mean energy loading for the different facial shielding combinations were as follows: metal facial shield combination (M = 136.80 J, SD = 65.80); polycarbonate facial shield combination (M = 127.29 J, SD = 56.03); followed by helmets with no facial shield (M = 122.28

J, SD = 55.59). The mean energy loading at the side location at a high neckform stiffness was statistically significantly higher in the helmet with metal facial shield compared to the helmet with the no shielding (p = .007).

Rear boss location. There was no statistically significant simple main effect for facial shielding on energy loading at the rear boss impact location at a high neckform stiffness F (1.21, 20.55) = 0.32, p = .731, η_p^2 = .02.

Rear location. There was a statistically significant simple main effect for facial shielding on energy loading at the rear impact location at a high neckform stiffness F (2, 34) = 12.97, p < .001, η_p^2 = .43. The mean energy loading for the different facial shielding combinations were as follows: polycarbonate facial shield combination (M = 156.97 J, SD = 87.92); metal facial shield combination (M = 142.50 J, SD = 87.49); and helmets with no facial shield (M = 135.02 J, SD = 88.34). The simple comparison revealed that at the rear location, helmets with polycarbonate facial shields had, more energy loaded onto them then helmets with no facial shields (p < .001); and metal facial shields (p = .002).

Discussion

Energy loading is a relatively new variable when it comes to helmet testing. The aim of this variable is to examine helmet performance in terms of the dynamic response of helmet materials across the various locations. This approach considers the deformation of helmet materials from the force generated in an impact (Zerpa et al., 2016). This approach could prove to be useful in understanding injury mechanisms in hockey (Namjoshi et al., 2013), as the amount of energy loaded onto the brain can potentially be determined.

Energy analyses can have applications for improving the design and protective properties of a helmet in areas where more energy is loaded onto the helmet and head, as the outer shell and

attenuation liner of a hockey helmet are currently unable to dissipate all forces and energy, meaning some are passed to the head and brain of the wearer (Cui et al., 2009; Zerpa et al., 2016). Such improvements could help reduce rebound velocity and decrease the probability of brain tissue damage from on ice head impacts (Barth et al., 2001; Zerpa et al., 2016).

Energy loading values for the current study are derived from the acceleration-time curves but are considered in relation to the mass of the system. This outcome measure, however, only utilizes the data from the initiation of the impact to the maximum linear acceleration value produced in the impact. To determine the energy loaded into the system, the testing protocol used in this study incorporated the mass of the helmet, headform, and table assembly as the mass of the whole system to compute the applied force. This approach can be beneficial in the helmet testing field, as it evaluates the ability of the helmet in combination with the head and neck to manage the loading force over the helmet deformation interval during the impact.

A major finding of the current study was that when the helmet was outfitted with full facial shielding, a higher amount of energy was significantly loaded into the system when compared the non-facial shielding condition. One rationale for this outcome may be that when facial shields were added to the helmet, the helmet's mass and momentum (of the stationary helmeted headform) also increased. As the momentum before and after the impact must be conserved in accordance with Newton's first and second laws of motion (Hall, 2007), the impact force of collision would then be elevated in helmets with facial shields since the impact time decreases. Determining the force causing the acceleration to headform, helmet, and neckform assembly is the first step in the energy loading calculations. Consequently, greater forces led to greater energy loading, which is what the results of this study illustrate.

A further investigation in the current study on the facial shielding energy loading relationship revealed that the metal facial shielding condition received the highest energy loadings 8 times out of the 12 significant impact locations while the polycarbonate shield received the other 4. This outcome emphasizes that the increased mass of the facial shields may not be solely responsible for the increased energy loading values as both facial shields had approximately the same mass. Other factors such as the material properties of the helmets may also come into play. As discussed in relation to the static stiffness testing, both facial shields caused the helmets to increase their overall stiffness properties.

This reduced elasticity of the helmet also means a decreased ability of the helmet to disperse the force upon impact (Hearn, 1997; Kostopoulos et al., 2002) possibly causing increased energy loadings. Greater helmet stiffness, however, has been shown to result in higher acceleration in motorcycle helmets (Kostopoulos et al., 2002) but this did not occur in peak linear acceleration results of the current study.

Kostopoulos et al.'s findings, as well as, the results of the energy loading section of this study, suggest that adding a facial shield could inhibit the protective properties of a hockey helmet due to the increased stiffness and mass. There were still some instances when the helmets with facial shields resulted in less energy loading onto the headform than the helmet with no facial shielding. Facial shields could, in this instance, be responsible for the reduction because facial shields are thought to help increase the area in which forces can be transferred, which is a protective property of the helmet (Graham et al., 2014). The reasons for these inconsistencies in the findings are unknown and, therefore, warrant further exploration to improve the understanding of how facial shielding influences the energy loading of a hockey helmet.

The interaction between facial shielding and impact location on measures of loading energy found in the current study also means that the impact locations must be examined closely by taking in consideration the type of facial shielding outfitted on the helmet during testing. The results highlighted statistically significant simple main effects for both impact location and facial shielding conditions.

To date, only two studies Carlson (2016) and Zerpa et al., (2016) have examined the energy loaded onto hockey helmets in dynamic impacts using this evaluation technique. In both studies (Carlson, 2016; Zerpa et al., 2016), the mass of the systems, the method of impacting, and the helmets were different than the presented work, making it difficult for energy loading comparisons.

Zerpa et al.'s (2016) work focused more on the energy dissipation of hockey helmets, rather than the energy loading experienced by the helmet. The study did report energy loading findings, but the findings were much lower than the results of the present study and Carlson's (2016) findings. This difference is more likely related to impact speed as Zerpa et al. (2016) impacted hockey helmets at a speed of 4.5 m/s, whereas in the current study, the helmet was impacted with speeds up to 5.13 m/s. Nevertheless, in the current study, a statistically significant difference was observed in energy loading measures at the various impact locations tested.

Carlson (2016) also observed a main effect among locations on energy loading, meaning that location in which the helmet was impacted did not manage the energy loaded onto the helmet, head and neckform equally. In Carlson's study, the front location (M = 162.29 J, SD = 59.86); followed by the rear (M = 155.06 J, SD = 54.10); rear boss (M = 150.88 J, SD = 53.30); front boss (M = 131.66 J, SD = 34.14); and, finally, the side (M = 105.28 J, SD = 30.93) experienced the most energy loaded onto them.

In the current study, the rear boss location experienced the greatest energy loadings of the five impact locations, while the front boss typically had the least. The front, side, and rear locations did not show consistency in their order as they allowed similar amounts of energy to be loaded into the systems and was dependent on the facial shielding condition. These results can be supported by the lack of significant pairwise comparisons found between these three impact locations.

Another factor to consider is the stiffness asymmetries in the structure of the neckform in combination with helmet structure in relation to the foam and geometry, which may cause differences between the impact locations (Carlson, 2016). The helmet foam's primary purpose, for example, is to absorb the impact energy and prevent it from being transferred to the head (Radziszewski & Saga, 2017). The foam undergoes large compressive deformations, due to the foam cell bending, buckling, or fracturing to perform this feat (Avalle, Belingardi, & Montanini, 2001). The thickness, density, and whether the foam is glued to shell of the helmet also varies greatly within the helmet (Di Landro et al., 2002) and would change the ability of the foam to absorb the energy.

Zerpa et al. (2016) also reported that the location of the impact influenced the amount of energy that the hockey helmets were able to dissipate, ranging from 10.47 % at the front boss location to 22.01 % at the side location. The front, front boss, and side locations of the helmets used in the present study had the same thickness of foam under the impact locations and could explain why these locations had similar energy loading. The rear boss location, had openings in the outer shell and the liner to allow ventilation. This lack of foam under the impact site could have been responsible for the large energy loading values experienced at this location. The rear impact site was protected by the thickest layer of foam compared to other locations of the

helmet. This location, however, received some of the higher energy loadings, meaning other factors such as the external geometry of the helmet may also be contributing to the elevated energy loadings.

For instance, Spyrou, Pearsall, and Hoshizaki (2000) found that geometry of the shell changes the elastic properties of the helmet, which could alter the absorption by 4-35% depending of the ridge shape (angle of inclination and width). The geometry and the ridges of the helmet were different for each location of the helmet. The rear location is generally flatter than other locations with several ridges nearby. Flatter areas have been associated with higher linear accelerations (Halstead et al., 2000). These differences and similarities across helmet locations could be another reason why the front and side locations are close in terms of their energy loadings.

Alternatively, the front boss location has a greater curvature which likely meant better dispersion of the forces and less energy loading. This location also had significant ridges to allow for ventilation. As mentioned previously, tiny fractures in the plastic were occurring at this location meaning that the elastic limit of the material had been exceeded (Hearn, 1997). This wear and tear of the helmet material in the current study could have aided in the energy dispersion at the impact site and reduced the energy loading at this impact location. This is a principle used in motorcycle helmet designs where the impact induces damage to the shell to aid in energy dispersions (Pinnoji & Mahajan, 2010).

The literature suggests that the energy loading onto the helmet should be reduced with increased neckform stiffness as this would decrease impact forces, leading to greater energy dispersion (Cantu, 1992; Johnston, McCrory, Mohtadi, & Meeuwisse, 2001). Neither the outcome of the present study nor Carlson's (2016) have found significant interactions or main

effects involving neckform stiffness levels. Carlson's research was the first to examine how neckform stiffness levels influenced energy loading onto a helmeted headform, but used a drop testing method which limited the influence of the neck.

The current study used a horizontal impactor which should have increased the influence that the neckform had on the finding as it allowed the headform movement to continue following the impact. Even with post impact movement of the neckform allowed by the impacting method used in this study, there was no effect found regarding stiffness. Perhaps, the stiffness of the neckform may not have been maintained after multiple impacts. Changes to the stiffness may have been caused by the rotation of the wire cable running longitudinally through the neckform changing the torque of the nut and possibly the material properties of the neckform. This problem should be addressed in future research using this neckform as well as considering using a wider range of neckform stiffness levels to determine whether this may create a difference in the amount of energy loaded onto the system.

Energy transfer and dissipation are thought to be useful variables for determining risk of injury (Monthatipkul et al., 2012), but have never been clearly validated with a standard measure of concussion risk or head injury risk. Carlson (2016) determined that there was a moderate correlation between SI and energy loading, with only 11.56% of the variance in energy loading explained by the relationship. The relationship failed to account for the majority of the variance, which could be attributed to the SI measure being based entirely on linear acceleration (Carlson, 2016). Although the two variables were moderately correlated, one would expect the correlation to be much higher as both calculations roughly began with the same impact data.

The calculations required to determine energy loading values are also more tedious than those required to determine SI. This brings into question the practicality of using this method to

assess head injuries and concussions. Although there are obvious downsides to this evaluation method, it is still relatively new and should be continued to be examined as a method of evaluating helmets and player's risk of injury.

Chapter 5 – Conclusion

This study examined the effect of the type of impact location, facial shielding condition, and neckform stiffness level on measures of peak linear acceleration, severity index (SI), and energy loading. Additionally, the static stiffness of helmets was tested at different impact locations with the various types of facial shielding. This project attempted to build upon previous helmet testing research with new and relevant findings regarding impact location, facial shielding, neckform stiffness. The data analysis presented in the current study provided an avenue to assess the effect of these variables on a player's risk of injury and implications for helmet manufacturers and researchers in the field of concussion.

This study found statistically significant three-way ANOVA interactions between impact location, facial shielding, and neckform stiffness levels for each of the three dependent variables examined including peak linear acceleration, SI, and energy loading. These findings support and build on the previous literature regarding hockey helmet impact testing (Carlson, 2016; Lemair and Pearsall, 2007; Rousseau & Hoshizaki, 2008) using a collision type injury mechanism.

Strengths

The primary strength of this study was the comparison of helmets with two types of facial shields against a helmet with no facial shield, using a horizontal impactor to simulate on ice hockey collisions. Only one prior study has examined the effects that facial shielding has on the attenuation abilities of a hockey helmet. Lemair and Pearsall (2007) directly impacted the facial shields in their study using a drop testing method. This study did not directly impact the facial

shields, rather chose to impact five NOCSAE impact locations. Finally, the energy loading of helmets was explored both statically and dynamically when considering facial shielding, building on the work of Zerpa et al., (2016) and Carlson (2016), respectively.

Limitations

This study had several limitations pertaining to the headform, neckform, helmet, and pneumatic impactor. It first must be stated that the results obtained from this study are specific to testing conditions set forth by the researcher. Meaning that the results may be different if other helmets, facial shields, head/neckforms, and impactors are used.

The NOCSAE headform used contained only linear accelerometers. The accelerometers only serve to provide an estimate of linear acceleration, SI, and energy loading that a typical human brain would experience upon impact and it is unknown how close this measure is to the true linear acceleration the brain would experience; however, this measure has been found to be highly correlated to estimated tissue strain measures during head impact simulations (Clark, Post, Hoshizaki, & Gilchrist, 2016).

The headform did not have the ability to measure rotational acceleration, a variable that is also associated with concussions and brain injuries (Gennarelli et al., 1971), however, the study was geared toward examining the effect of neckform stiffness levels on helmet impact location and facial shields on measures of peak linear acceleration, risk of injury and energy.

The neckform used to simulate the various neckform stiffness conditions in the study was also supposed to simulate a response similar to a human's neck during an impact. It was designed to imitate the response of a 50^{th} percentile human neck, the same as the Hybrid III neckform, but it does not differ for neck strength in relation to gender. It was reported that, strong correlations between the custom neckform and the Hybrid III were observed based on the

research of Carlson (2016), which stated that “the behaviour of the custom neckform is similar to the Hybrid III when the headform is impacted at different locations” (p, 103). The custom neckform used in this study, however, has not yet been compared to the Hybrid III when using a horizontal impacting device.

Before the helmets were tested dynamically, one helmet underwent a durability test. A limitation of this preliminary test was that it was unable to test all the impact sites (front boss, rear boss, and side). Furthermore, the repetitive impactor used for the wear and tear test was unable to match the maximum impact force administered by the horizontal impactor at the top testing velocities. Testing at the maximum force would be preferable when determining the number of impacts a helmet can take before the helmet’s energy attenuation properties are compromised (Carlson, 2016). Ideally, this test would have been completed on the same impactor used to dynamically test the helmets, but would have added hundreds of impacts to the study.

The horizontal impactor also had several limitations. As with any machinery, there is wear on the system as it is used. This could lead to slight changes in the delivery of the impactor arm. Typically, impactors have timing gates to monitor the control of the delivery, but at the time of data collection the custom-built timing gate system was not functional. Therefore, the velocities reported are based off a high-speed motion capture analysis, which are still accurate but it is tedious process. Additionally, the cap of the impactor arm is slightly smaller and not convex liked the recommendations outlined in the NOCSAE testing protocol guidelines. Difference in the size of the striker cap has been shown to influence the dynamic response of the headform (Dawson, Ouer, Rousseau, & Hoshizaki, 2012). Having a different cap, however, did not influence the reliability of the results as the same cap was used for all testing. Future

researching using this impactor should address these limitations and make the appropriate modifications.

The final limitation concerns the energy loading variable used in this study. The energy loading was not computed solely for the helmet but rather for the helmet, headform, neckform, and table assembly. To compute the energy loading solely for the helmet or helmet facial shielding combinations, similar impacts would have to be conducted on a headform with and without helmets/facial shielding. The differences between the energy computations for the various conditions would indicate the exact amount of energy loaded onto the helmet based on the location. This approach would allow researchers to determine areas of the helmet that allow higher amounts of energy to be loaded onto it. The issue with this is approach, however, is that impacting a bare headform will likely cause irreversible damage to the mechanical structure and compromise its dynamic response to impacts. Furthermore, the calculations required to determine energy loading values are quite tedious and require the creation of scripts in excel to perform them.

Future Research

Future research should continue to explore the relationship that the combination of facial shielding and helmets have on reducing the severity of an impact. This strain of research could aid manufacturers in improving the design of facial shield itself or how it is secured to the helmets to help players manage with the impacts demands encountered into the sport of hockey. Testing organizations should also consider incorporating facial shielding in their impact assessments, as most players in the sport wear full facial protection.

Helmet testing research should be continued to be examined from a comprehensive perspective, as there are many complex relationships among variable concerning the risk of injury or concussion a player has. The relation neck stiffness level has with concussion is still unclear. Future research considerations should be aimed at examining current neckforms and whether they are biofidelic enough to simulate the dynamic response experienced by a human neck during impact. Furthermore, novel techniques such as principle component analyses, should be used to incorporate variables such as linear and rotational acceleration, SI, and HIC to form a more comprehensive variable to assess the severity of concussion (Greenwald et al. 2008) in hopes of understanding how variables interact.

Finally, future research also needs to examine how the helmet performs in the impact rather than the system in its entirety. A better understanding of how helmets perform during impacts will highlight areas of the helmet should be improved. This technique could be accomplished via impacting helmeted and unhelmeted headforms. Comparisons could be made between the two, allowing the energy dissipation characteristics of the helmet to be determined.

References

Agel, J., & Harvey, E. J. (2010). A 7-year review of men's and women's ice hockey injuries in the NCAA. *Canadian Journal of Surgery*, *53*(5), 319-323.

Andriessen, T. M., Jacobs, B., & Vos, P. E. (2010). Clinical characteristics and pathophysiological mechanisms of focal and diffuse traumatic brain injury. *Journal of Cellular and Molecular Medicine, 14*(10), 2381-2392.

Arciniegas, D. B., (2012). *Hypoxic-ischemic brain injury.* Retrieved from: http://www.internationalbrain.org/articles/hypoxicischemic-brain-injury/

Arciniegas, D., Anderson, A., Topkoff, J., & McAllister, T. (2005). Mild traumatic brain injury: A neuropsychiatric approach to diagnosis, evaluation, and treatment. *Neuropsychiatric Disorder Treatment*, *1*(4), 311-327.

Ashrafiuon, H., Colbert, R., Obergefell, L., & Kaleps, I. (1996). Modeling of a deformable manikin neck for multibody dynamic simulation. *Mathematical and Computer Modelling*, *24*(2), 45-56.

Asplund, C., Bettcher, S., & Borchers, J. (2009). Facial protection and head injuries in ice hockey: A systematic review. *British Journal of Sports Medicine, 43*(13), 993-999.

ASTM (2016). *Standard Performance Specification for Ice Hockey Helmets*. (F1045-16). West Conshohocken, USA, American Society for Testing and Materials.

Avalle, M. Belingardi, G., & Montanini, R. (2001). Characterization of polymeric structural foams under compressive impact loading by means of energy-absorbing diagram. *International Journal of Impact Engineering, 25*(5), 455-472.

(Bailes, J. E., Petraglia, A. L., Omalu, B. I., Nauman, E., & Talavage, T. (2013). Role of subconcussion in repetitive mild traumatic brain injury. *Journal of Neurosurgery*, *119*(5), 1235-1245.

Barth, J. T., Freeman, J. R., Broshek, D. K., & Varney, R. N. (2001). Acceleration-deceleration sport-related concussion: The gravity of it all. *Journal of Athletic Training*, *36*(3), 253-256.

Baumgart, F. (2000). Stiffness – an unknown world of mechanical science? *International Journal of the Care of the Injuries, 31(2)*, S-14-S-B2.

Benson, B. W., Hamilton, G. M., Meeuwisse, W. H., McCrory, P., & Dvorak, J. (2009). Is protective equipment useful in preventing concussion? A systematic review of the literature. *British Journal of Sports Medicine*, *43*(1), i56-i67.

Benson, B., Mieeuwisse, W., Rizos, J., Kang, J., & Burke, C. (2011). A prospective study of concussions among National Hockey League players during regular season games: the NHL-NHLPA Concussion Program. *Canadian Medical Association Journal, 183*(8), 905-911.

Benson, B. W., Mohtadi, N. G., Rose, M. S., & Meeuwisse, W. H. (1999). Head and neck injuries among ice hockey players wearing full face shields vs half face shields. *Journal of the American Medical Association*, *282*(24), 2328-2332.

Benson, B. W., Rose, M. S., & Meeuwisse, W. H. (2002). The impact of face shield use on concussions in ice hockey: A multivariate analysis. *British Journal of Sports Medicine*, *36*(1), 27-32.

Biasca, N., Wirth, S., Maxwell, W., & Simmen, H. (2005). Minor traumatic brain injury (mTBI) in ice hockey and other contact sports. *European Journal of Trauma, 31*(2), 105-116.

Biasca, N., Wirth, S., & Tegner, Y. (2002). The avoidability of head and neck injuries in ice hockey: an historical review. *British Journal of Sports Medicine*, *36*(6), 410–427.

Brainard, L. L., Beckwith, J. G., Chu, J. J., Crisco, J. J., McAllister, T. W., Duhaime, A. C., ... & Greenwald, R. M. (2012). Gender differences in head impacts sustained by collegiate ice hockey players. *Medicine and science in sports and exercise*, *44*(2), 297-304.

Cantu, R. C. (1992). Cerebral concussion in sport. *Sports Medicine, 14*(1), 64-74.

Cantu, R. V., & Cantu, R. C. (2011). Skull Fracture. In *Encyclopedia of Sports Medicine.* (Vol. 4, pp. 1341-1343). Thousand Oaks, CA: SAGE Publications, Inc.

Clark, J. M., Post, A., Hoshizaki, T.B., & Gilchrist, M. D. (2016). Protective capacity of ice hockey helmets against different impact events. *Annals of Biomedical Engineering, 44*(12), 3693-3704.

Carlson, S. (2016). The influence of neck stiffness, impact location, and angle on peak linear acceleration, shear force, and energy loading measures of hockey helmet impacts. (Master's thesis). Lakehead University, Thunder Bay, Canada.

Carlson, S., Zerpa, C., Hoshizaki, T., Elyasi, S., Paterson, G., Przyucha, E., & Sanzo, P. (2016, July). *Evidence of reliability and validity for the use of a helmet impact drop system*. Poster session presentation at the meeting of 34th International Conference on Biomechanics in Sports, Tsukuba, Japan. 391-394.

Caswell, S., & Deivert, R. (2002). Lacrosse helmet designs and the effects of impact forces. *Journal of Athletic Training, 37*(2), 164-171.

Chamard, E., Théoret, H., Skopelja, E. N., Forwell, L. A., Johnson, A. M., & Echlin, P. S. (2012). A prospective study of physician-observed concussion during a varsity university hockey season: metabolic changes in ice hockey players. Part 4 of 4. *Neurosurgical focus*, *33*(6), E4.

Charkrabratty, S. N. (2013). Best split-half and maximum reliability. *IOSR Journal of Research & Method in Education, 3*(1), 01-08.

Clement, L. & Jones, D. (1989) Research and development of hockey protective equipment: A historical perspective, in C. Castaldi & E. Hoerner (eds): Safety in Ice Hockey. Philadelphia, American Society for Testing and Material, 1989, 164-186.

Cobb, B. R., Zadnik, A. M., & Rowson, S. (2016). Comparative analysis of helmeted impact response of Hybrid III and National Operating Committee on Standards for Athletic Equipment headforms. *Journal of Sports Engineering and Technology, 230*(1), 50-60.

Collins, C. L., Fletcher, E. N., Fields, S. K., Kluchurosky, L., Rohrkemper, M. K., Comstock, R. D., & Cantu, R. C. (2014). Neck strength: A protective factor reducing risk for concussion in high school sports. *The Journal of Primary Prevention*, *35*(5), 309–319.

Cui, L., Kiernan, S., & Gilchrist, M. (2009). Designing the energy absorption capacity of functionally graded foam materials. *Materials Science and Engineering,30*, 3405-3413

Cook, D. J., Cusimano, M. D., Tator, C. H., & Chipman, M. L. (2003). Evaluation of the ThinkFirst Canada, Smart Hockey, brain and spinal cord injury prevention video. *Injury Prevention*, *9*(4), 361–366.

CSA. (2015a). *Ice hockey helmets.* (Z262.1-15). Toronto, Canada, Canadian Standards Association.

CSA. (2015b). *Face protectors for use in ice hockey.* (Z262.2-15*)*. Toronto, Canada, Canadian Standards Association.

Davenshvar, D., Nowinski, C., McKee, A., & Cantu, R. (2011). The epidemiology of sport-related concussion. *Journal of Sports Medicine, 30*(1), 1-17.

Dawson, L., Oeur, A., Rousseau, P., Hoshizaki, T. B. (2014). The influence of striker cap size on the dynamic response of a Hybrid III headform [Abstract]. *STP1552 Mechanism of Concussion in Sport*, 13-22.

Decloe, M. D., Meeuwisse, W. H., Hagel, B. E., & Emery, C. A. (2014). Injury rates, types, mechanisms and risk factors in female youth ice hockey. *British Journal of Sports Medicine*, *48*(1), 51-56.

Di Landro, L., Sala, G., & Olivieri, D. (2002). Deformation mechanisms and energy absorption of polystyrene foam for protective helmets. *Polymer Testing, 21*, 217-228.

Emery, C. A., & Meeuwisse, W. H. (2006). Injury rates, risk factors, and mechanisms of injury in minor hockey. *The American Journal of Sports Medicine*, *34*(12), 1960-1969.

Fekete, J. F. (1968). Severe brain injury and death following minor hockey accidents: The effectiveness of the "safety helmets" of amateur hockey players. *Canadian Medical Association Journal*, *99*(25), 1234-1239.

Foreman, S. G. (2010). The dynamic impact response of a Hybrid III head- and neckform under four neck orientations and three impact locations. (Master's thesis). University of Ottawa, Ottawa, Canada.

Furr, R., & Bacharach, V. (2008). *Psychometrics: An introduction.* Thousand Oaks, CA: Sage Publications, Inc.

Gadd, C. Use of a weighted impulse criterion for estimating injury hazard. In: *Proceedings of the*

10th Stapp Car Crash Conference, Society of Automotive Engineering, 1966, pp. 95-100.

Gennarelli, T., Ommaya, A., & Thibault, L. (1971). Comparison of translational and rotational head motions in experimental cerebral concussion. *Stapp Car Crash Conference,* 797-803.

Gessel, L. M., Collins, C. L., & Dick, R. W. (2007). Concussions among United States high school and collegiate athletes. *Journal of Athletic Training*, *42*(4), 495.

Gimbel, G., & Hoshizaki, T. (2008). A comparison between vinyl nitrile foam and new air chamber technology on attenuating impact energy for ice hockey helmets. *International Journal of Sports Science and Engineering, 2*(3), 154-161.

Giza, C.C., & Hovda, D.A. (2001). The neurometabolic cascade of concussion. *Journal of Athletic Training, 36*(3), 228-235.

Graham, R., Rivara, P., Ford, M., & Spicer, C., (2014). *Sports-Related Concussion in Youth.* Washington, DC: The National Academies Press.

Greenwald, R., Gwin, J., Chu, J., & Crisco, J. (2008). Head impact severity measurement for evaluating mild traumatic brain injury risk exposure. *Neurosurgery, 62*(4), 789-798.

Gurdjian, E. (1972). Recent advances in the study of the mechanism of impact injury the head-a summary. *Clinical Neurosurgery, 19*, 1-42.

Gurdjian, E., Hodgson, V., Thomas, L., & Patrick, L. (1968). Significance of relative movements of scalp, skull, and intracranial contents during impact injury of the head. *Journal of Neurosurgery, 29*(1), 70-72.

Gurdjian, E., Roberts, V., & Thomas, L. (1966). Tolerance curves of acceleration and intracranial pressure and protective index in experimental head injury. *Journal of Trauma (6)*, 600-604.

Gurdjian, E., Webster, J., & Lissner, H. (1955). Observations on the mechanism of brain concussion, contusion, and laceration. *Journal of Surgery, Gynecology, and Obstetrics, 101*(6), 680-690.

Guskiewicz, K. M., & Mihalik, J. P. (2006). The biomechanics and pathomechanics of sports-related concussion. In S. M. Slobounov & W. J. Sebastianelli (Eds.), *Foundations of sports-related brain injuries* (65-80). New York, NY: Springer Science + Business Media, Inc.

Gwin, J. T., Chu, J. J., Diamond, S. G., Halstead, P. D., Crisco, J. J., & Greenwald, R. M. (2010). An investigation of the NOCSAE Linear impactor test method based on in vivo measures of head impact acceleration in American football, *Journal of Biomechanical Engineering, 132*(1), 1-9.

Gwin, J., Chu, J., McAllister, T., & Greenwald, R. (2009). In situ measures of head impact acceleration in NCAA Division I men's ice hockey: Implications for ASTMF1045 and other ice hockey helmet standards. *Journal of ASTM International, 6*(6), 1-10.

Gysland, S. M., Mihalik, J. P., Register-Mihalik, J. K., Trulock, S. C., Shields, E. W., & Guskiewicz, K. M. (2012). The relationship between subconcussive impacts and concussion history on clinical measures of neurologic function in collegiate football player. *Annals of Biomedical Engineering, 40*(1), 14-22.

Hall, S. J. (2007). Basic biomechanics. (6th e.d.). New York, NY: McGraw-Hill.

Halstead, D. (2001). Performance testing updates in head, face, and eye protection. *Journal of Athletic Training, 36*(3), 322-327.

Halstead, P. D., Alexander, C. F., Cook, E. M., & Drew, R. C. (2000). Hockey headgear and the adequacy of current designs and standards. In *Safety in Ice Hockey: Third Volume*. ASTM International.

Halstead, M., Walter, K., & The Council on Sports Medicine and Fitness. (2010). Clinical report – sport-related concussion in children and adolescents. *Pediatrics, 126*(3), 597-615.

Higgins, M., Halstead, D., Snyder-Mackler, L., & Barlow, D. (2007). Measurement of impact acceleration: Mouthpiece accelerometer versus helmet accelerometer. *Journal of Athletic Training, 42*(1), 5-10.

Hockey Canada. (2015). *2014-2015 annual report.* Retrieved from: https://az184419.vo.msecnd.net/hockey-canada/Corporate/About/Downloads/2014-15_annual_report_e.pdf

Hodgson, V. R. (1975). National Operating Committee on Standards for Athletic Equipment football helmet certification program. *Medicine & Science in Sports Fall 1975*, *7*(3), 225-232.

Hodgson, V.R., Thomas, L.M., & Khalil, T.B. (1983). The role of impact location in reversible cerebral concussion. *Proceedings of the 27st Stapp Car Crash Conference*, SAE Paper No. 831618.

Honey, C. (1998). Brain injuries in ice hockey. *Clinical Journal of Sports Medicine, 8*(1), 43-46.

Hoshizaki, T. B., & Brien, S. E. (2004). The science and design of head protection in sport. *Neurosurgery*, *55*(4), 956-967.

Hoshizaki, B., Post, A., Kendall, M., Karton, C., & Brien, S. (2013). The relationship between head impact characteristics and brain trauma. *Journal of Neurology & Neurophysiology,* 5(1), 1-8.

Hoshizaki, T.B., "The relationship between helmet standards and head protectors safety in ice hockey", in *IIHF International Symposium on Medicine and Science in Hockey*, Biasca, N., Montag, W., & Gerber, C., University of Zurich, Zurich, 1995, pp. 90-95.

Hutchison, M. G. (2011). *Concussions in the National Hockey League (NHL): The Video Analysis Project* (Doctoral dissertation). University of Toronto. Toronto, Canada.

Hutchinson, J., Kaiser, M. J. & Lankarani, H. M. (1998). The head injury criterion (HIC) functional. *Applied Mathematics and Computation, 96*(1), 1-16.

Jeffries, L., Zerpa, C., Przysucha, E., Sanzo, P., & Carlson, S. (2017). The use of a pneumatic horizontal impact system for helmet testing. *Journal of Safety in Engineering, 6*(1), 8-13.

Johnston, K., McCrory, P., Mohtadi, N., & Meeuwisse, W. (2001). Evidence-Based Review of Sport-Related Concussion: Clinical Science. *Clinical Journal of Sport Medicine*, *11*(3), 150-159.

Kaplan, S., Driscoll, C. F., & Singer, M. T. (2000). Fabrication of a facial shield to prevent facial injuries during sporting events: A clinical report. *The Journal of Prosthetic Dentistry*, *84*(4), 387-389.

Kazim, S. F., Shamim, M. S., Tahir, M. Z., Enam, S. A., & Waheed, S. (2011). Management of penetrating brain injury. *Journal of Emergencies, Trauma and Shock*, *4*(3), 395-402.

Kendall, M., Walsh, E. S., & Hoshizaki, T. B., (2012). Comparison between Hybrid III and Hodgson-WSU headforms by linear and angular dynamic impact response. *Journal of Sports Engineering and Technology, 226*(3-4), 260-265.

Keppel, G. (1991). *Design and analysis: A researcher's handbook.* (3rd e.d.). Englewood Cliff, NJ: Prentice-Hall, Inc.

Kimpara, H., & Iwamoto, M. (2012). Mild traumatic brain injury predictors based on angular accelerations during impacts. *Annals of Biomedical Engineering, 40*(1), 114-126.

King, A., Yang, K., Zhang, L., & Hadry, W. (Eds). (2003). Is head injury caused by linear or rotational acceleration? Proceedings from IRCOBI 2003: *International Research Council on the Biomechanics of Injury.* Lisbon, Portugal.

Kis, M., Saunders, F. W., Kis, M., Irrcher, I., Tator, C. H., Bishop, P. J., & ten Hove, M. W. (2013). A method of evaluating helmet rotational acceleration protection using the Kingston Impact Simulator (KIS unit). *Clinical Journal of Sport Medicine*, *23*(6), 470-477.

Kostopoulos, V., Markopoulos, Y. P., Giannopoulos, G., & Vlachos, D. E. (2002). Finite element analysis of impact damage response of composite motorcycle safety helmets. *Composites: Part B, 33*(2), 99-107.

Lemair, M. (2007). Evaluation of impact attenuation of facial protectors in ice hockey helmets. (Master's thesis). McGill University, Montréal, Canada.

Lemair, M., & Pearsall, D. J. (2007). Evaluation of impact attenuation of facial protectors in ice hockey helmets. *Sports Engineering*, *10*(2), 65-74.

Lissner, H., Lebow, M., & Evans, F. (1960). Experimental studies on the relation between acceleration and intracranial changes in man. *Surgery, Gynecology & Obstetrics, 111*, 329-338.

Marsh, P., McPherson, M., & Zerpa, C. (2008). Impact forces and material properties of a soccer headgear. *ISBS - Conference Proceedings Archive*, Ottawa, ON.

Matic, G. T., Sommerfeldt, M. F., Best, T. M., Collins, C. L., Comstock, R. D., & Flanigan, D. C. (2015). Ice hockey injuries among United States high school athletes from 2008/2009–2012/2013. *The Physician and Sports Medicine*, *43*(2), 119-125.

Mayo Clinic. (2017). Concussion. Retrieved April 25, 2017, from http://www.mayoclinic.org/diseases-conditions/concussion/home/ovc-20273153

McAllister, A. (2013, September). Surrogate Head Forms for the Evaluation of Head Injury Risk. *Brain Injuries and Biomechanics Symposium*.

McAllister, T., Sparling, M., Flashman, L., & Saykin, A. (2001). Neuroimaging finding in mild traumatic brain injury. *Journal of Clinical and Experimental Neuropsychology, 23*(6), 775-791.

McIntosh, A. S. (2001). Equipment testing and concussion. *British Journal of Sport Medicine, 35*(5), 374.

McKenzie, B. (2017, May 15). Episode 15. The TSN Hockey Bobcast. Podcast retrieved from http://www.tsn.ca/the-tsn-hockey-bobcast-episode-15-1.743970

Meaney, D., & Smith, D. (2011). Biomechanics of concussion. *Clinics in Sports Medicine, 30*(1), 19-31.

Mihalik, J. P., Blackburn, J. T., Greenwald, R. M., Cantu, R. C., Marshall, S. W., & Guskiewicz, K. M. (2010). Collision type and player anticipation affect head impact severity among youth ice hockey players. *Pediatrics*, *125*(6), e1394-e1401.

Mihalik, J. P., Guskiewicz, K. M., Marshall, S. W., Blackburn, J. T., Cantu, R. C., & Greenwald, R. M. (2012). Head impact biomechanics in youth hockey: Comparisons across playing position, event types, and impact locations. *Annals of Biomedical Engineering*, *40*(1), 141-149.

Montgomery, D. L. (2006). Physiological profile of professional hockey players – a longitudinal comparison. *Applied Physiology, Nutrition, and Metabolism, 31*(2), 181-185.

Monthatipkul, S., Iovenitti, P., & Sbarski, I. (2012). Design of facial impact protection gear for cyclists. *Journal of Transportation Technologies*, *2*(3), 204-212.

Namjoshi, D., Good, C., Cheng, W., Panenka, W., Richards, D., Cripton, P., & Wellington, C. (2013). Towards medical management of traumatic brain injury: A review of models and mechanisms from a biomechanical perspective. *Disease Models and Mechanisms, 6*(6), 1325-1338.

National Aeronautics and Space Administration (1965). Dictionary of technical terms for aerospace use: NASA SP-7. Cleveland, Ohio: NASA.

NOCSAE. (2006). *Standard linear impactor test method and equipment used in evaluating the performance characteristics of protective headgear and face guards.* (ND 081-04m04). Overland Park, USA: National Operating Committee on Standards for Athletic Equipment.

NOCSAE. (2016a). *Standard performance specification for newly manufactured ice hockey helmets.* (ND 030-11m16). Overland Park, USA: National Operating Committee on Standards for Athletic Equipment.

NOCSAE. (2016b). *Standard pneumatic ram test method and equipment used in evaluating the performance characteristics of protective headgear and face guards.* (ND 081-14m15). Overland Park, USA: National Operating Committee on Standards for Athletic Equipment.

NOCSAE. (2017). *Standard test method and equipment used in evaluating the performance characteristics of headgear/equipment.* (ND 001-17m17). Overland Park, USA: National Operating Committee on Standards for Athletic Equipment.

Ommaya, A. K., Goldsmith, W., & Thibault, L. (2002). Biomechanics and neuropathology of adult and paediatric head injury. *British Journal of Neurosurgery, 16*(3), 220-242.

Ono, K., Kaneoka, K., Hattori, S., Ujihashi, S., Taknounts, E., Haffner, M., & Eppinger, R. (2003). Cervical vertebral motions and biomechanical responses to direct loading of human head. *Traffic Injury Prevention, 4*(2)*,* 141-152.

Ouckama, R. (2013). *Time series measurement of force distribution in ice hockey helmets during varying impact conditions*. Unpublished doctoral dissertation, McGill University, Montreal, Canada.

Pinnoji. P. K. & Mahajan, P. (2010). Analysis of impact-induced damage and delamination in the composite shell of a helmet. *Materials and Design, 31*(8), 3716-3723.

Pittella, J. E., & Gusmão, S. N. (2003). Diffuse vascular injury in fatal road traffic accident victims: Its relationship to diffuse axonal injury. *Journal of Forensic Science*, *48*(3), 1-5.

Post, A., Oeur, A., Hoshizaki, B., & Gilchrist M. D. (2011). Examination of the relationship between peak linear and angular accelerations to brain deformation metrics in hockey helmet impacts. *Computer Methods in Biomechanics and Biomedical Engineering, 16*(5), 511-519.

Radziszewski, L., & Saga, M. (2017). Modeling of non-elastic properties of polymeric foams used in sports helmets. *Procedia Engineering*, *177*, 314-317.

Richardson, J.T. (2011). Eta squared and partial eta squared as measures of effect size in educational research. *Educational Research Review, 6*(2), 135-147.

Rousseau, P., & Hoshizaki, T. B. (2009). The influence of deflection and neck compliance on the impact dynamics of a Hybrid III headform. *Proceedings of the Institution of Mechanical Engineers, Part P: Journal of Sports Engineering and Technology*, *223*(3), 89-97.

Rousseau, P., Post, A., & Hoshizaki, T. (2009). The effects of impact management materials in ice hockey helmets on head injury criteria. *Journal of Sports Engineering and Technology, 223*, 159-165.

Rowson, S., Bland, M. L., Campolettano, E. T., Press, J. N., Rowson, B., Smith, J. A., … & Duma, S. M. (2016). Biomechanical perspectives on concussion in sport. *Sports Medicine and Arthroscopy Review, 24*(3), 100-107.

Rowson, S., & Duma, S. M. (2011). Development of the STAR evaluation system for football helmets: Integrating player head impact exposure and risk of concussion. *Annals of Biomedical Engineering*, *39*(8), 2130-2140.

Rowson, B., Rowson, S., & Duma, S. M. (2015). Hockey STAR: A methodology for assessing the biomechanical performance of hockey helmets. *Annals of Biomedical Engineering, 43*(10), 2429-2433.

Schick, D. M., & Meeuwisse, W. H. (2003). Injury rates and profiles in female ice hockey players. *The American Journal of Sports Medicine*, *31*(1), 47-52.

Schmidt, J. D., Guskiewicz, K. M., Blackburn, J. T., Mihalik, J. P., Siegmund, G. P., & Marshall, S. W. (2014). The influence of cervical muscle characteristics on head impact biomechanics in football. *The American Journal of Sports Medicine, (42)*9, 2056-2066.

Silverthorn, D. U., Johnson, B. R., Ober, W. C., Garrison, C. W., & Silverthorn, A. C. (2010). *Human physiology: An integrated approach* (5th e.d.). San Francisco, CA: Pearson Education INC.

Smith, A. W., Bishop, P. J., & Wells, R. P. (1985). Alterations in head dynamics with the addition of a hockey helmet and facia shield under inertial loading. *Canadian Journal of Applied Sport Science. 10*(2), 68-74.

Spyrou, E., Pearsall, D. J., & Hoshizaki, T. B., (2000). Effect of local shell geometry and material properties on impact attenuation of ice hockey helmets. *Sports Engineering, 3*(1), 25-35.

Stevens, S. T., Lassonde, M., de Beaumont, L., & Keenan, J. P. (2006). The effect of visors on head and facial injury in National Hockey League players. *Journal of Science and Medicine in Sport*, *9*(3), 238-242.

Stuart, M. J., Smith, A. M., Malo-Ortiguera, S. A., Fischer, T. L., & Larson, D. R. (2002). A comparison of facial protection and the incidence of head, neck, and facial injuries in Junior A hockey players. A function of individual playing time. *The American Journal of Sports Medicine*, *30*(1), 39-44.

Tuominen, M., Stuart, M. J., Aubry, M., Kannus, P., & Parkkari, J. (2015a). Injuries in men's international ice hockey: A 7-year study of the International Ice Hockey Federation adult World Championship tournaments and Olympic Winter Games. *British Journal of Sports Medicine*, *49*(1), 30-36.

Tuominen, M., Stuart, M. J., Aubry, M., Kannus, P., Tokola, K., & Parkkari, J. (2015b). Injuries in women's international ice hockey: An 8-year study of the World Championship tournaments and Olympic Winter Games. *British Journal of Sports Medicine*, *50*(22), 1406-1412.

Walsh, E., Rousseau, P., & Hoshizaki, T. (2011). The influence of impact location and angle on the dynamic impact response of a Hybrid III headform. *Sports Engineering*, *13*(3), 135-143.

Wennberg, R. A., & Tator, C. H. (2003). National Hockey League reported concussions, 1986-87 to 2001-02. *Canadian Journal of Neurological Sciences*, *30*(3), 206-209.

Wilcox, B. J., Beckwith, J. G., Greenwald, R. M., Chu, J. J., McAllister, T. W. Flashman, L. A., ... & Criso, J. J. (2014). Head impact exposure in male and female collegiate ice hockey players. *Journal of Biomechanics, 47*(1). 109-114.

Yoganandan. N., & Pintar, F.A. (2003). Biomechanics of temporo-parietal skull fracture. *Clinical Biomechanics, 19*(3). 225-239.

Young, J. W. (1993). Head and face anthropometry of adult US civilians. *Federal Aviation Administration Civil Aeromedical Institute*, 1963-1993. *(*Final Report, 1993).

Zerpa, C., Carlson, S., Elyasi, S., Przysucha, E., & Hoshizaki, T. (2016). Energy dissipation measures on a hockey helmet across impact locations. *Journal of Safety Engineering*, *5*(2), 27-35.

Zerpa, C., Carlson, S., Sanzo, P., Przysucha, E., Hoshizaki, T., & Kivi, D. (2017). *The effect of angle of impact, neck stiffness, and impact location on measures of shear forces during helmet testing.* Oral session presentation at the meeting of 35th International Conference on Biomechanics in Sports, Cologne, Germany. 1020-1023.

Zhang, L., Yang, K. H., & King, A. I. (2004). A proposed injury threshold for mild traumatic brain injury. *Journal of Biomechanical Engineering, 126*(2), 226-236.

Zhang, L., Yang, K.H., & King, A. I. (2011). Comparison of brain responses between frontal and lateral impacts by finite element modelling. *Journal of Neurotrauma, 18*(1), 21-30.

Zumdahll, S. S., & Zumdahl, S. A. (2010). *Chemistry*. (8th e.d.). Belmont, CA: Brooks Cole.

Appendix A

Impact Condition Scenario

45 Different impact conditions for a total of: 810 impacts

Neck Torque 1 → No cage → 18 Speeds to Front Location
Neck Torque 1 → No cage → 18 Speeds to Front Boss Location
Neck Torque 1 → No cage → 18 Speeds to Side Location
Neck Torque 1 → No cage → 18 Speeds to Rear Boss Location
Neck Torque 1 → No cage → 18 Speeds to Rear Location

Neck Torque 2 → No cage → 18 Speeds to Front Location
Neck Torque 2 → No cage → 18 Speeds to Front Boss Location
Neck Torque 2 → No cage → 18 Speeds to Side Location
Neck Torque 2 → No cage → 18 Speeds to Rear Boss Location
Neck Torque 2 → No cage → 18 Speeds to Rear Location

Neck Torque 3 → No cage → 18 Speeds to Front Location
Neck Torque 3 → No cage → 18 Speeds to Front Boss Location
Neck Torque 3 → No cage → 18 Speeds to Side Location
Neck Torque 3 → No cage→ 18 Speeds to Rear Boss Location
Neck Torque 3 → No cage → 18 Speeds to Rear Location

Neck Torque 1 → Metal cage → 18 Speeds to Front Location
Neck Torque 1 → Metal cage → 18 Speeds to Front Boss Location
Neck Torque 1 → Metal cage → 18 Speeds to Side Location
Neck Torque 1 → Metal cage → 18 Speeds to Rear Boss Location
Neck Torque 1 → Metal cage → 18 Speeds to Rear Location

Neck Torque 2 → Metal cage → 18 Speeds to Front Location
Neck Torque 2 → Metal cage → 18 Speeds to Front Boss Location
Neck Torque 2 → Metal cage → 18 Speeds to Side Location
Neck Torque 2 → Metal cage → 18 Speeds to Rear Boss Location
Neck Torque 2 → Metal cage → 18 Speeds to Rear Location

Neck Torque 3 → Metal cage → 18 Speeds to Front Location
Neck Torque 3 → Metal cage → 18 Speeds to Front Boss Location
Neck Torque 3 → Metal cage → 18 Speeds to Side Location
Neck Torque 3 → Metal cage → 18 Speeds to Rear Boss Location
Neck Torque 3 → Metal cage → 18 Speeds to Rear Location

Neck Torque 1 → Polycarbonate cage → 18 Speeds to Front Location
Neck Torque 1 → Polycarbonate cage → 18 Speeds to Front Boss Location
Neck Torque 1 → Polycarbonate cage → 18 Speeds to Side Location
Neck Torque 1 → Polycarbonate cage → 18 Speeds to Rear Boss Location
Neck Torque 1 → Polycarbonate cage → 18 Speeds to Rear Location

Neck Torque 2 → Polycarbonate cage → 18 Speeds to Front Location
Neck Torque 2 → Polycarbonate cage → 18 Speeds to Front Boss Location
Neck Torque 2 → Polycarbonate cage → 18 Speeds to Side Location
Neck Torque 2 → Polycarbonate cage → 18 Speeds to Rear Boss Location
Neck Torque 2 → Polycarbonate cage → 18 Speeds to Rear Location

Neck Torque 3 → Polycarbonate cage → 18 Speeds to Front Location
Neck Torque 3 → Polycarbonate cage → 18 Speeds to Front Boss Location
Neck Torque 3 → Polycarbonate cage → 18 Speeds to Side Location
Neck Torque 3 → Polycarbonate cage → 18 Speeds to Rear Boss Location
Neck Torque 3 → Polycarbonate cage → 18 Speeds to Rear Location

Appendix B

Descriptive Statistics for All Impacts at Low, Medium, and High Neckform Stiffness Levels

Table 5

Descriptive Statistics (Mean; SD) for all impacts at low neckform stiffness

Facial Shielding	Location	Peak Linear Acceleration (g)	Severity Index (SI)	Energy Loading (J)
No Facial Shielding	Front	140.51 (68.93)	536.58 (444.04)	131.03 (56.04)
	Front Boss	125.11 (68.50)	434.92 (382.93)	107.84 (36.10)
	Side	111.50 (65.24)	313.19 (292.58)	114.81 (58.48)
	Rear Boss	145.68 (91.11)	503.73 (477.55)	144.89 (75.01)
	Rear	71.14 (26.27)	193.61 (138.34)	142.08 (73.01)
Metal Facial Shielding	Front	108.46 (52.63)	350.56 (286.37)	152.77 (73.03)
	Front Boss	108.56 (60.67)	333.56 (296.67)	109.86 (38.29)
	Side	110.89 (61.60)	324.00 (284.80)	129.19 (61.76)
	Rear Boss	164.81 (103.83)	634.11 (611.78)	154.05 (77.91)
	Rear	74.25 (30.24)	207.73 (150.79)	123.64 (70.70)
Polycarbonate Facial Shielding	Front	100.33 (42.32)	318.78 (233.33)	119.13 (62.79)
	Front Boss	116.12 (64.34)	389.92 (306.56)	100.48 (34.93)
	Side	109.54 (63.19)	306.56 (279.10)	124.04 (59.72)
	Rear Boss	148.50 (97.67)	540.10 (203.84)	148.86 (78.49)
	Rear	73.16 (29.31)	203.84 (145.82)	152.17 (79.71)

Table 6

Dependent Statistics (Mean; SD) for all impacts at medium neckform stiffness

Facial Shielding	Location	Peak Linear Acceleration (g)	Severity Index (SI)	Energy Loading (J)
No Facial Shielding	Front	140.43 (70.24)	527.67 (450.00)	137.03 (59.68)
	Front Boss	124.38 (69.47)	448.07 (409.19)	109.16 (38.79)
	Side	114.94 (66.17)	328.08 (296.00)	118.03 (60.26)
	Rear Boss	163.20 (99.23)	624.36 (594.47)	145.44 (70.04)
	Rear	72.25 (30.41)	195.30 (149.57)	140.76 (85.96)
Metal Facial Shielding	Front	113.63 (53.12)	362.82 (289.56)	150.30 (69.87)
	Front Boss	112.98 (64.63)	347.27 (319.30)	105.36 (40.96)
	Side	111.57 (61.75)	319.57 (281.00)	128.86 (63.59)
	Rear Boss	171.65 (104.68)	671.28 (634.78)	153.17 (70.79)
	Rear	77.34 (41.11)	218.58 (188.62)	141.25 (89.29)
Polycarbonate Facial Shielding	Front	108.96 (42.89)	343.30 (228.87)	119.27 (49.82)
	Front Boss	115.73 (65.17)	346.93 (316.93)	104.95 (41.12)
	Side	112.54 (63.77)	316.93 (285.14)	128.52 (63.22)
	Rear Boss	152.92 (96.09)	556.68 (540.52)	155.15 (79.90)
	Rear	76.97 (38.56)	219.13 (183.55)	158.51 (84.81)

Table 7

Dependent Statistics (Mean; SD) for all impacts at high neckform stiffness

Facial Shielding	Location	Peak Linear Acceleration (g)	Severity Index (SI)	Energy Loading (J)
No Facial Shielding	Front	149.64 (72.07)	578.12 (470.99)	135.94 (52.90)
	Front Boss	118.55 (64.14)	395.41 (343.38)	108.40 (35.75)
	Side	115.00 (65.87)	326.03 (293.04)	122.28 (55.59)
	Rear Boss	168.99 (100.76)	663.88 (628.88)	149.78 (68.38)
	Rear	72.72 (31.47)	198.68 (153.73)	135.02 (88.34)
Metal Facial Shielding	Front	112.29 (53.85)	354.32 (289.75)	144.43 (69.33)
	Front Boss	107.19 (62.34)	333.40 (311.14)	102.42 (40.31)
	Side	102.54 (60.33)	294.79 (270.45)	136.80 (65.80)
	Rear Boss	152.48 (100.60)	565.50 (586.43)	147.94 (83.27)
	Rear	73.40 (32.76)	250.11 (157.99)	142.50 (87.49)
Polycarbonate Facial Shielding	Front	95.55 (34.05)	266.36 (169.06)	121.21 (64.89)
	Front Boss	118.87 (64.71)	392.01 (350.83)	104.14 (43.16)
	Side	109.89 (61.13)	303.17 (264.89)	127.29 (56.03)
	Rear Boss	164.83 (100.18)	641.25 (605.34)	150.45 (71.46)
	Rear	79.59 (43.24)	230.65 (204.09)	156.97 (87.92)